

**ALMA MATER STUDIORUM - UNIVERSITA' DI BOLOGNA**

Second Cycle Degree Programme in

**Digital Humanities and Digital Knowledge**

Dissertation Title

**A semi-automatic procedure for 3D survey of cultural heritage  
objects: the case of the archaeological *Dynamic Collections***

Final Dissertation in

**Digital Heritage and Multimedia**

Supervisor **Sofia Pescarin**

Co-supervisor **Nicolò Dell'Unto**

Co-supervisor **Diego Ronchi**

Presented by **Luisa Ammirati**

**Third Session – March 2023**

Academic year

**2021/2022**



## Table of contents

<b>Index of Figures.....</b>	<b>3</b>
<b>Index of Tables .....</b>	<b>6</b>
<b>1. Introduction.....</b>	<b>9</b>
<b>2. The Digital Archaeology: the context of the Dynamic Collections.....</b>	<b>12</b>
<b>2.1 Surveying technology and museum collections: State of Art.....</b>	<b>12</b>
<b>2.2 Digital libraries of semantically annotated 3D objects .....</b>	<b>18</b>
<b>2.3 The design of a survey campaign.....</b>	<b>24</b>
2.3.1 Dynamic Collections.....	24
2.3.2 The educational purpose .....	30
<b>3. First phase of the survey: the object.....</b>	<b>34</b>
<b>3.1 Artefact classification .....</b>	<b>34</b>
3.1.1 Intrinsic aspects.....	34
3.1.2 Extrinsic aspects.....	42
<b>3.2 Surveying aims: input and output metrics .....</b>	<b>44</b>
<b>3.3 Model complexity index.....</b>	<b>46</b>
<b>3.4 Complexity classes.....</b>	<b>48</b>
<b>4. Second phase of the survey: planning and acquisition .....</b>	<b>51</b>
<b>4.1. The choices of the devices and the equipment.....</b>	<b>51</b>
4.1.1. Basic photogrammetric instrumentation .....	51
4.1.2. Equipment for macro photography and cross polarization .....	55
<b>4.2. The camera setting.....</b>	<b>58</b>
4.2.1. Aperture, shutter speed and ISO .....	58
4.2.2. Arrangement of lighting and associated filters .....	61
4.2.3 Equipment and camera setting for the case studies.....	61
<b>4.3. Image acquisition .....</b>	<b>63</b>

4.3.1. Turntable interval rotation .....	63
4.3.2. Camera height intervals .....	64
4.3.3. Artefact orientations.....	65
4.3.4. The use of polarized filter and lights with laminated polarizing sheets.....	68
<b>5. Third phase of the survey: 3D photogrammetric processing.....</b>	<b>71</b>
<b>5.1. Feature matching .....</b>	<b>72</b>
<b>5.2. Bundle adjustment .....</b>	<b>74</b>
<b>5.3. Dense reconstruction.....</b>	<b>79</b>
<b>5.4. Network triangulation .....</b>	<b>81</b>
<b>5.5. Texturing.....</b>	<b>82</b>
<b>6. Guiding the 3D photogrammetric survey .....</b>	<b>85</b>
<b>6.1. Result of the semi-automatic procedure in Twine .....</b>	<b>86</b>
<b>Conclusion.....</b>	<b>87</b>
<b>References .....</b>	<b>89</b>
<b>Sitography .....</b>	<b>103</b>

# Index of Figures

<b>Figure 1</b> Taxonomy of 3D modelling techniques (Remondino and El-Hakim, 2006; Talha et al., 2019).	13
<b>Figure 2</b> Laser triangulation range finding	14
<b>Figure 3</b> Output of SfM (left) and MVS (right) algorithms (“Photogrammetry: the technology behind the magic”).	16
<b>Figure 4</b> Homepage of 3D Virtual Museum.	19
<b>Figure 5</b> Examples of two 3D objects on Sketchfab: a globular aryballos published by Museo etrusco di Populonia - Collezione Gasparri - (on the left), and a bust statue from Pompei by a user called fginestrini (on the right).	19
<b>Figure 6</b> Collage of a 3D models with the related metadata available in Europeana.	21
<b>Figure 7</b> Visualisation of a 3D model within its metadata (on the left) in Smithsonian platform.	22
<b>Figure 8</b> Example of a window (on the right) with metadata and paradata (written in Swedish) for an artefact chosen from the entire collection.	23
<b>Figure 9</b> A graphic representation of the different annotation approaches (Ponchio et al., 2020)	23
<b>Figure 10</b> Artefacts from the campaign acquisition of June 2022 (Dynamic Collections).	29
<b>Figure 11</b> Example of annotation related general Notes (Dynamic Collections)	32
<b>Figure 12</b> Example of annotations related to Views of the related model (Dynamic Collections)	33
<b>Figure 13</b> Example of a model with annotation related to Spot (Dynamic Collections)	33
<b>Figure 14</b> Bounding box of the 3D model of the artefact LUHM13188c	35
<b>Figure 15</b> Bounding box of the 3D model of the artefact LUHM21015.20.	35
<b>Figure 16</b> Bounding box of the 3D model of the artefact LUHM25561.	35
<b>Figure 17</b> Bounding box of the 3D model of the artefact LUHM32125.81.	36
<b>Figure 18</b> Representation of the Cavity ratio ( $W$ in the left, $D$ in the right picture) of LUHM32125.81 through its untextured model	37
<b>Figure 19</b> Representation of the Cavity ratio of LUHM21015.20 through its textured (left) untextured model (right)	37
<b>Figure 20</b> Designs of different types of fibulas by (Håkansson et al., 1999)	38
<b>Figure 21</b> (a) reflectance and (b) transmissivity measurements (Lu, 2016, 28).	38
<b>Figure 22</b> (a) Basic reflectance models of the incoming light (in red): perfect diffuse (light blue), glossy (purple), and perfect specular (blue). In (b-d) renderings of diffuse, glossy and specular spheres are shown, places inside a Cornell box (Guarnera et al., 2016, 3)	39
<b>Figure 23</b> LUHM25561 and LUHM13188c from different perspectives.	43

<b>Figure 24</b> Untextured LUHM25561 from different perspectives, with a focus on the central hole.	44
<b>Figure 25</b> The suggested shift from object complexity, throughout model complexity, up to process complexity (Pritchard et al., 2022, 52).....	47
<b>Figure 26</b> Constant representing the incremental growth of the model's complexity.....	49
<b>Figure 27</b> The four case studies displayed along the constant of the model's complexity within a differentiation of the complexity classes. ....	50
<b>Figure 28</b> Multi-viewpoint camera approach (left); the rotary approach (right). The model shown in the figure is LUHM32125.81.....	53
<b>Figure 29</b> Scale bar of 10 cm. The model shown in the figure is LUHM25561.....	54
<b>Figure 30</b> Different artefact positioning supported by two rubber pads. The model shown in the figure is LUHM25561.....	55
<b>Figure 31</b> Scale bars of different dimension. ....	56
<b>Figure 32</b> Different optical lens. ....	56
<b>Figure 33</b> Interaction of light sources, the object and the camera with polarizer (Miyazaki et al., 2004, 6). ....	57
<b>Figure 34</b> Aperture measures and related image of the lens. ....	59
<b>Figure 35</b> Explanation of the reciprocal relationship with aperture and shutter speed (Verhoever, 2016). ....	59
<b>Figure 36</b> Explanation of relative aperture and f-stop series. ....	60
<b>Figure 37</b> The ISO-A-S triangle exposure. ....	60
<b>Figure 38</b> Example of the turntable interval rotation with LUHM13188c. ....	64
<b>Figure 39</b> Example of the camera height intervals with LUHM32125.81.....	64
<b>Figure 40</b> The four artefact orientations used for LUHM13188c.....	65
<b>Figure 41</b> On the left, the frontal symmetric face of LUHM21015.20; on the right, its thin lateral side. ....	66
<b>Figure 42</b> Disposition of LUHM21015.20 on the turntable with rubber pads. The first representation is relative to the first artefact orientation; the images on the centre and the right side are related to the second orientation. ....	67
<b>Figure 43</b> The four artefact orientations used for LUHM21015.20.....	67
<b>Figure 44</b> Arrangement of the polarised filter (attached to the camera) and of lights with laminated polarising sheets, during the camera acquisition. The model shown in the figure is LUHM13188c.....	69
<b>Figure 45</b> Object rotation in relation to the camera and polarizer. The model used is LUHM21015.20.....	70
<b>Figure 46</b> A sample of typical workflow offered by Metashape (PhotoScan) GUI (Rahaman and Champion, 2019).....	71

<b>Figure 47</b> Flowchart of feature extraction, in a comparison among SIFT and AKAZE (Xu et al., 2022, 5). .....	73
<b>Figure 48</b> Align photo menu of Agisoft Metashape Professional.....	74
<b>Figure 49</b> Camera calibration mechanism.....	75
<b>Figure 50</b> Results from the estimation of camera properties and geometry. At the bottom of the figure, the sparse point-cloud formed from the feature points matching (Collins et al., 2019, 7).....	75
<b>Figure 51</b> Result of the camera calibration and the generation of the sparse cloud.....	76
<b>Figure 52</b> The reprojection error is the distance between the projected image point $p$ and the observed image point $\tilde{p}$ (Nguyen et al., 2012). .....	77
<b>Figure 53</b> Gradual selection and Reprojection error windows of Agisoft Metashape Professional. ....	77
<b>Figure 54</b> Screenshot of Add Marker action, by pointing on the images and click right button on the mouse (top); result of the scaled model in Metashape (bottom).....	78
<b>Figure 55</b> (a) A patch $p$ is a three-dimensional rectangle with centres and normal represented as $c(p)$ and $n(p)$ , respectively. (b) A patch's photometric discrepancy $f(p, I_1, I_2)$ is equal to one minus the normalised cross correlation score between sets of sampled pixel colours $q(p; I_i)$ (Furukawa and Ponce, 2010, 1364).....	79
<b>Figure 56</b> They use visible pictures to keep track of image projections of reconstructed patches to execute essential tasks like as accessing nearby patches, enforcing regularization, and so on (Furukawa and Ponce, 2010). .....	80
<b>Figure 57</b> Build Dense Cloud button and menu on Agisoft Metashape Professional.....	80
<b>Figure 58</b> The following are the results of normal orientation and meshing: (a) default point normals; (b) mesh before normal orienting; (c) point normals after orienting; and (d) mesh after normal orienting. (Xu et al., 2022, 8).....	82
<b>Figure 59</b> Example of texture mapping mechanism. ....	83
<b>Figure 60</b> Results of the four steps (feature matching, bundle adjustment, network triangulation and texturing) for the object LUHM25561. From left to right: sparse point cloud, dense point cloud, solid model (mesh), textured model.....	84
<b>Figure 61</b> Overview of the macro areas proposed by the semi-automatic procedure written with Twine.....	85
<b>Figure 62</b> Structure of the decision tree (graph) obtained with Twine Version 2.6.0 (2.6.0).....	86

# Index of Tables

<b>Table 1</b> SWOT analysis of Laser Scanning (Artec Space Spider scanner).....	26
<b>Table 2</b> SWOT analysis of photogrammetry.....	27
<b>Table 3</b> Matrix of complexity value for different materials and surfaces. ....	41
<b>Table 4</b> Complexity index of the four case studies .....	48
<b>Table 5</b> Equipment and camera setting for the four case studies. ....	62
<b>Table 6</b> Number of photos, revolutions (rows) and orientations with different optical axis inclinations around the object. ....	68



# Abstract

Virtual reality and 3D modelling are becoming increasingly popular in the field of Cultural Heritage, specifically in archiving, restoration, valorisation in virtual tourism, and educational programmes. However, the practical process of digitization might be an intricate task that requires the competence of specialised operators. This thesis highlights the need for tools that enable non-expert users working in museums to easily and effectively realize 3D replicas of artefacts with Image-based model approach. The study then documents the most significant moments of critical reflection during the 3D photogrammetric survey, to stimulate operators in identifying a model's complexity factors and suggest how to deal with them. It provides a case study of Dynamic Collections, its pedagogical and research purposes. The proposed methodology introduces a semi-automatic procedure to generate accurate 3D models from photographs, that is further implementable.

**Keywords:** digital archaeology, photogrammetry, 3D survey campaign, digital heritage, image-based modelling



# 1. Introduction

Over the centuries, the care and preservation of Cultural Heritage have undergone significant changes, driven by the continuous evolution of computational and technological sciences. While photography was traditionally responsible for preserving, presenting, and appreciating Cultural Heritage in the last century, virtual reality and 3D modelling have taken on this role today. This shift emphasizes the growing importance of these technologies in the CH field and their potential to transform how we engage with and comprehend the past.

In modern times, 3D modelling is an essential part of archiving practices, documentation, and "*preventive digital memory*" (Carlucci, 2016), especially in high-risk areas or during invasive operations such as archaeological site excavations. It's also widely used for restoration, enhancing virtual tourism experiences, and supporting educational resources. The literature demonstrates that the field of archaeology recognized the potential of blending digital and analogue methods as early as the latter half of the previous century. Thus, there is a deeper understanding of reality-based 3D modelling techniques, such as image-based and range-based rendering, and a concerted effort to enhance the Findability, Accessibility, Interoperability, and Reusability (FAIR principles) of digital assets. As a result, digital libraries of semantically annotated 3D objects are becoming increasingly popular. These collections of 3D models are stored in digital formats and enhanced with semantic information, including standardized labels and descriptions of their traits, features, and attributes, to enable easy machine searching and interpretation.

However, the integration of these technologies into the network of Italian Cultural Institutions is still an objective that cannot be considered achieved for most of these public Entities.

On the other hand, there is an urgent demand for tools enabling non-expert users to easily and effectively capture complicated reality-based 3D scenarios.

Thus, the **goals** of this thesis are twofold: firstly, to document the most significant moments of critical reflection during the 3D photogrammetric survey, which precedes mechanical steps of acquisition; and secondly, to walk alongside non-experienced operators throughout the survey to stimulate them to identify a model's complexity factors and suggest how to deal with them.

The subject and the aims of this study stem from my practical and direct encounter with Digital Archaeology and the theoretical reflections that followed. During the spring of 2022 (April-June), I had the pleasure and honour of completing my curricular internship at the Laboratoriet för Digital Arkeologi (DARK Lab), which is coordinated by Professor Nicolò Dell'Unto and is part of the Department of Archaeology and Ancient History at Lund University in Sweden.

I was involved in the Dynamic Collection project, designed in 2018 by DARK Lab in collaboration with the Visual Computing Lab of ISTI-CNR, Pisa, with the aims to develop a novel 3D web infrastructure designed to support higher education and research in archaeology. Its dataset, composed of 3D replicas of pieces from the Lund University Historical Museum, is now used in the basic level course ARKA21 of Lund University's BA degree in Archaeology, which focuses on the cultural history and material culture of the Scandinavian and European Stone and Bronze Ages.

Some artefacts were considered most suitable for photogrammetric acquisition, others for laser scanner acquisition. During my internship, I was in charge of the first instances, in collaboration with the archaeologist and Project Assistant at Lund University Domenica Dinunno.

Through a process of iterative and dynamic inquiry, a keen interest emerged to explore the diverse array of factors that can impact the course and outcomes of an acquisition campaign. These factors span a wide range, from the technical aptitude of the operator conducting the campaign, to the characteristics of the object being acquired, and ultimately to the underlying objectives and intended audience of the project. Such factors collectively shape the resolution and overall quality of the output, underscoring the complex nature of acquisition campaigns and the importance of taking a holistic approach to understanding their intricacies.

For museum collections, photogrammetric acquisition is never a closed black box which follows a single linear path and has rigid and unbreakable rules. Rather, it is the outcome of a process that questions itself at every turn and envisions embedding, piece by piece, feature by feature, of the project and the object of its interest, producing its own history.

Thus, the study follows a scalar approach, further implementable and not properly covering all possible cases: its main goal it's therefore methodological.

The thesis is organized as follows. Chapter 2 provides an overview of the current State of Art of survey technologies for museum collection and an explanation of semantic digital libraries, including what they are and the opportunities they present. Then it moves from the theoretical to the practical, describing the case study of Dynamic Collections and their pedagogical and research purpose. The design of an acquisition campaign is therefore outlined, motivating through a SWOT analysis why photogrammetry was chosen for the case study.

In Chapter 3, the first phase of the survey is defined. It is devoted to assessing the artefact to deeply understand its intrinsic and extrinsic features. This evaluation, as well as the surveying aims, such as input and output metrics, marks the equipment selection and subsequent steps. The chapter concludes with a classification of models based on a complexity index calculated from their related original artefact properties and the desired 3D resolution. Then, Chapter 4, explains the moment of instrumentation planning and camera set-up. It suggests some good practices to follow during the actual image acquisition, such as turntable rotation intervals and artefact orientations, together with

some tips on the correct functioning of cross polarisation. Finally, Chapter 5 deepens the theory behind the operation of image-based modelling software (Agisoft Metashape in the case study) and then examines some of the most popular algorithms for constructing sparse point clouds, dense point clouds, meshes and textures. The last stage of this thesis, Chapter 6, provides a design proposal for a semi-automated procedure, aimed at framing the complexity class of the model to be created and the recommended set of instrumentation and procedure. The interactive route structure was created with Twine and works with a range of cases but has the potential to be expanded and enriched in the future.

## 2. The Digital Archaeology: the context of the Dynamic Collections

### 2.1 Surveying technology and museum collections: State of Art

Similar to photography at the end of the nineteenth century, 3D modelling is now driving a revolution in Cultural Heritage recording, becoming an ever-growing area of interest in academic and cultural circles. Despite the difficulties of non-experts in creating easily good 3D models, their high "cost" and the presence of prejudice condemning 3D to being mainly an additional "aesthetic" factor (Bitelli et al., 2007), for Cultural Heritage, the encounter between the digital and analogic worlds has proven to yield exciting results in many different sectors. From the archiving practice to documentation and, in cases of loss or damage (i.e. in high-risk areas and or during invasive operation, such as archaeological site excavations), the creation of a "*preventive digital memory*", which is very similar to preventive conservation (Carlucci, 2016); from restoration to valorization, but also in education resources and virtual tourism. In the last decades many steps forward have been made, a huge amount of literature has already been published on the topic (Marín-Buzón et al., 2021). Techniques have been perfected and although excellent 3D scanners are still beyond the usual small museum and conservation institute's budget, they are spreading in shape and size and the costs of tools and hardware have largely even off, making high-level technical equipment more affordable to people who wish to invest in it (Apollonio et al., 2021; Caine and Magen, 2017, 2). 3D digitization is currently applicable to artefacts ranging in size from the tiniest (De Paolis et al., 2020) to the largest, assisting scholars by giving greater resolution (sampling surface density) and enhanced accuracy.

3D models can also be created by the means of 3D modelling software (i.e., Maya, 3D Studio Max, Blender, etc.). Such tools enable, with varying degrees of approximation, three-dimensional modelling, and digital visual representation not only for project simulation but also for real world items. Their use, however, requires, as for IMB or ranging methods, extensive training, and longer time (Nguyen et al, 2012).

On the other hand, urgent demand for tools enabling non-expert users to simply and effectively capture complicated 3D scenarios lead to a variety of image-based modelling (IBM) software and ranging systems, providing a simple way to capture reality-based 3D models. This chapter therefore aims at categorizing *reality-based modelling* in order to finalize 3D deliverables into an interactive Real Time Rendering (RTR) application, designed to host models and metadata for visualization.

Thus, according to the most general categorization of 3D object measurement we'll deal with *non-contact methods*, implementing active or passive sensors (i.e. laser scanner, photogrammetry), rather than *contact systems* (i.e., coordinate measuring devices, calipers, rulers, bearings) (Remondino et al, 2006). Before delving into our issue, it is essential to draw distinctions between various surveying approaches. Nowadays, three techniques of documenting, preservation, and visualization of cultural heritage sites and artefacts may be distinguished: range-based methods, image-based approaches, and a mix of the two them, when no one method can meet all recording needs at the same time (Talha and Fritsch, 2019; Remondino and El-Hakim, 2006; Bitelli et al., 2007, 2; Caine and Magen, 2017; Bourke, 2016; Grassi et al., 2022; Koutsoudis et al., 2013).

In this regard, it's worth mentioning another visualization technique: the Image-based rendering (IBR). This method generates innovative perspectives and virtual views of 3D worlds straight from input pictures, without entailing the creation of a geometric 3D model. This is the reason why its application covers an intriguing area in virtual reality and interactive photo-realistic experiences, but it is less suitable for artefacts or architectural structure than other techniques (Szeliski, 2011).

The literature is replete with comparative analysis involving various tangible heritage objects, but there is no obvious winner or a single solution for all circumstances (Remondino et al., 2006, 272). Each technology has a role to play, as well as relative benefits and drawbacks. Heritage institutions may and should embrace all three while scientifically assessing their success in their unique setting and requirements (Caine and Magen, 2017).

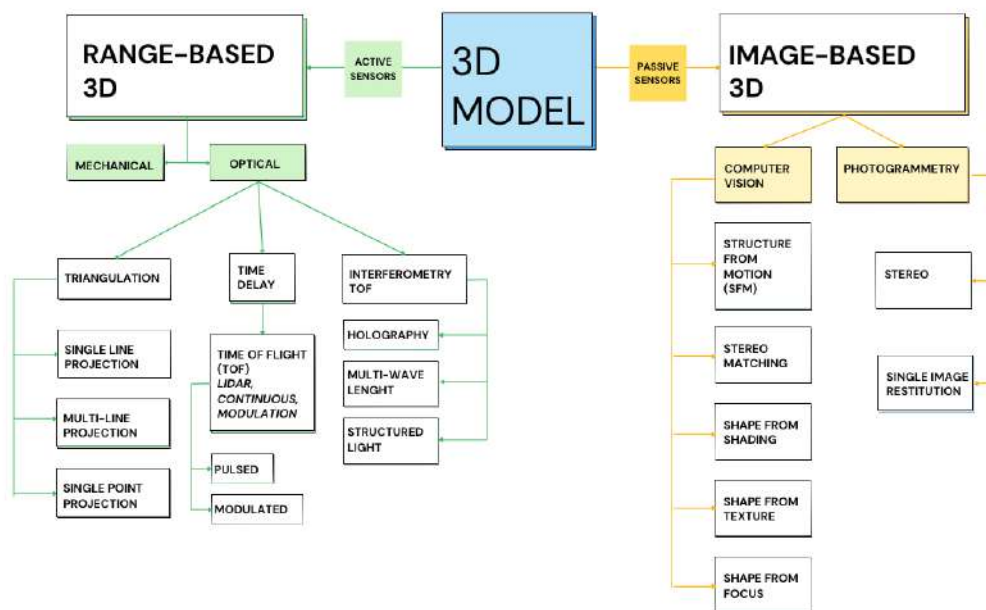


**Figure 1** Taxonomy of 3D modelling techniques (Remondino and El-Hakim, 2006; Talha et al., 2019).

### 1) *Range-based modelling*

This approach, based on laser radiation or pattern projection and so named for its usage of ranges (intervals) of values, directly captures an object's 3D geometric features (Talha and Fritsch, 2019; Remondino and El-Hakim, 2006). Active sensors also depend on surface typology and operational conditions (Caine and Magen, 2017; Bourke, 2016; Remondino and El-Hakim, 2006). Various breakthroughs have been achieved in the last 25 years, making many solutions available to the market: Structure light scanner (SLS), *triangulation scanner*, Terrestrial laser scanner (TLS), based on time of flight or phase interference etc.

As (Blais, 2004) recalls in his review about 20 years of range sensors, the notion of triangulation-based range measuring is millennia old, having been proved by the Greeks for navigation and astronomy. Even during the two world wars, the military made extensive use of passive optical range finders. It was in the early 1980s that CCD (charge-coupled device) arrays were introduced and at the end of the decade, low-cost laser diodes replaced the need for gas lasers, allowing the development of very tiny sensor heads.

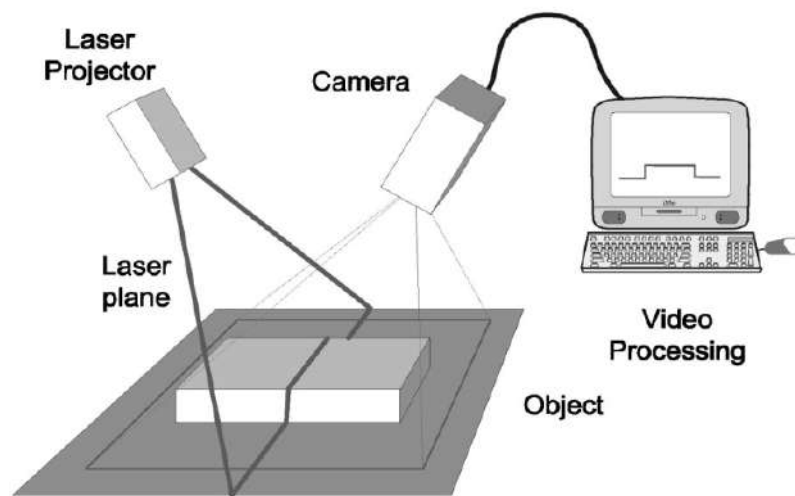


**Figure 2** Laser triangulation range finding.

The majority among today's systems are just focused on 3D geometry acquisition, providing often only an intensity value for each given range or, most of the time, a very poor RGB texture (Caine and Magel, 2017, 6). In the former case, the scanner, using a frame camera, captures pixel color information, stored as RGB attribute to the point cloud, and, as for handheld models, some provide color per vertex and UV atlas.

This method, nevertheless, may not yield the greatest results since the optimal conditions for capturing the photos may not match with those for scanning (Caine and Magel, 2017; Morena et al.,



2019). As a result, textures produced from different high-resolution color digital cameras are frequently used to create higher-level realistic 3D models (De Paolis et al., 2020; Polo et al., 2022). Performing the data acquisition phase of the intended object with a single scan is impractical in most circumstances. Due to item size, shape, and occlusions, as well as scanner accuracy, it is frequently essential to make multiple scans from various positions to capture any aspect of the object. It is not difficult to guess that the alignment and integration of these scans, as it corresponds to a further manipulation step of the data, involves other possible errors, and might impact the final accuracy of the 3D model (Morena et al., 2019). Furthermore, long-range sensors frequently have edge issues, resulting in mistakes or smoothing effects (Koutsoudis et al., 2013). Range-based approaches, on the other hand, may offer precise and comprehensive features with a high degree of automation for tiny and medium-sized objects (approximately the size of a human or a statue) (Talha and Fritsch, 2019).

## 2) *Image-based modelling* (IBM)

IBM is a method enabling the generation of 3D coordinates from a set of 2D images from numerous viewpoints using a mathematical model (Elkhrachy, 2022). It is founded, indeed, on the premise that, whereas a single photograph may only offer two-dimensional coordinates, height and width (X-Y), two overlapping photographs of the same scene taken slightly apart from each other can yield the third dimension (Z) via triangulation (Caine and Magen, 2017, 3). Digital photogrammetric surveys are, indeed, frequently used in archaeology to create three-dimensional assets of artefacts, as well as landscape and architectural features, due to their ability to perform the analysis at a low cost (Gonizzi Barsanti et al., 2014) and without contact with the object.

Close-range photogrammetry (CRP) is among the most commonly observed forms of this technique in archaeological research (Marn-Buzón, 2021, 15), though it was not until years later, in 2000, that the use of close-range photogrammetry demonstrated its use in virtual reality and integration into archaeology (Addison and Gaiani, 2000). Close-range photogrammetry can refer to a variety of close-distance measurements. Indeed, it has no image acquisition limitations, whereas the existence of surrounding buildings or other impediments in the urban environment frequently limits capturing photographs from random points of view around the item of interest (De Paolis et al., 2020, 376).

Photogrammetry makes use of the Structure from Motion (SfM) method (Xu et al. 2022; Rahaman and Champion, 2019; Remondino et al., 2017; Nocerino et al., 2017; Koutsoudis et al., 2013; Nguyen et al., 2012; Remondino and El-Hakim, 2006) and the Multi View Stereo (MVS) algorithm (Apollonio et al., 2021; Collins et al., 2019; Furukawa and Ponce, 2010). Following the initial phase of camera calibration, the Structure from Motion method correctly places the photos in a 3D space, using a geometric reconstruction algorithm that matches identical feature points (patterns of pixels

recognizable by the computer) in two or more pictures (Remondino and El-Hakim, 2006). This step produces camera location data using a sparse point cloud. Thus, the MVS method inherits the result of SfM and allows a pixel in an image to create a 3D optic ray that goes through the pixel and the photo's camera centre. The comparable pixel on another picture can only be found on the optic ray's projection onto the second image. By repeating this technique on all pixels in each image, depth maps may be generated, resulting in a dense point cloud (“Photogrammetry: the technology behind the magic”).

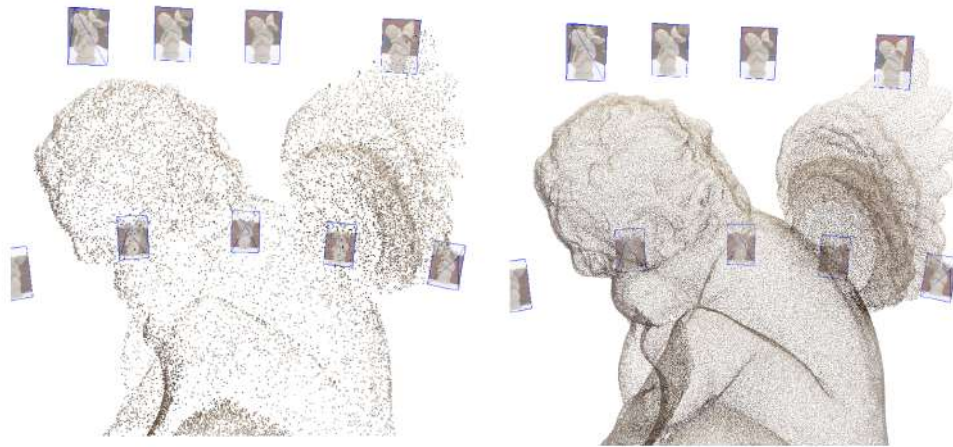


**Figure 3** Output of SfM (left) and MVS (right) algorithms (“Photogrammetry: the technology behind the magic”).

Over the last few years, the key advances in the automated pipeline have actually been in SfM and MVS algorithms (Xu et al., 2022; Collins et al., 2019; Remondino et al., 2017): scalable tie point retrieval, large-scale bundle correction, and dense point cloud production. The workflow then ends with mesh generation and texture production (Apollonio et al., 2021; Bolognesi and Fiorillo, 2018). So, back to the core point, IBM sensors can be extremely portable and usually affordable (Rahaman and Champion, 2019; Koutsoudis et al., 2013, 4455). Furthermore, with the introduction of high-megapixel mobile-phone cameras in the 2010s, despite their differences from SLR cameras (Collins et al., 2019), digital cameras on smartphones began to be employed as imaging tools in photogrammetric applications high-quality SLR lenses and acquisition sensors are also being replaced by compact, affordable hardware that has been enhanced by software (Apollonio et al., 2021). This technology advances rapidly year after year, attaining levels of picture resolution, color accuracy and sharpness, that are comparable, but not identical, to SLR cameras. The advantages afforded by this low-cost option can, of course, be accompanied by certain drawbacks (i.e. geometric distortion, high noise, lens shading and light scattering). They can, at least, be much improved, as seen by the results of image denoise (Apollonio et al., 2021). Nowadays, it is therefore possible to generate satisfactory

3D textured models, containing all the details required for a precise documentation of the find, in digital form utilizing cheap digital cameras and photographs obtained by non-expert surveyors (Bedford et al., 2017; Bitelli et al., 2007).

### 3) *Combination of range-based and image-based modelling*

Another popular option is to combine these two procedures (Polo et al., 2022; Talha and Fritsch, 2019; Remondino and El-Hakim, 2006). In many cases, indeed, a single modelling technique does not meet all of the project needs: photogrammetry and laser scanner have been coupled in particular for sophisticated or massive architectural items, when no approach alone can generate a full and accurate model in a rapid and efficient way (Fiorillo et al., 2021). The advantage of an integrated approach is that it allows to exploit the potential of both techniques to obtain the best completeness and quality of the resulting representations. On the other hand, the disadvantage is the complexity of the procedure to integrate active and passive sensor data and the more complex definition of an efficient workflow (Fiorillo et al., 2021). Consider data gathering with a LiDAR technique, then add the time it takes to acquire all of the required images to create the model with the required information. For an artefact in a museum collection, for example, with simple geometry but a challenging texture, it may be worthwhile to extract the forms and surface using a scanner and export the texture details with high-quality lens sensors (Caroti et al., 2015; Polo et al., 2022). The traditional method for obtaining textures from photos is to derive camera orientation parameters from a single take, generate the UV map using texture mapping of the single-frame model's projection (Apollonio et al., 2010; Baldissini et al., 2010; Guidi et al., 2010), and finally merge the various partial UV maps to generate the texture of the model as a whole. Textures obtained in this manner enable the creation of high-quality 3D models in terms of geometric, morphological, and chromatic characteristics (Fantini et al., 2012). However, this technique is time-consuming and requires regular operator intervention in the collimation of points on the model and photographs (Caroti et al., 2015).

## 2.2 Digital libraries of semantically annotated 3D objects

Archaeologists, restorers and museum curators have the unique privilege of handling objects that almost all people will only see in the display window of a museum or, at a considerable distance, in reported images (whether in books or, increasingly, on internet); indeed, a significant portion of archaeological material is strongly, and often forever, out of field of vision in museum storage (Dudley, 2010). For everyone, from academics and students to a larger interested audience, the emergence of 3D technology for producing both digital and printed models have already enabled new types of encounters with places and objects (an example in the domain of archaeology, Di Giuseppantonio Di Franco et al. 2012). 3D models offer the significant advantage of bridging the gap between cultural heritage and its users (Di Giuseppantonio Di Franco et al., 2015), and museums and research institutions seem to have realised this potential (Eros and Bornaz, 2017).

The wider way to simply access data, as well as dynamically interacting with it, through 3D object manipulation (with rotation, zoom, application of different lighting effects) and even personal replication, with 3D printing, is a matter of knowledge democratisation (Di Giuseppantonio Di Franco et al., 2015). One famous example comes from the popular online platform Sketchfab<sup>1</sup> (Ekengren et al., 2021), which hosts 3D models generated by the work of individuals as well as major institutions like the Kunsthistorisches Museum Wien, the British Museum and Faculty of Archaeology University of Warsaw. They are progressively providing full access to interactive digital models from their collections. Even private no profit organization for research and education, such as CyArk<sup>2</sup>, Global Digital Heritage (GDH)<sup>3</sup> and ARC/K<sup>4</sup> rely on Sketchfab platform.

In reference to Italian scenario, instead, a noteworthy project is the 3D Virtual Museum<sup>5</sup>, a web portal hosting 3D models of art pieces from Italian museums, created by Giulio Bigliardi, the founder of 3D ArcheoLab, a company specializing in 3D technology for Cultural Heritage preservation. The project is a collaborative initiative where the end user can both utilize the service and contribute to it. The platform brings together various 3D collections and locations and makes them accessible through Sketchfab.

---

<sup>1</sup> Sketchfab, <https://sketchfab.com/>

<sup>2</sup> CyArk, <https://cyark.org/>

<sup>3</sup> Global Digital Heritage, <https://globaldigitalheritage.org/>

<sup>4</sup> ARC/K, <https://arck-project.org/>

<sup>5</sup> 3D Virtual Museum, <http://www.3d-virtualmuseum.it/>



**Figure 4** Homepage of 3D Virtual Museum.

Sketchfab, on the other hand, is utilized primarily for display and is constrained to the single-object browsing paradigm, limiting support for more sophisticated engagement. Besides the author's name, model name, and online upload date, there's no obligation to provide metadata and acquisition process information in a machine-readable format. Accredited cultural institutions, as those mentioned above, often include annotations and scientifically document their models' characteristics (Fig. 5, on the left), but Sketchfab has also uncertified productions that lack proper sourcing and methodology (Fig. 5, on the right). While this vast and accessible knowledge has its benefits, it's also challenging to verify, presenting both strengths and weaknesses.

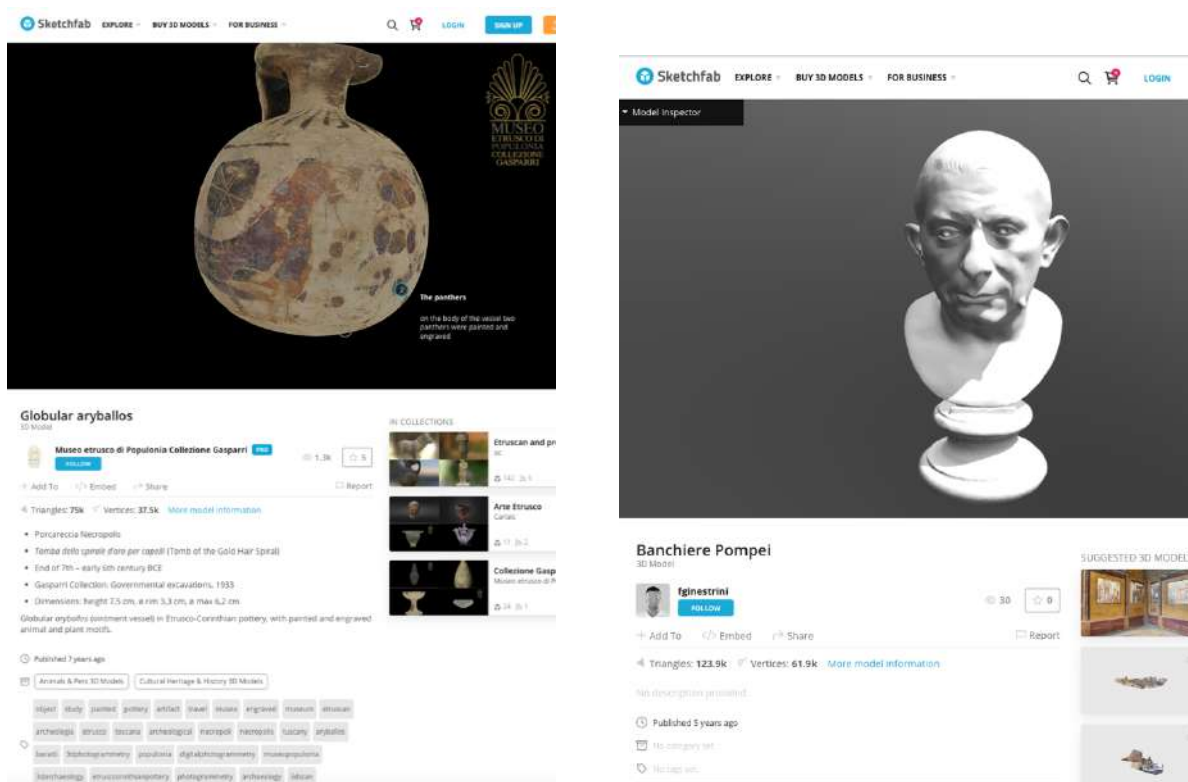


**Figure 5** Examples of two 3D objects on Sketchfab: a globular aryballos published by *Museo etrusco di Populonia - Collezione Gasparri* - (on the left), and a bust statue from Pompei by a user called *fginestrini* (on the right).

The use of commercial platforms (such as Google, Sketchfab etc.) to publish digitised cultural heritage materials risks sacrificing some of their potential as public and social information carriers in favour of their market value (Ekengren et al., 2021). These applications, anyway, revealed the impact of technology on the archaeological field, in its double value of "tool" (or even "digital toy") to be passively deployed or as a "medium," a "science," capable of affecting interpretation and research orientation (Morris et al., 2018).

In this regard, this latter point requires further observation: when one aspires to accurate and scientific knowledge, the mere manipulation and observation of the virtual replica may be not enough (Ekengren et al., 2021). This is where one of the substantial differences between a commercial platform such as Sketchfab and a digital library managed by a public cultural organization arises: the type and quality of knowledge and documentation to be transmitted through 3D models. When visual data, such as the 3D models of artefacts, are enhanced with standardized descriptions and linked to reliable sources, users can have a richer experience and deeper understanding of the project, leading to a more effective utilization of the provided data (Mi and Pollock 2018, 285). Moreover, since digital cultural heritage initiatives frequently entail interdisciplinary partnerships, they need interoperability and the usage of common languages and systems (Mi and Pollock 2018).

Therefore, a digital library of semantically annotated 3D objects is a collection of 3D models kept in digital format and described with semantic information, such as labels and descriptions about their traits, features, and attributes, to make them searchable and interpretable.

Moreover, there are also semantic enrichment processes involving machine-understandable terms derived from an ontology (or set of ontologies), which aid in categorizing and describing objects in a standardized manner, allowing for advanced searching, and indexing capabilities and making it easier to understand the context and meaning of the objects (Yu, 2014). In addition to improving interoperability and quality control, ontology-based annotations are useful because they enable new knowledge, reasoning and inference, as well as linking 3D digital objects to the wider Semantic Web and Linked Data cloud (Yu and Hunter, 2013).

In the Cultural Heritage area, this element has significant promise for autonomously inferring high-level descriptive information and reasoning about the origin and authenticity of museum objects (Yu and Hunter, 2013). Thus, 3D artefacts intended to be effectively used by a large community must adhere to the FAIR principles, so being Findable, Accessible, Interoperable, and Reusable (FAIR Principles; Wilkinson et al., 2016).

Europeana<sup>6</sup> is an excellent example of how to adopt FAIR principles. As Europe's digital library for Cultural Heritage, it has become a flourishing reality, fostering the formation of a robust network of EU national and thematic aggregators (Pritchard et al., 2022). It has also brought together a diverse, multidisciplinary community of professionals and technical experts in the field of Cultural Heritage to drive innovation, collaboration, and the creation of new digital multimedia content. Today it disposes of a dataset of 5889 3D models.

**Figure 6** Collage of a 3D models with the related metadata available in Europeana.

<sup>6</sup> Europeana, <https://www.europeana.eu/en>

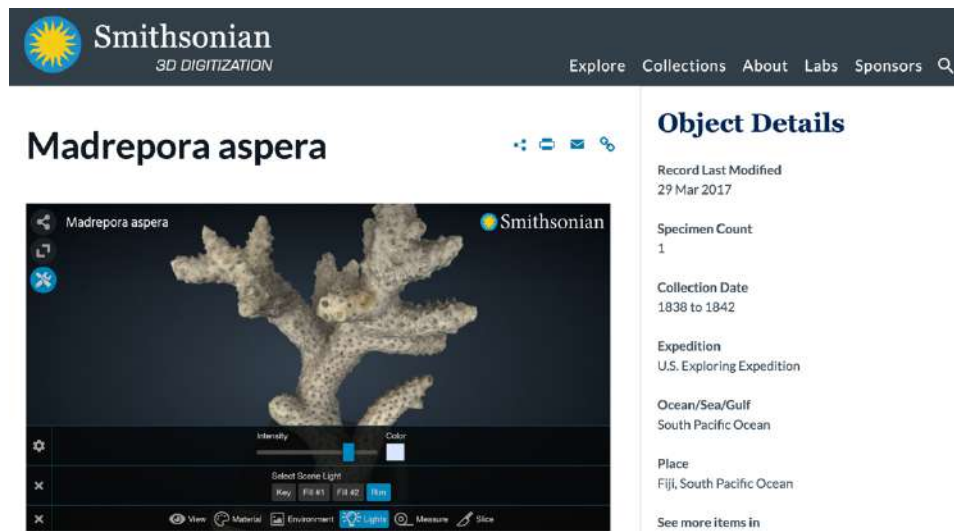


**Figure 7** Visualisation of a 3D model within its metadata (on the left) in Smithsonian platform.

Nevertheless, some argue that much more can and must be done to conform with this worldwide trend (Amico et al., 2013; Börjesson et al., 2020). Indeed, although pictures and visualizations have a significant influence on (pre-)historical knowledge (Börjesson et al., 2020), many archaeological visualizations, whether 3D models (Champion, 2018) or other visual objects, are still lacking in both descriptive data about the process (Piccoli, 2017). Research emphasizes the parallel importance of documenting how these information objects were created (Börjesson et al., 2020). Indeed, the rapid development and proliferation of new digital methods underscores the need to document not only the results, but also the logic behind them and the processes employed (Edmond and Morselli, 2020). Paradata can assist to comprehend what was done and how it was done, make projects and their outputs sustainable (Edmond and Morselli, 2020), and validate hypotheses and the authenticity of models (Kastanis, 2019).

The Dynamic Collections (Callieri, 2020), which will be further explored in the following chapters, is among the projects that aim to respect these principles, overcoming cultural, environmental and management barriers for their information to be easily and widely disseminated (Ekengren et al., 2021). The project, indeed, assists to the following three parts of the process of creation:

- 1) 3D artefact generation
- 2) Metadata and paradata implementation
- 3) Development (or adoption) of a visualization system used for presenting the data (Ekengren et al., 2021).



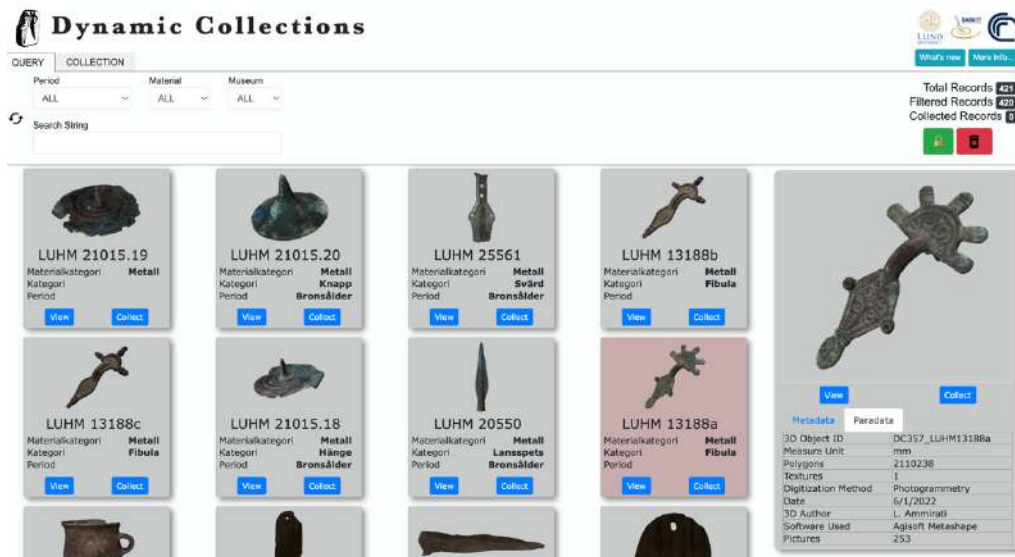


**Figure 8** Example of a window (on the right) with metadata and paradata (written in Swedish) for an artefact chosen from the entire collection.

To conclude, it is also worth clarifying the existence of several forms of semantic annotations. To the standardized attribution of metadata and paradata descriptions of 3D artefacts, (Ponchio et al., 2020) also adds:

- *Semantic segmentation* (see Fig. 9), in which a functional subset or structural subdivision in sections is specified over a given form. Metadata can be defined for each of its sub-components.

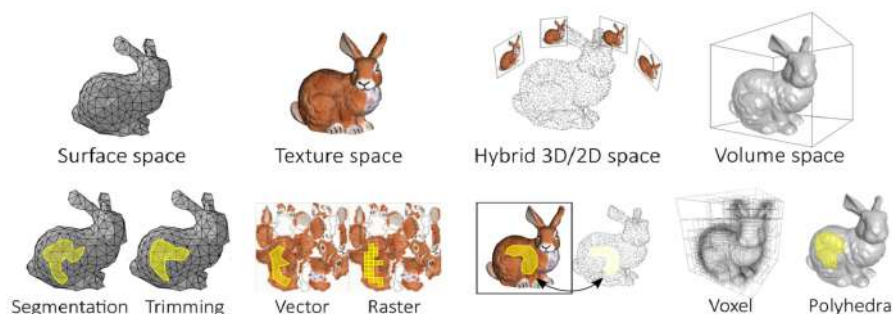


**Figure 9** A graphic representation of the different annotation approaches (Ponchio et al., 2020)

- *User-driven characterization*<sup>8</sup>, in which each annotated region is selected based on a specific user request or insight (e.g., a small region affected by some degradation process) and is linked to some metadata or to some descriptions. In this situation, most programmes provide a user-driven selection mechanism, because the identification of such locations and the accompanying data frequently rely on the expertise of a human expert and/or are the results of a visual examination.

<sup>8</sup> In the 2.3.2. *The educational purpose*, a practical example related to Dynamic Collections will provide.

## 2.3 The design of a survey campaign

### 2.3.1 Dynamic Collections

In 2018, to explore the potential of the impact of technology on archaeological interpretation and research orientation, the University of Lund, Sweden, in collaboration with the Visual Computing Lab of ISTI-CNR, Pisa, developed the project of Dynamic Collections<sup>9</sup> (Ekengren et al., 2021). DARK Lab handled the programme, which was inspired by the purpose of promoting and encouraging higher education and research in archaeology. The system would enable teachers, students, and researchers:

- to browse through the catalogue of 3D artefacts kept on the Lund University server, organized in chronological order as well as grouped based on material, form, technical elements;
- to connect directly and compare meta- and paradata associated with the 3D objects;
- to select objects, results of specific queries, and to create with them a personal collection, which can be downloaded on a personal computer;
- to customise the collection and its objects, adding notes and descriptions to them;
- to engage with the 3D items through several tools available through the online visualisation system of 3DHOP<sup>10</sup>, that enable a high-level of interaction and analysis (Ekengren et al., 2021, 338).

The artefacts selected are on permanent loan from Lund University's Historical Museum and belong to the Scandinavian Stone and Bronze Ages and kept in the research collection at Lund's Department of Archaeology and Ancient History. The dataset is constantly expanding and during the starting two years, many tests have been conducted to determine which data acquisition strategy, between Range-based Modelling (RBM) and Image-based Modelling (IBM), would be most suited in each case. The DARK Lab team's equipment includes an Artec Space Spider scanner and an Artec Eva Scanner for large artefacts, as well as a Canon EOS 6D Mark II DSLR camera with a variety of zoom lenses. The scanner was linked to a laptop running Artec Studio 14, which was used to observe the scanning process in real time and then for the majority of the scan processing, whereas the photogrammetric

---

<sup>9</sup> Dynamic Collections, [https://models.darklab.lu.se/dynmcoll/Dynamic\\_Collections/](https://models.darklab.lu.se/dynmcoll/Dynamic_Collections/)

<sup>10</sup> 3DHOP is a package of tools and templates developed by Visual Computing Lab del ISTI – CNR di Pisa and released under the GPL licence so that it can be installed on any server and create customised 3D galleries (Potenziani et al., 2015)

processing is done in the software Agisoft Metashape<sup>11</sup> Professional, version 1.5.2, and occasionally MeshLab<sup>12</sup>, for the final editing of the surfaces (Ekengren et al., 2021, 340).

The first acquisition campaign had the primary aims of populating the archive and evaluating the system's functionality. However, the advent of the COVID-19 epidemic turned the plans up, forcing DARK Lab to speed the procedure up to face the upcoming online lessons. Time therefore has been a variable that has marked the team choices. And hence the choice of focusing on covering a wide range of items rather than relying on fewer but more accurate models. Difficult materials and surfaces of some artefacts played a role in driving the team to evaluate the acquisition techniques. Typically, the most important aspects to consider are the size and form of the item, as well as the reflecting characteristics of light on its surface (whether it is opaque, glossy or translucent) (De Paolis et al., 2020, 378). An issue, for instance, has been colour fidelity (Battini, 2015): the texture created by the scanner was frequently insufficiently detailed and the web rendering is not designed to provide proper colour control. However, during the acquisition campaign in which I contributed (April/June 2020), the major difficulties were caused by reflecting materials and small sizes.

Certain material types afflict indeed both approaches. With shiny surfaces, basic image-based modelling fails because the feature point stage identifies features inside reflections, resulting in an inaccurate depth computation, but due to the technique being based on reflected light, laser scanning was not optimal as well (Bourke, 2016). Moreover, experiments and tests conducted in advance and reported in literature have confirmed that scanner results are highly reliant on material properties. Because the laser is reflected in various directions, shiny, translucent, and reflective materials such as marble, gold leaf, or gemstones were almost hard to record with active scanning (Bourke, 2016; Caine and Magen, 2017). Finally, photogrammetry's flexibility in terms of range, using lenses and equipment, such as polarized lenses and lights, prevailed. For this reason, starting with the following chapter, the core focus will exclusively be on close-range photogrammetry.

The motivations behind this direction also emerged from the following SWOT analyses for the use of laser scanning and photogrammetry respectively.

---

<sup>11</sup> Agisoft Metashape, <https://www.agisoft.com/>

<sup>12</sup> MeshLab, <https://www.meshlab.net/>

	Positive	Negative
I n t e r n a t i o n a l	<b>Strengths</b> <p>S1: Ambient light does not alter the result.</p> <p>S2: Rapid data capture. If the operator has good manual skills and expertise with the equipment, he or she can capture many artefacts in a matter of hours.</p> <p>S3: During the acquisition, possibility to get quick feedback from the software on the future result, although the alignment phase is not yet underway.</p> <p>S4: For medium size objects, it produces excellent results in terms of the geometry</p>	<b>Weaknesses</b> <p>W1: For acquisition in external, tool difficult to carry and problematic with natural light. .</p> <p>W3: Complex objects need many scanning positions and field efforts.</p> <p>W4: Missing data in correspondence with occlusions or shadows. During the acquisition phase, detecting the connection areas between the artefact's inner and exterior surfaces can be challenging (i.e., the mouth of a pot).</p> <p>W5: Limited range and measurement volume.</p> <p>W6: Inadequate for reconstructing minute features, smooth edges, or break lines, making them unsuitable for extremely small objects.</p> <p>W7: Inadequate for shiny surfaces.</p> <p>W8: In some cases, minimally sophisticated textures.</p>
E x t e r n a l	<b>Opportunities</b> <p>O1: Production software: Depends on qualified commercial and technical people</p> <p>O2: Depending on the operator and the process of manufacturing, the performance of a laser scanner can be higher or lower and more or less time efficient.</p> <p>O3: Data merging from several sensors leads to the possibility of new products.</p>	<b>Threats</b> <p>T1: More care should be taken in the scanner's setup.</p> <p>T2: Heavy device, which requires dexterity and strength in the operator's arms. This aspect has an impact on the scanning time and so on the number of scans produced for each object.</p> <p>T3: The usage of a laser source poses a safety risk (use of protective lenses is recommended).</p> <p>T4: The preset performance cannot be changed and improved, as digital cameras can do with different lens and lights.</p>

**Table 1** SWOT analysis of Laser Scanning (Artec Space Spider scanner)

	Positive	Negative
I n t e r n a t i o n a l	<b>Strengths</b>  S1: Generally simple to use and affordable. S2: Lightweight and easy to handle equipment, ideal for acquisition in external. S3: Flexible in terms of range using lens. With the equipment of a standard lens (i.e. 50 mm), a macro lens, polar filters a wide range of objects can be covered. S4: High accuracy, especially about textures. S5: With the proper safeguards taken during camera acquisition (such as using a matte black background to minimize shadows, etc.), the subsequent work with the software is simplified to a few easy steps. S6: Open-source drivers and software are available.	<b>Weaknesses</b>  W1: Difficulties in case of limited texture. W2: Large objects lead to larger post processing efforts and require more high-resolution imagery. W3: It may take several attempts to shoot complicated geometries before finding the ideal combination of pictures that covers the full surface of the item and is accurately matched during the alignment step. In many circumstances, the acquisition process might be long. W4: To get the appropriate exposure with a macro lens and a polarized filter on a shiny object, the operator may need to use a prolonged shutter time and thus face a long-lasting acquisition campaign.
E x t e r n a l	<b>Opportunities</b>  O1: Requires a good knowledge of the camera device, but not too specific skills. O2: Given the ease of training the equipment and method, it is highly adapted to include new operators (e.g., Archaeology students) who may occasionally contribute to the project, allowing it to progress. O3: Ample room for improvements to make software algorithms and computation hardware more efficient.	<b>Threats</b>  T1: Lack of feedback about the acquired data, till the alignment phase. T2: The absence of scale information requires additional manual work; in some case, for reasons of accuracy, it needs a second data acquisition. T3: Depending on the performance of the computer device, software can be very slow in the computing of dense clouds and mesh. T4: Not always reliable if automated modality is used, especially at large scales.

**Table 2** SWOT analysis of photogrammetry

For the acquisition campaign of June 2022, a set of heterogeneous artefacts were chosen from the Historical Museum at Lund University (i.e., the largest museum for archaeological finds, coins, and mediaeval church art in southern Sweden), hosted inside their storage in Gastelyckan. Among several pieces, I chose to describe four of them as case studies due to their variety and representativeness. The brief categorization is followed, where available, by a metadata description of the object by Fredrik Ekengren.

1. **LUHM13188c**<sup>13</sup>: Fibula, Bronze Age, bounding box = **40x77x14mm**, highly reflective surface, (Fig. 10 a).
2. **LUHM21015.20**<sup>14</sup>: Metal conical tutulus, Bronze Age, bounding box = **42x21x41mm**, highly specular skin and tiny details. Category of buttons (*knapp* in Swedish). Found in Skane (Fig. 10 b).

*Bronze tutulus with a conical centre section, decorated with concentric circles in the form of closely spaced ribs and finished with a short, undecorated pik.*

3. **LUHM25561**<sup>15</sup>: Sword, Bronze Age, bounding box = **49x8x131mm**, non-homogeneous material (made by metal and legacy of copper), lateral side very thin. Found in Normandie (Fig. 10 c).

*The grip for a bronze grab handlebar, with a wide grip tab with raised edges. The tongue ends with extended tips, one of which is broken. The shoulder of the shutter is sloping. Both the grab tab and the shoulders are equipped with rivet holes. The sheet is missing.*

4. **LUHM32125.81**<sup>16</sup>: Pottery vessel, (Late Roman) Iron Age, bounding box = **156x116x130mm**, quite damaged, dark material. Found in Skane. (Fig. 10 d).

*Low abdomen and curved orifice duck vessels. The Hanken is attached to the neck and the transition between the shoulder and the abdomen. Decorated with carved ornaments on the lower half of the neck in the form of angular bands and horizontal lines. The handle is adorned with vertical lines and two rows of small, pressed-in pits. Parts of the vessel are reconstructed.*

<sup>13</sup> [https://models.darklab.lu.se/dynmcoll/Dynamic\\_Collections/single\\_viewer.html?obj=DC354\\_LUHM13188c](https://models.darklab.lu.se/dynmcoll/Dynamic_Collections/single_viewer.html?obj=DC354_LUHM13188c)

<sup>14</sup> [https://models.darklab.lu.se/dynmcoll/Dynamic\\_Collections/single\\_viewer.html?obj=DC351\\_LUHM21015.20](https://models.darklab.lu.se/dynmcoll/Dynamic_Collections/single_viewer.html?obj=DC351_LUHM21015.20)

<sup>15</sup> [https://models.darklab.lu.se/dynmcoll/Dynamic\\_Collections/single\\_viewer.html?obj=DC352\\_LUHM25561](https://models.darklab.lu.se/dynmcoll/Dynamic_Collections/single_viewer.html?obj=DC352_LUHM25561)

<sup>16</sup> [https://models.darklab.lu.se/dynmcoll/Dynamic\\_Collections/single\\_viewer.html?obj=DC358\\_LUHM32125.81](https://models.darklab.lu.se/dynmcoll/Dynamic_Collections/single_viewer.html?obj=DC358_LUHM32125.81)



a)



b)



c)



d)

**Figure 10** Artefacts from the campaign acquisition of June 2022 (Dynamic Collections).

### 2.3.2 The educational purpose

Before embarking on a 3D survey campaign, the objectives and scope must be carefully considered, as the end result may be directly related to them (De Paolis et al., 2020). As (Dell’Unto, 2018, 25) suggests, the order of steps in a 3D survey campaign should follow this general rule:

1. to undertake an accurate assessment of the artefact to be modelled or acquired;
2. to analyse the characteristics that define the object (e.g. geometry, materials, colours);
3. to **establish (before acquisition or modelling) how the model will be employed once generated;**
4. to evaluate all sources available to
5. determine the best modelling techniques and/or acquiring equipment to employ;
6. to embrace a specific proper language for documenting the interpretation.

Depending on the Level of Detail (LoD) and purposes, (Apollonio et al., 2021, 5) suggested a differentiation between “*master model*” and “*derived model*”. The first typology is intended for professional usage and provides the finest quality reproduction of the original object in terms of spatial and color information contents. It is the case of photogrammetric acquisitions in an archaeological or museum environment that might have documentary or divulgation significance (different to the commercial advertising purpose), in support of scientific study, archiving, and restoration (De Paolis et al., 2020, 377). On the other hand, the models of the second category are useful for museum visitors or for inventory purposes in a web application. These replicas have a reduced resolution and various characteristics, particularly in terms of the components.

The evolution of Dynamic Collections databases experienced both these types of replicas. In the paragraph above (2.3.1 *Dynamic Collections*), I mentioned one of the main goals for the first acquisition campaign, such as to start populating the repository with the whole study collection at the department<sup>17</sup> (leaving open the possibility of extending it with more specimens from local museums and surrounding colleges) and evaluate the system's functionality.

« The onset of the COVID-19 pandemic, however, forced us to accelerate the process in order to provide objects for the necessary online classes. For these reasons, we focused on covering a wide variety of objects instead of concentrating on fewer, but more accurate, models. When

---

<sup>17</sup> Department of Archaeology and Ancient History, Lund University, Sweden.



evaluating the produced models, we found problems with some of the objects, especially caused by challenging materials and surfaces. » (Ekengren et al., 2021, 342)

Furthermore, once uploaded the first 300 models, the project entered a second phase, where “*derived models*” began to be replaced by new “*master models*”. To date, the educational and research goals remain central. In this latter case, according to the research team (Ekengren et al., 2021, 341), one crucial aim is to identify possible issues with gathering data for certain types of archaeological materials (for example, artefacts with thin edges or shiny surfaces) and then build specific procedures and workflows for these materials. The camera settings, for example, change depending on the classification of artefacts, their composition and surface properties, whilst the number of scans is determined mostly by the size of the item and the richness of the geometry. All of this information, retrievable in the objects’ metadata and paradata section, about the intrinsic and extrinsic features of artefacts was the focus of my work during the Internship and also the main focus of the following chapters.

Nevertheless, the core of the Dynamic Collections project is its implementation in teaching. While (Hermon, 2008) argued that at the turn of the millennium, studies on virtual archaeology were overly focused on computer graphics innovations and not enough on their potential use in supporting the interpretation process, today's literature devotes ample space to the theme, beginning with its functionality and progressing through the educational field (Lock, 2006; Alugo and Velasques De Velasco, 2007; Agbe-Davies et al., 2014; Noblet et al., 2019; Derudas and Berggren, 2021; Arias et al., 2022).

Thus, the Dynamic Collections dataset is used in the basic level course ARKA21 of Lund University's BA degree in Archaeology<sup>18</sup>, which focuses on the cultural history and material culture of the Scandinavian and European Stone and Bronze Ages. An integral part is devoted to artefact training and the examination method includes a written dissertation and an artefact exam. Far from the *educational atomism* of the Instruction Paradigm (Barr and Tagg, 1995), the adopted learning method goes in the direction of *object-based* and practical learning (Chatterjee et al., 2015). During the pandemic and distance learning mode, professors still intended to keep this aspect of the course, replacing face-to-face sessions in the laboratory with taped lectures and tutorials on Canvas - the online educational platform adopted by Lund University- and the online 3DHOP models (Potenziani et al., 2015). The Dynamic Collections platform was tested as a pedagogic tool for the first time on this occasion. The result of the ARKA21 for the artefact exam session spring/summer 2020 was better than previous ones: more students passed it at the first attempt (Ekengren et al., 2021). The

---

<sup>18</sup> *Archaeology: Level 2 | The joint faculties of humanities and theology.* Humanistiska och teologiska fakulteterna. <https://www.ht.lu.se/en/course/ARKA22/VT2016/>

hypothetical reasons for this success are several (such as the lower amount of stress for a remote mode, greater confidence in university exams during the second semester of the year), but the change of tool and modality must have played an important role (Ekengren et al., 2021). According to some students (Ekengren et al., 2021) and previous educational experiments, 3D models cannot totally replace the tangibility of real things (Newell, 2012; Di Giuseppantonio et al., 2015). The physical engagement of the tactile experience, intended as an active experience involving information gathered from a variety of senses related to touch, such as texture and temperature, is not comparable to 3D object manipulation (Galeazzi et al., 2015). On the other hand, the accessibility, which is a crucial factor in the educational environment, of digital tools cannot be underestimated (Nobles et al., 2019; Arias et al., 2022). Whereas in-person lessons on artefacts were constrained by lab opening hours, limited lab space (space for limited material), staff availability and so on, the online platform allows students to become familiar with the objects with no space or time constraints (Nobles et al., 2019). Furthermore, the ability to personalize a collection of objects and add exportable notes, both to the collection and to a single artwork, allows students to attach their own meaning and develop their own knowledge by connecting with an item, as a social constructivist approach proposes (Willcocks, 2015). Therefore, Dynamic Collections allows semantic annotation of the *User-driven characterization* typology (deepen in section 2.2). The user can annotate an artefact or some region of it, detected by a frame (Views) or a detail (Spot) of the model, with a personal description in natural language and export these annotations in a Json file (Fig. 11, 12 and 13). The annotations can also be loaded, enabling an integration and the interchange of descriptions and data.



**Figure 11** Example of annotation related general Notes (Dynamic Collections)

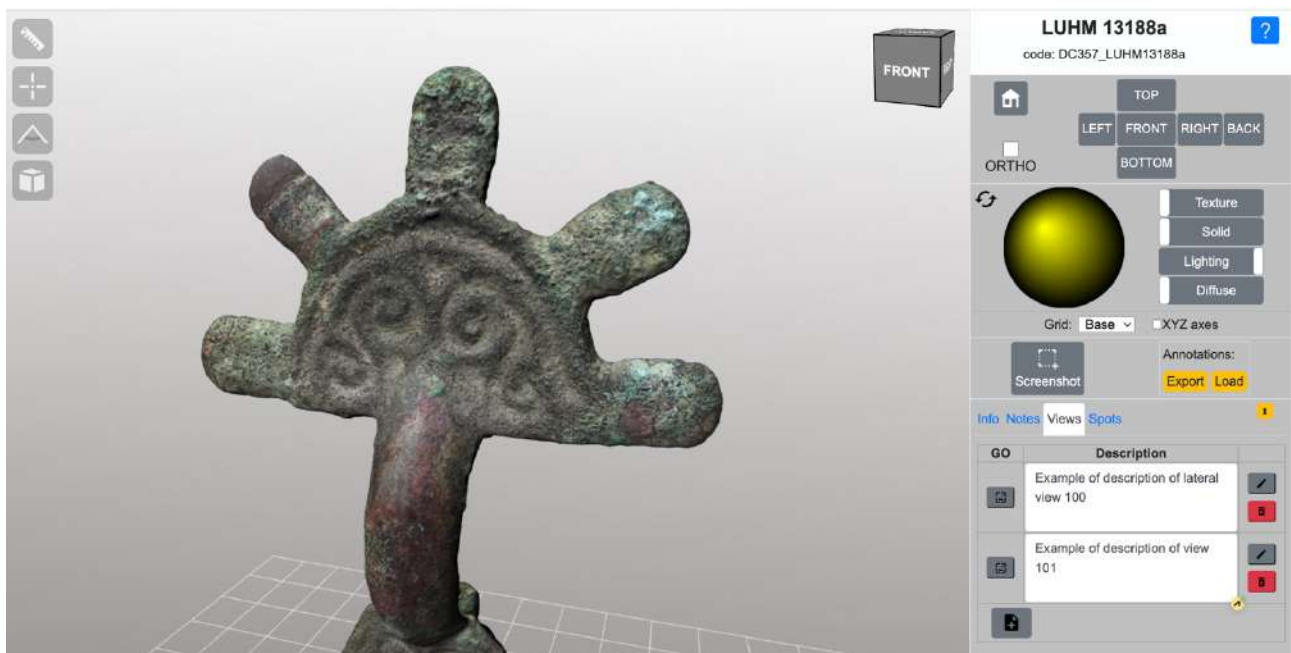


**Figure 12** Example of annotations related to Views of the related model (Dynamic Collections)



**Figure 13** Example of a model with annotation related to Spot (Dynamic Collections)

### 3. First phase of the survey: the object

#### 3.1 Artefact classification

Analysing different types of artefacts to evaluate their characteristics and quality in terms of accuracy, tolerances, form features, and surface qualities is a critical stage in reality-based 3D model generation for CH. This is crucial **to pick the most effective procedure** that will provide the desired quality (Apollonio, et al. 2021). To evaluate the complexity of an item intended for being the source of a 3D replica, I follow the example of previous experiments (Budiono and Hadiwardoyo, 2021; Apollonio et al., 2021), proposing to assign a complexity index to it. Thus, the following is a typing of objects according to their intrinsic and extrinsic aspects: both will be considered in the complexity index assignment.

##### 3.1.1 Intrinsic aspects

An intrinsic quality is a property that is inherent in or of a system or substance. It is unaffected by the amount of material present, as well as the shape of the substance, which might be a huge chunk or a group of smaller bits. Intrinsic characteristics are mostly determined by a material's chemical composition or structure. According to (Apollonio et al., 2021), the intrinsic aspects of an object can be described by  **$D/d$  ratio (where  $D$  is the diagonal length of the bounding box enclosing an item and  $d$  is the needed average length distance between vertices to describe the minimum detail, i.e. the model resolution)**, surface characteristics and Cavity Ratio (that is a variable indicating the feasibility of digital capture for some areas of the surveyed item). Intricate geometry and/or size, complex surface features (roughness, high reflectivity, cracks, decay, occlusions) may mean complexity on the digitization of heritage objects (Pritchard et al., 2022).

Now consider the  $D/d$  ratio. From an eye assessment of the real object, based on the characteristics of its geometry and the depth of its surface features, we can estimate the desired resolution quality of the model, and therefore of its geometry, that we want to obtain. As an example, if the minimum distance between two vertices of an incision on an effigy is 0.010m, the modeler could point to create a 3D replica with a minimum detail level of 0.005m ( $d$ ), a half of the length distance between those vertices. So, a higher detail requires a lower  $d$  value, furthermore the higher  $D/d$  ratio results in survey complexity (Apollonio et al., 2021, 12).

$$D = \sqrt{x^2 + y^2 + z^2}$$

The computed of the  $D/d$  ratio for the selected case studies produces the following results:

1. The fibula, **LUHM13188c**, has a xyz bounding box of 40x77x14mm. The diagonal length, so  $\sqrt{40^2 + 77^2 + 14^2} = 88.477\text{mm}$ . The minimum distance between two vertices of the surface incisions hovers around 3mm. I decided to impose a value of 1mm to  $d$ .  $D/d = 88\text{mm}$ .



**Figure 14** Bounding box of the 3D model of the artefact LUHM13188c.

2. The titulus, **LUHM21015.20**, has a bounding box of 42x21x41mm. Its diagonal length  $D$  is 62.846mm, whereas the desired model resolution  $d$  is 1mm.  $D/d$  ratio = 62mm.

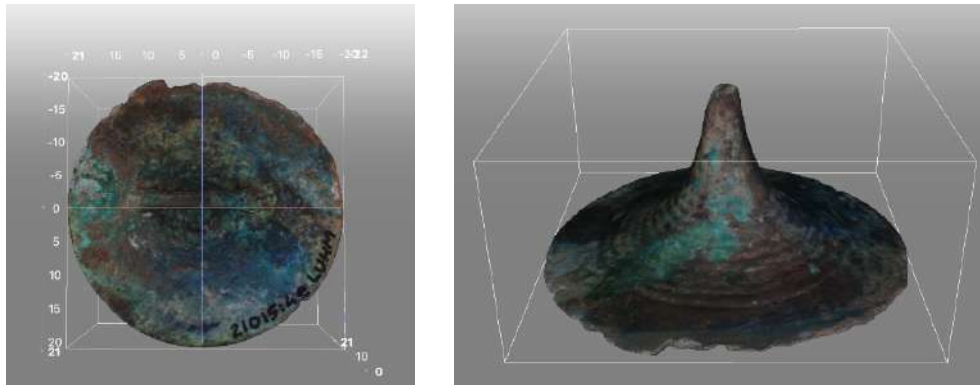


**Figure 15** Bounding box of the 3D model of the artefact LUHM21015.20.

3. The sword, **LUHM25561**, has a bounding box of 49x8x131mm. Its diagonal length  $D$  is 140.42mm, whereas its model resolution  $d$  is 2mm.  $D/d$  ratio = 70mm.

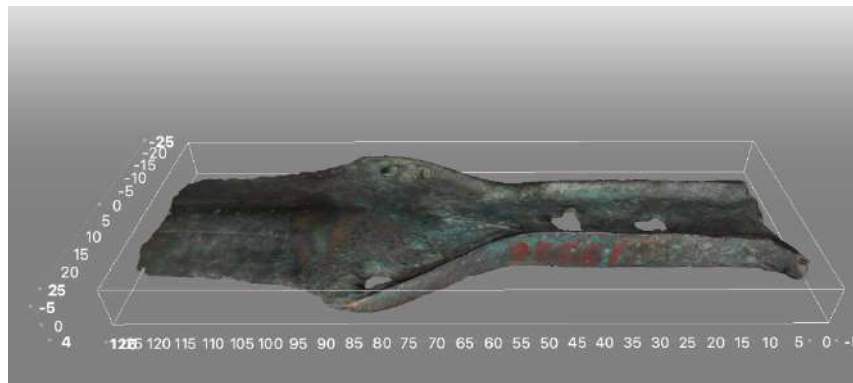


**Figure 16** Bounding box of the 3D model of the artefact LUHM25561.

4. The vase, **LUHM32125.81**, has a bounding box of 156x116x130mm. Its diagonal length  $D$  is 234.58mm, whereas its model resolution  $d$  is 2.  $D/d$  ratio = 117mm.



**Figure 17** Bounding box of the 3D model of the artefact LUHM32125.81.

Regarding the size of the object, and thus its bounding box, studies show that in relation to a high level of detail desired, the more voluminous an object is, the more the complexity of the process increases (Apollonio et al., 2021). Although true, it is also good to pay attention to the complexity of acquisition for objects that present the reverse problem, i.e., they are particularly small in size, so capturing their detail requires appropriate skills and equipment (Gallo et al. 2014; Percoco and Sanchez, 2015; Nicolae et al., 2014). As a result, I decided to assign 1 extra point for very small objects, i.e., those objects that have a  $D$  (diagonal of the bounding box)  $< 10\text{cm}$ .

**Cavity ratio (CR)**, instead, is a measure that defines the inability of specific areas of the surveyed item to be digitally acquired. It is determined by the ratio of  $D/W$ , where  $D$  is the depth and  $W$  is the hole width, depending on the surveying approach and instrument used. The surveying planning is straightforward for values between 0 and 1, but it becomes increasingly hard for values larger than 1 (Apollonio et al., 2021, 12).

From the direct observation of the objects, the presence of cavities among the case studies was found only in two out of four, such as the titulus and the vase. The fibula, LUHM13188c, presents some small engravings on the surface, but they are not properly cavities, whereas the sword, LUHM25561, has no relevant cavities at all. For both CR values is  $< 1$ , with a complex value related to this feature equal to 1.



The vase, LUHM32125.81, despite its fluctuation in  $W$  throughout the  $D$  length, has not a complex geometry, since its cavity is approximately equally wide and deep ( $CR < 1$ ).

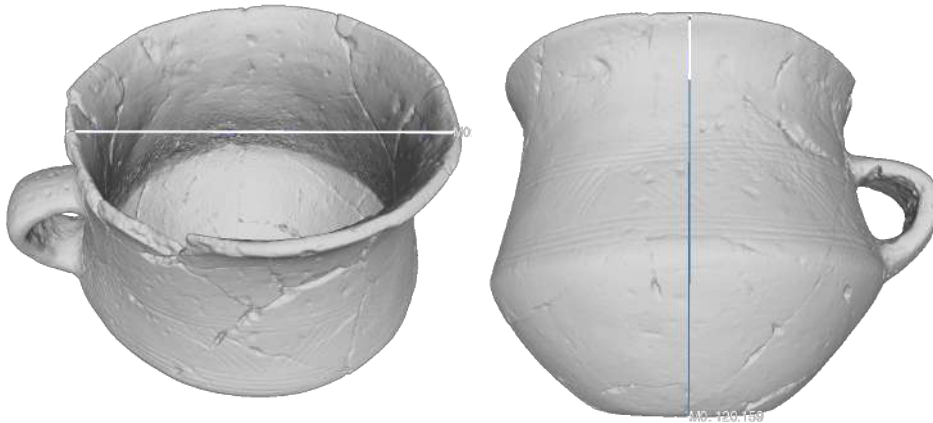


**Figure 18** Representation of the Cavity ratio ( $W$  in the left,  $D$  in the right picture) of LUHM32125.81 through its untextured model

The cavity of the titulus, LUHM21015.20, instead, is slightly more challenging, and not for a high value of depth and therefore of the  $D/W$  ratio (reason why I decided to describe the complexity of its CR with **1**), but rather for the presence of a piece of bronze, which hampers the direct framing of the cavity.

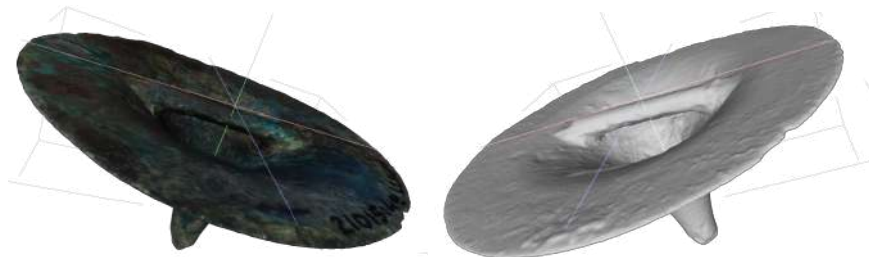


**Figure 19** Representation of the Cavity ratio of LUHM21015.20 through its textured (left) untextured model (right)

It's a case of **self-occluded surfaces survey** (Dang et al., 2020). Indeed, we're dealing with a circular buckle with a strong point in the middle, typical of a titulus format, that originally also included a pin made of iron on the back (Håkansson et al., 1999) (Fig. 20). To underline this sophisticated geometry, I later increase the **value of its topological complexity**.

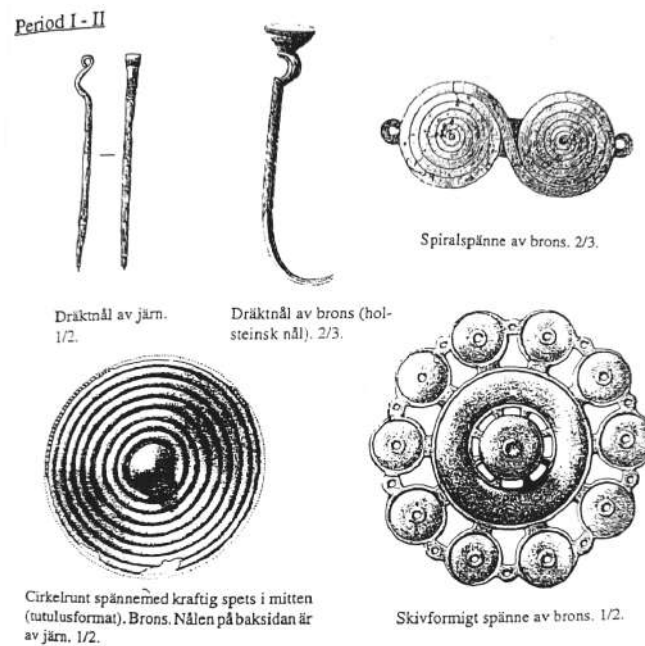


**Figure 20** Designs of different types of fibulas by (Håkansson et al., 1999).

For what concerns materials and surfaces, their reflectance and transmissivity degree (Fig. 21) deserve a brief deepening.

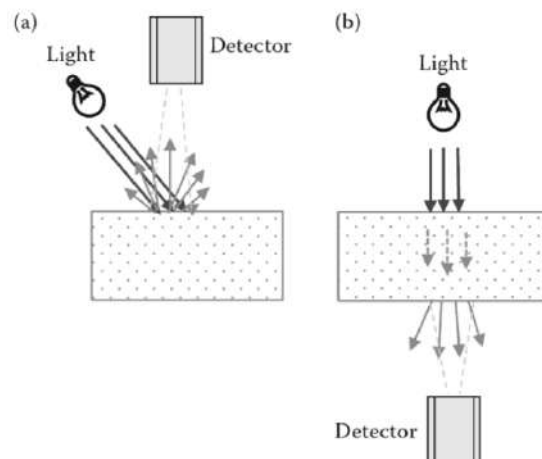


**Figure 21** (a) reflectance and (b) transmissivity measurements (Lu, 2016, 28).

The optical properties of materials, such as colour, surface texture, translucency and gloss, can be replicated and visualized through the acquisition of the Bidirectional Reflectance Distribution Functions (BRDF) (Guarnera et al., 2016), which quantitatively represents the true light reflection taking into account the complete hemisphere surrounding the light/surface collision site (Apollonio



et al., 2021). The analysis of this function leads to reflectance models, such as the diffuse<sup>19</sup>, the glossy and the specular one, as visually described in the following figure by (Guarnera et al., 2016, 3).

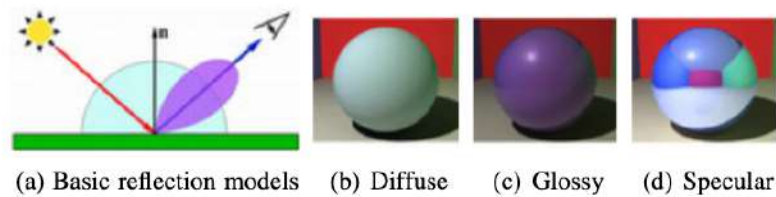


**Figure 22** (a) Basic reflectance models of the incoming light (in red): perfect diffuse (light blue), glossy (purple), and perfect specular (blue). In (b-d) renderings of diffuse, glossy and specular spheres are shown, places inside a Cornell box (Guarnera et al., 2016, 3).

In other words, in material analysis, also related to archaeological artefacts (Gebhard, 2003), we cope with:

- *Lambertian materials*: they are ideal "matte" or diffusely reflecting (Goral, 1984). When they are viewed from any angle, they have an apparent uniform radiance, which means the same brightness perceived by human eyes (Lu, 2016, 27).
- *Dielectric materials*<sup>20</sup>: they are poor conductors of electricity but effective supporters of electrostatic fields. They represent the most commonly occurring situation (Atkinson and Hancock, 2005): from a piece of metal to air to human bone. Most dielectric materials are solid (Awati, 2022), such as porcelain (ceramic), glass and plastic.
- *Conductor materials*: ideal conductors ignore masking, shadowing, and interreflections, yielding a BRDF with highly complex radiance expressions consisting of a (off-)specular spike and a specular lobe (Pont and Koenderink, 2003, 213). They are metals, such as gold, bronze etc.

Finally, there are also mixed materials. Furthermore, when the identification of the material of the object is not immediate, analysing the degree of polarisation of the artefact can help to detect the surface reflection, which, in the light of the above, provides important details for the definition of the material itself (Koshikawa and Shirai, 1987; Miyazaki et al., 2004).

According to the models characterizing the object, its complexity index could vary (Apollonio et al., 2021). The majority of techniques for determining object shape is based on the *body reflection* component of object surface reflections and so, it is intended to deduce the shapes of opaque

<sup>19</sup> "Diffuse reflection is the reflection of light from a surface such that an incident ray is reflected at many angles, rather than at just one angle as in the case of specular reflection. An illuminated ideal diffuse reflecting surface will have equal luminance from all directions in the hemisphere surrounding the surface, i.e. Lambertian reflectance." (Choudhury, 2014, 53)

<sup>20</sup> In this regard, the Dielectric Replica Measurement, the method of material identification proposed by (Robinson et al., 2019), represents a noticeable method for providing useful information about the properties and composition of dielectric materials of objects intended for a 3D replica in a non-destructive way.

inhomogeneous surfaces (Miyazaki et al., 2004; Pont and Koenderink, 2003). However, some materials are more complex to capture than others: because of their reflectance behaviour, which interfered with the depth sensor (Hagg et al., 2017; Miyazaki et al., 2004), current object recognition methods fail on object sets that include reflective or refractive (such as metals) as well as transparent and dark materials (Hagg et al., 2017). Indeed, the interactions between lights and materials are modelled as scale-dependent phenomena in order to better match the rendering engine's characteristics and behaviour (Apollonio et al., 2021).

In light of the above, I assigned 1 to the material “Stone” (which also included marble artefacts), since the problems for 3D relief are not severe and likely to be present in instances with low-feature artefacts (Koutsoudis et al., 2013). In fact, the quality of the data produced by image-based methods is greatly affected by the surface feature richness (e.g., strong feature points, texture with frequent colour alterations) (Koutsoudis et al., 2013). Instead, unfinished wood has nearly Lambertian reflectance, and despite the fact that wood polished with a glossy layer of polyurethane does not (since the glossy coating causes specular highlights) (Lu, 2016, 27), I opted to assume the general first scenario, assigning 1 to “Wood” material. “Clay” follows the same principle of wood: natural, therefore without paints or varnishes, it has an opaque surface and follows a reflectance model easy to manage during the acquisition (Morris et al., 2018). I assigned 1 to this material. In the case of metal, however, specular reflection occurs (Hagg et al., 2017). In fact, its material reflection risks not letting the system reproduce the correct geometry of the object, so its depth information. Polarization study (Miyazaki et al., 2004) shows that it is now possible to deal with this item material, but because it requires sophisticated equipment, I gave value of 4 to “Metal”.

Fabrics are complex nonlinear viscoelastic materials that move when stressed and only gradually return to rest when the force is removed (Maksimović, 2020). Their simulation is problematic due to their difficult to define and anticipate behaviour (Moskvin et al., 2019), so I gave value of 3 to “Fabric”. The “leather” is a fabric with a relatively rigid structure, but partially reflective, so I scored 2. In contrast, “Glass” and “Plastic” have a pattern that is reflected away from the active RGB-D camera or is irrevocably damaged due to their transparency (Hagg et al., 2017, 6). Transparency issues mean that depth is missing, making it difficult to record the object's 2D contour, especially if they are textureless and therefore with “non-collaborative” surfaces (Morelli et al. 2022, 77). Thus, score 4. To “Paper”, defined as a genuinely Lambertian surface (Atkinson and Hancock, 2005, 109), I assigned 1.

Fur is one of the most difficult surface materials to work with because of the relatively low contrast in reflections, especially for black hair, and the potential damage of light penetration if the hair is thin and sparse (Chen et al. 2018). Its 3D reconstruction from multi-views stereo is very hard to do outside of a laboratory environment with high-quality results, and although the objective in many applications

is to capture general hair geometry rather than fine detail of each strand, the outcome is frequently unreliable (Chen et al., 2018). Thus, score 4.

In the absence of polarized lenses and appropriate equipment, evaluating the colour and reflection of the glaze layer can be challenging (Zhang and Neu, 2021). As such, I assign a value of 2 to the Glaze. For what concerns the transmissivity of the material, so the finishing of the surface, the existing literature in this regard (Morelli et al., 2022; Hagg et al., 2017; Marroquim et al., 2017; Pont and Koenderink, 2004; Miyazaki, 2004) helped me produce this assessment. “Opaque” = 1; “Glossy” = 2; “Reflective” = 3; “Transparent” = 4; “Dark” = 2; “Not consistent” = 3; “Featureless” = 2; “Repetitive” = 2.

	Opaque (1)	Glossy (2)	Reflective (3)	Transparent (4)	Dark (2)	Not consistent (3)	Featureless (2)	Repetitive (2)
Stone (1)	2	3	4	5	3	4	3	3
Wood (1)	2	3	4	5	3	4	3	3
Clay (1)	2	3	4	5	3	4	3	3
Metal (4)	5	6	7	8	6	7	6	6
Fabric (3)	4	5	6	7	5	6	5	5
Leather (2)	3	4	5	6	4	5	4	4
Glaze (2)	3	4	5	6	4	5	4	4
Glass (4)	5	6	7	8	6	7	6	6
Fur(4)	5	6	7	8	6	7	6	6
Paper (1)	2	3	4	5	3	4	3	3
Plastic (4)	5	6	7	8	6	7	6	6

**Table 3** Matrix of complexity value for different materials and surfaces.

### 3.1.2 Extrinsic aspects

A property that is not essential or intrinsic is called an extrinsic property. For example, mass is an intrinsic property of any physical object, whereas weight is an extrinsic property that depends on the force of the gravitational field in which the object is placed. In the 3D survey campaign, extrinsic study of the artefact includes how the object is displayed throughout the acquisition phase, how it interacts with the context, and whether it is fixed or removable from it. Furthermore, surveying activity is influenced by *spatial distribution* (SD). The possible scenarios are summarized below:

- If the spatial distribution is described by  $X \simeq Y \simeq Z$ , it's the case of a 3D object.
- $X \simeq Y \gg Z$  means a 2D item.
- $X \simeq Y \ll Z$  means a 1D item.

The most undesirable scenario occurs when one dimension dominates the other two ( $X \simeq Y \ll Z$ ), followed by the case when the distribution of the masses that comprise the object is two-dimensional ( $X \simeq Y \gg Z$ ) (Apollonio et al., 2021, 12). In our campaign, we always deal with artefacts, so three-dimensional objects. Nevertheless, in two of these objects, the slight disproportion of depth (z) compared to height (y) and length (x) made image processing more problematic, resulting in the initial trials in a failure in image alignment with the software and, therefore, in further acquisition campaigns. In the instance of the sword and notably the fibula, without a significant number of images of the object's lateral sides, the software could not realize that the front and back were two faces of the same artefact. They were not challenging cases, but they generated more inventiveness for artefact orientation (in order to enhance the side of the object) than other instances, thus I would assign a rating of 1.5 to them. The titulus and the vase, instead, have a uniform spatial distribution following the formula  $X \simeq Y \simeq Z$ . To their SD variable, I can assign 1.



**Figure 23** LUHM25561 and LUHM13188c from different perspectives.

One of the strategies for describing connections between spatial entities is topology. As a result, it serves as the foundation for many spatial operations (Zlatanova et al., 2004). In 3D surveys, *topological complexity* (TC) is important because it affects every operation of the proposed workflow: when the object is not a simply connected space, for example, it presents through holes, or even if it has blind holes, acquisition planning and subsequent phases (parameterization, texturing, and so on) will become increasingly complex (Apollonio et al., 2021, 12). Among the presented case studies, only the vase, LUHM32125.81, is characterized by a hole, inside the handle, so has a TC higher than 1. However, although the cavity of the titulus cannot be properly defined as a hole, the item's topology is affected by this self-occluded surface region, which makes it almost impossible to handle the area under the iron pin (Dang et al., 2020). That's why I assign it a  $TC = 2$ .

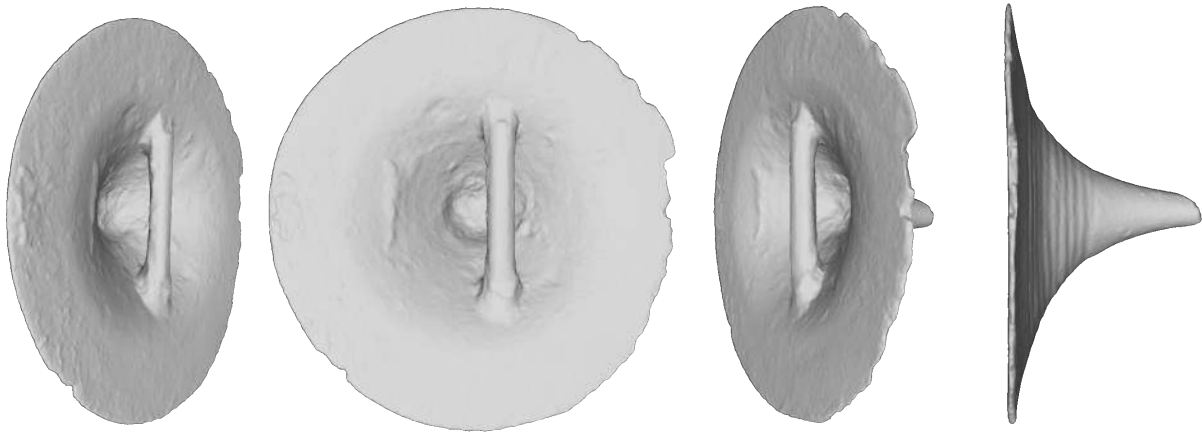


**Figure 24** Untextured LUHM25561 from different perspectives, with a focus on the central hole.

The last extrinsic features worth mentioning are *boundary conditions* (BC) and the possible presence of movable parts. The first aspect studies the availability of object's adjacent working areas that are free of barriers. For example, a statue in a public park adjacent to a tree is difficult to recreate from some angles. As a result, there is an impediment that makes the perception and construction of some viewpoints of the item impossible. Furthermore, the mobility of the item affects this point. Photographs and paintings are examples of *movable heritage*, as they are metals, pottery, glass, wood, leather, textiles, and other composites. It can be two-dimensional or three-dimensional, formed of one or more materials, and generally meet less boundary obstacles than immovable items (Pritchard et al., 2022, 44). On the other hand, *immovable heritage* includes buildings, lands, and other historically significant assets, often with stable foundations tied to the landscape (Pritchard et al., 2022, 46). In museum collections, like the one involved in Dynamic Collections, modelers generally deal with movable objects. The four case studies are therefore all moveable items that display all sides free of physical obstructions. Additionally, when an item is formed by several components, it is necessary to determine if these parts are movable or not, since this may affect the model acquisition process. Even in this case, the chosen artefacts do not meet this characterization.

### 3.2 Surveying aims: input and output metrics

The effort to obtain a 3D replica is measured by the combination of intrinsic, extrinsic features and sampling. Thus, now the modeler can consider the sample to whom his/her attention and interest is addressed. The survey aims (*l'esigenza mensoria* in Italian) addresses two fundamental spheres of operation: input metrics and output metrics.

This is a critical stage. A model arises from the measurements taken here, which with its resolution and refinement will be the means of conveying information. (Vitelli, 2011) emphasizes the delicate nature of this passage:

« The technologies of our interest, therefore, have the peculiarity of providing the operator with a new and different type of data, a new "product" that is at the same time not only carrier of heterogeneous information (metric, radiometric, colorimetric, etc.) but also a new concept of "measuring", which asks the operator for new types of processing so that, from this set of non-interpretative instrumental type data, a representation can arise, an interpretative model that, we have seen, constitutes "the metric knowledge" of the artefact and, at the same time, the mainstay of the entire information system from which the knowledge of the cultural heritage will flow, the first fundamental stage of the conservation project. »<sup>21</sup> (Vitelli, 2011, 34).

Thus, Input metrics are concerned with image generation, how the object occurs in the act of its acquisition, whereas output metrics are focused on measurement requests from the final model (Having et al. 2007, 2). Starting from the input metrics, the 3D survey passes through some question points: What do I want to measure of my object? Is the concerned part of the digital replica a specific feature (like a scratch on the surface) of the object, or is the object as such (like a pot), in its entirety, the ultimate goal?

In this regard, the reason for the survey is intimately connected with the sampling portion. In the four case studies in question, such as artefacts of small size, all are replicated as a whole in their geometry. However, in the instance of a medium-high dimension complex of statues, the modeler may decide it is necessary to sample only a fraction of the area. Furthermore, most applications that use 3D models require them to be geometrically precise, as well as clear of noise, outliers, and missing data or holes. Such errors not only render the models worthless for documentation or reproduction, but also produce an unpleasant visual experience (Gonizzi Barsanti et al., 2014, 145). The details should be of high quality, which is commonly characterized as having a high geometric precision, a low level of uncertainty and completeness.

---

<sup>21</sup> In the original text «Le tecnologie di nostro interesse, dunque, hanno la peculiarità di fornire all'operatore una nuova e diversa tipologia di dati, un nuovo "prodotto", per così dire, che è al tempo stesso non solo portatore di informazioni eterogenee (informazioni metriche, radiometriche, colorimetriche ecc.) ma anche di una nuova concezione del "misurare", che chiede all'operatore nuovi tipi di elaborazioni affinché, da tale insieme di dati di tipo strumentale non-interpretativo, possa scaturire una rappresentazione, un modello interpretativo che, abbiamo visto, costituisce "la conoscenza metrica" del manufatto e, al tempo stesso, l'asse portante di tutto il sistema informativo da cui scaturirà la conoscenza del bene culturale, primo fondamentale stadio del progetto di conservazione. »

Then, it is time to examine the output metrics. Once the chosen software has been exposed to the input data, the operator should set the dense cloud, mesh and texel values. For several reasons (i.e. model weight, efficiency of the host web application etc.) related to the final use of the model (i.e. visualization purpose, gamification), the operator could opt for submitting a simplification process to the replica (Preim and Botha, 2014) or to complete the model with the highest accuracy and fidelity to the original object. Thus, the modeler can define the maximal *error* that can be introduced in a single simplification step (i.e. while simplifying the mesh), that we call *approximation error* (Cignoni et al., 1998). The numerical comparison of two triangle meshes of the same 3D artefact surface, created by following two different maximum values of uncertainty of the model, clarifies the gap between the adoption of a *Master model* or of a *Derived one* (Apollonio et al., 2021, 5).

### 3.3 Model complexity index

As explained in the previous chapters, the main aspects of object complexity are geometric/structural features, surface/texture, and material characteristics.



Moreover, it is desirable to state specifically that the use of the complexity index proposed in this place (especially in sections 3.1.1 and 3.1.2) is meant to convey the sense of complexity of the artefact that the modeler must replicate and to stimulate his/her critical spirit before proceeding with acquisition. It is not intended to be a calculating phase that actively engages the modeler before the survey. The most general recognition and relief of the artefact's intrinsic and extrinsic characteristics, as well as its measurements, is instead an essential premise to the 3D survey campaign. (Pritchard et al., 2022) supports this approach, stating that a precise *object complexity* can only be identified after all assessments of the object have been accomplished, which means that, as an indicator of complexity, it is useless for 3D digitization planning and decision-making, because it only occurs once the process is concluded. This is the reason why our emphasis focuses on "*Model Complexity*", rather than "*Object Complexity*" (Pritchard et al., 2022). Thus, not on the complexity of the real object (which is solely related to the data collection phase), but rather on the complexity of the created model, which is related to the complete data acquisition and processing workflow.

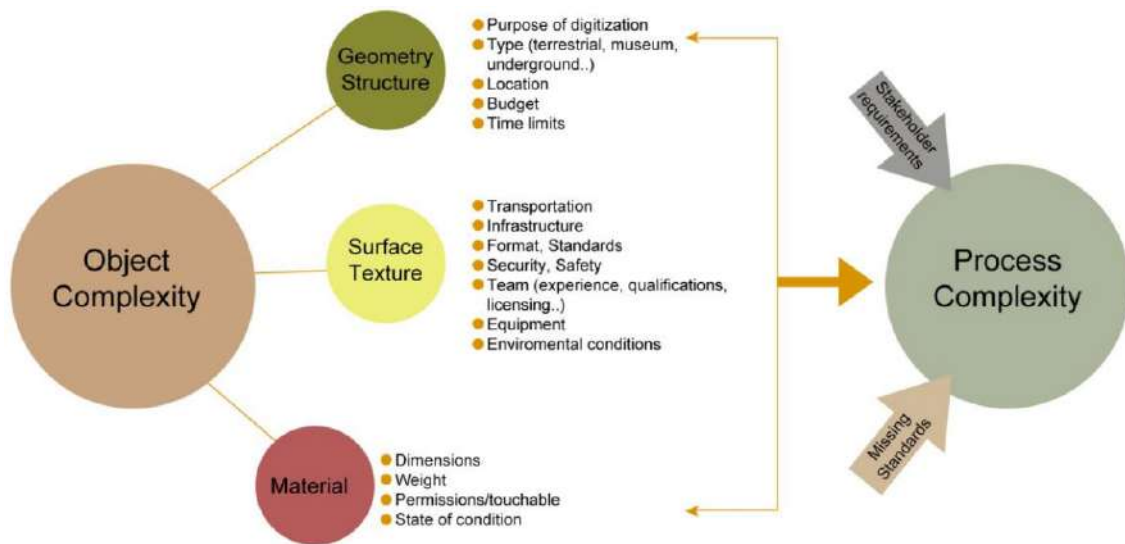






**Figure 25** The suggested shift from *object complexity*, throughout *model complexity*, up to *process complexity* (Pritchard et al., 2022, 52).

The following is the table of complexity index for the 3D models of the four case studies:

	Intrinsic aspects						Extrinsic aspects				
Collection piece	D/d	Very small object	Cavity Ratio (CR)	Surface Characteristics			Spatial distribution (SD)	Topological Complexity (TC)	Boundary Condition (BC)	Presence of movable part	Score
				Material reflective	Material transmissive	Texture					
	8,8 cm	Yes (1)	<1 (1)	Metal (4)	Reflective (3)	Even distribution (1)	3D (1.5)	0 hole (1)	All sides free (1)	No (1)	14,5
	6,2 cm	Yes (1)	<1 (1)	Metal (4)	Glossy (2)	Even distribution (1)	3D (1)	1 hole (2)	All sides free (1)	No (1)	14

	7,0 cm	No (0)	<1 (1)	Metal (4)	Opaque (1)	Even distribu tion (1)	3D (1.5)	0 holes (1)	All sides free (1)	No (1)	11,5
	11,7 cm	No (0)	<1 (1)	Clay (1)	Mix (opaque/ glossy /dark) (1), (2), (2)	Even distribu tion (1)	3D (1)	1 hole (2)	All sides free (1)	No (1)	9-10

**Table 4** Complexity index of the four case studies

### 3.4 Complexity classes

After evaluating the physical and structural aspects that make an item more or less complicated to recreate in 3D, we may now proceed to postulate the complexity classes.

These findings are accompanied with an incremental representation, in the form of a diagram, in a normalized vector space. The y axis indicates minimum value and maximum value of complexity: from a c.i.(min) = 8, computed by combining the lowest intrinsic (CR, surface features), extrinsic (SD, TC, BC), and removable-parts values that an object may have, to c.i.(max) = 26.5. The incremental value of the model complexity index is indeed 0.5. Tanking as a reference the set of complexity parameters grouped in Table 4, we can hypothesises a model that has all complexity features score 1 but a SD=1.5, motivated by a slight disproportion of the lateral surface, such that c.i.= 8.5 .

To construct the line that describes the behaviour of the complexity index, it is necessary to calculate the normalized value for the elements of the range on the ordinate axis y. In the graph below, therefore, since c.i. (min) = 8 this coincides with the y = 0, and so c.i. = 8.5 is represented with y= 0.5, c.i.= 9 is y=1 and so on.



**Figure 26** Constant representing the incremental growth of the model's complexity.

Therefore, the constant, which represents the incremental growth of the model's complexity, allows us to create classes of complexity. Based on an item's complexity index (c.i.), I opted to focus on four classes:

- a. Class A: **Low complexity** (8-13.5 c.i.)
- b. Class B: **Medium complexity** (13.5-17.5 c.i.)
- c. Class C: **High complexity** (17.5-21.5 c.i.)
- d. Class D: **Very high complexity** (21.5-26.5 c.i.)

Thus, the first stage of the acquisition campaign may be summarized with these conclusions:

- a. If the artefact intended for 3D replication has no cavities or holes (or none that are noteworthy in size), is made of *Lamberian material* (*wood materials wood*, stone, or clay material), with an opaque surface and a distribution in the homogeneous and observable space at 360°, then it will need minimal effort.
- b. Contrary, if a model has a medium complexity index, this complexity can be traced back to the presence of a few difficult elements, such as the involvement of a conductive or dielectric material, or a reflective surface, or an obstructing or precarious element in the geometry of the object, such as to prevent its framing.
- c. A model will require a high commitment (and, in some cases, also means sophisticated equipment) to be reconstructed three-dimensionally if it includes several elements of complexity

(both intrinsic and extrinsic), or a few but of huge proportions, such as a featureless and/or textureless surface, spatial distribution, and intricate topological complexity.

- d. We'd face a very difficult model if it was obstructed by one or more sides, had movable parts that may be damaged (which would rule out certain orientations), or was found in a space exposed to direct sunlight and had a reflecting or transparent conducting surface.

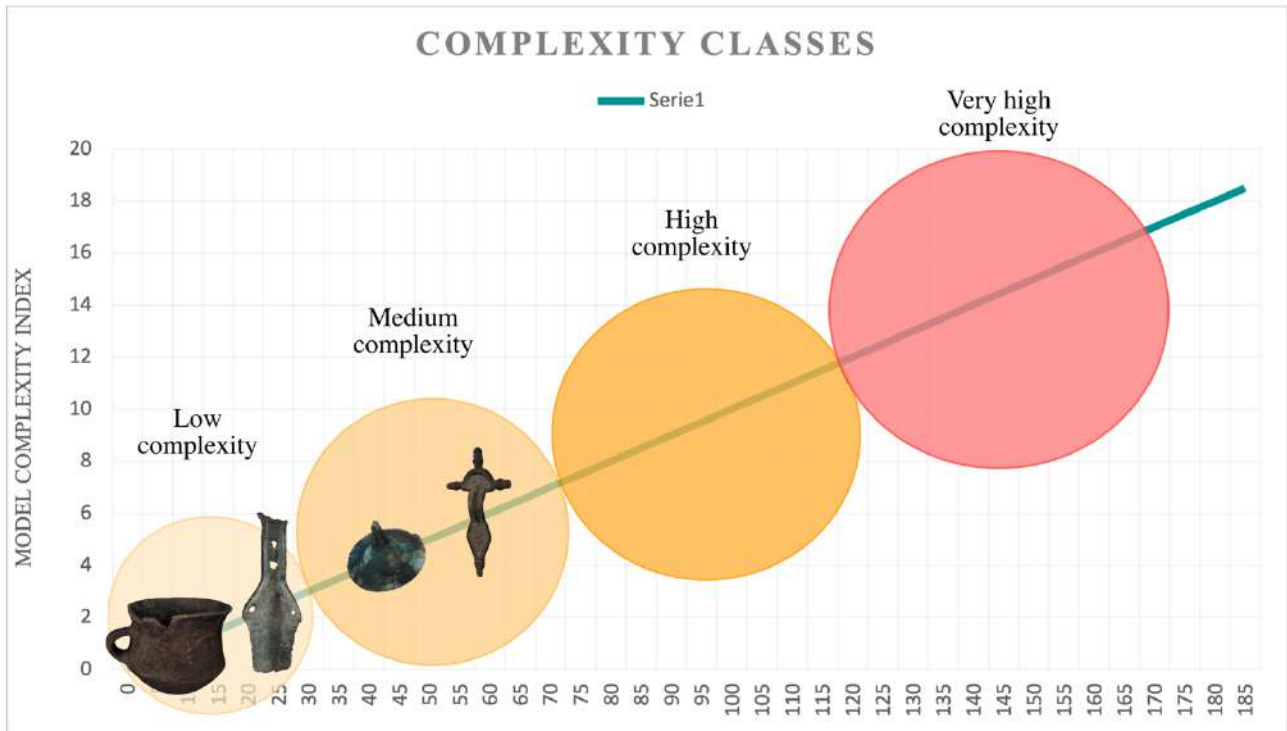


**Figure 27** The four case studies displayed along the constant of the model's complexity within a differentiation of the complexity classes.

## 4. Second phase of the survey: planning and acquisition

The assessment of the object's features is a crucial stage in the survey campaign since it allows the operator to select the most relevant tools and techniques to proceed with the effective acquisition of the model.

«In order to optimize the accuracy and reliability of 3D point measurement, particular attention must be given to the design of the network (“mesh”). Designing a network includes deciding on a suitable sensor and image measurement scheme; which camera to use; the imaging locations and orientations to achieve good imaging geometry; and many other considerations. » (Remondino and El-Hakim, 2006, 276)

This section of the study is devoted to analysing the choices of the devices and the camera setting, to explore the risks and the good practices of the image capture.

### 4.1. The choices of the devices and the equipment

This is a phase of planning, a brainstorming, before the action, such as the time to make a list of the needed equipment.

#### 4.1.1. Basic photogrammetric instrumentation

There is a highly recommended instrumentation, in some cases even necessary, which is the minimum common denominator of most professional photogrammetric capture campaigns for small-medium objects (Apollonio et al., 2021; Bedford, 2017; Verhoeven, 2016). They are summarized below:

- Digital single-lens reflex: (DSLR) cameras
- Essential lens (prime lens or zoom lens)
- Tripod
- Turntable
- Scale bar
- Illuminator kit (static lighting set)
- Resizable box structure to host objects to be captured
- Curtain made of (black) matte surfaces
- Rubber pads for artefact positioning

Now I'll go through each one in detail. The utilization of 2D pictures is the basis upon which photogrammetry is built (Elkhrachy, 2022). Recent researches have proven that even cutting-edge smartphone cameras may give adequate, if not reasonably good, high resolution photos for 3D reproductions (Apollonio et al., 2021; Nocerino et al., 2017; Poiesi et al., 2017). Thus, an initial hypothesis in producing the resulting 3D model is a smart phone camera with a minimum image resolution of 8 megapixels (Thomas et al., 2019, 3). These investigations, however, also demonstrate that, if in the hands of someone who knows how to use it, a digital camera can provide for even more detailed outcomes (Cardinal, 2020; Apollonio et al., 2021). When discussing digital cameras, it is necessary to distinguish between digital still cameras (DSC) and digital single-lens reflex cameras (DSLR). If, in the first case, the camera is equipped with a digital image sensor for capturing pictures and a storage device for saving the obtained image signals in a digital way, the latter one provides a useful (and often necessary, as we'll see later) degree of control over the entire photographic process, also due to the high-range using lens (Verhoeven, 2016, 163).

If you have the chance to use a DSLR camera, (Bedford, 2017, 3) suggests favoring this option over others because of the ability to change lenses. For the Dynamic Collections project, a Canon EOS 6D Mark II is used. As a result, although a medium-high-performance camera body is recommended, due to low-end consumer devices not offering proper control of exposure components, resulting in JPEG compression (Collins et al., 2019), its full potential is shown only when combined with an equally high-performing lens. In truth, «*better results will be obtained by using better quality lenses*» (Bedford, 2017, 28). Poor lenses will therefore produce photographs that lack sharpness and clarity even on a high-quality camera (Fryer, 1986).

Then, it is time to choose an essential standard lens to use, which, despite the wide range of lens types, may be divided into two major categories: zoom lenses (with variable focal lengths) and prime lenses (with fixed focal lengths). There are advantages and disadvantages for both: the first are heavier, optically often inferior (though there are exceptions), their largest aperture is smaller and their focal length risks changing during camera acquisition (posing a problem in calibration challenges during the subsequent stages of the survey) (Wang et al., 2017), but they cover the focal lengths required in 95% of the photographic cases (Verhoeven, 2016, 172). In contrast, with top-tier optical quality and big apertures, typical of prime lenses, the operator pays the price of carrying multiple prime lenses to cover the same zoom range (as, for example, a 50mm and an 85mm prime) (Nocerino et al., 2014). Thus, it is just a question of preference, based on the operator and project goals. The standard lens adopted for some objects of the Dynamic Collections is a Canon EF 24-105mm f/4L IS II USM.

Therefore, in addition to the main instrument that records 2D photos of the artefact, the basic and essential equipment for a museum acquisition campaign includes a roundtable and a tripod. If we

envision the campaign items, such as those mentioned as the case studies, to be of small dimensions (thus 32cm) (Pritchard et al., 2022), the operator can choose between a multi-viewpoint camera approach of a fixed artefact or a rotary photogrammetric approach, exploiting a fixed camera and a moving turntable (as shown by Fig. 28 below) (Collins et al., 2019).

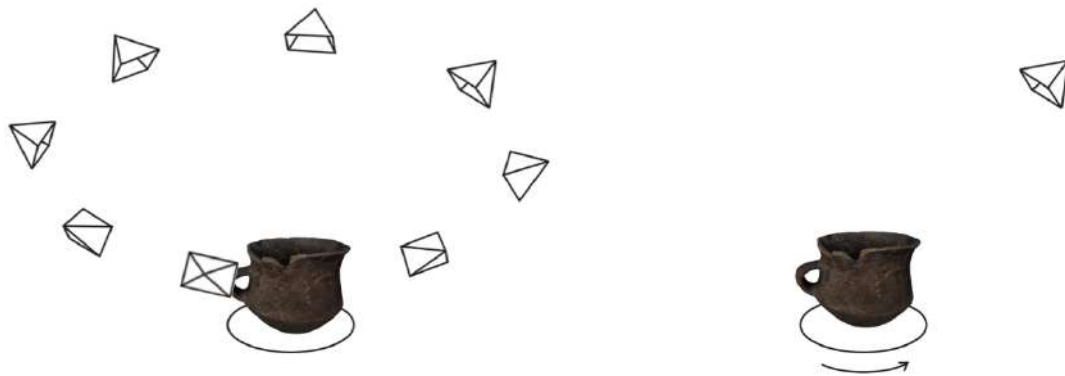


**Figure 28** Multi-viewpoint camera approach (left); the rotary approach (right). The model shown in the figure is LUHM32125.81.

When a fixed-camera technique is used, the findings show an improvement in monitoring quality. Even when the lens model is poorly determined, such a technique enhances the measurement accuracy of the SfM-MVS procedure (Parente et al., 2019). As a result, the combo tripods-turntable simplifies picture acquisition by allowing the item to be shot from all sides, capturing every feature of the object in a continuous loop, with controlled lighting and background, and ensuring consistency of the overlapping photos obtained (Thomas et al., 2019, 3). This advantageous turntable configuration has been proved effective in a variety of close-range photogrammetry initiatives such as historical preservation (Marshall et al., 2019; Collins et al., 2019; De Paolis et al., 2020; Menna et al., 2017; Morena et al. 2019). The turntable, on the other hand, poses a new issue since the extracted scene characteristics belong to at least two independent motion systems, namely the background and the item. Moving objects or a rich environment (background with high-frequency information, for example) may introduce ambiguous features (Eldefrawy et al., 2022, 2). Nonetheless, in this study, it is shown how to decrease or eliminate this potential risk. The turntable can be analogic, with the operator manually rotating it, and in this case the degrees should be marked on the border (Thomas et al., 2019), or it can be automated (Collins et al., 2019; Marshall et al. 2019).

Furthermore, according to (Verhoeven, 2016, 224), shooting the image series from a tripod is required for the best results since it substantially reduces any camera shaking. When no tripod is available, there is a major risk of causing image blur: even with extremely short focal lengths, 1/15 s is typically too lengthy an integration time to hold a camera and lens absolutely stable (Verhoeven, 2016, 213). Scale bars placed around the object on the turntable can be very useful for tiny subjects when formal

control is not possible (Bedford, 2017, 49). In the example studies presented, it was decided to use a scale bar of 10 cm (in Fig. 29) for the sword, the vase and other objects. Based on the size of the object, you may use scales with even smaller measurements, as we did for the titulus and the fibula. This small and low-cost component allows you to scale the model correctly using the software you've chosen for modelling, ensuring accuracy of the final result.



**Figure 29** Scale bar of 10 cm. The model shown in the figure is LUHM25561.

Then, an illuminator kit to ensure controlled and high-quality light to get uniform and diffuse illumination is required. If possible, the best option is to use external or studio lighting (Bedford, 2017, 75). Setups more often associated with product photography, such as light tents or resizable box structure consisting of translucent whitewalls suitable to diffuse the light, can be employed. The item is imaged within the structure, and lights are utilized outside the tent to disperse the light, or internally allowing for diffuse and equal coverage if many lights are employed. In our case, for not reflective material, an internal light of the box structure is used.

Finally, to complete the kit of the setting background, a curtain made of matte surface, possibly black, can help to mitigate the Fresnel effect on contours of reflective materials or to avoid the creation of the shadows on the turntable. A black backdrop reduces reflections from nearby objects and absorbs refracted light that flows through the item. (Morelli et al., 2022, 79). The last item on the basic equipment list concerns rubber pads for artefact positioning. Having a cheap and versatile support such as rubber pads, which are not harmful to artefacts, allowed us to position artefacts as best suited to a correct and strategic alignment of the objects. In the case of the fibula or the sword, for example, it was useful to position the objects standing along the y-axis to better frame the thin sides of the object during rotation (Fig. 30).



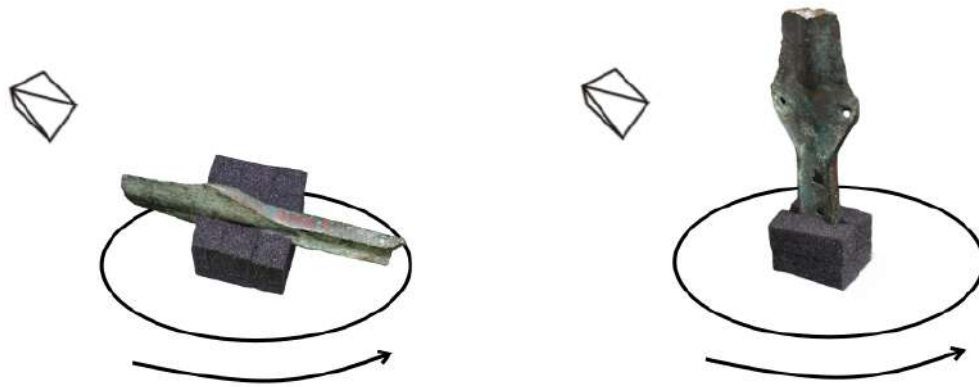


**Figure 30** Different artefact positioning supported by two rubber pads. The model shown in the figure is LUHM25561.

#### 4.1.2. Equipment for macro photography and cross polarization

Now, as we have seen in the analysis on the object complexity index, there will be some acquisition campaigns that are more complex than others and that require more specific equipment than that analyzed above (Pritchard et al., 2022). In order not to get into a digression that could be long-winded, I have preferred to delve more deeply into those tools that more or less concerned the Dynamic collections acquisition campaign of last spring, in particular the equipment necessary for the four case studies of the research.

- Scale bar for very small objects
- Different lenses (a wide range and a long length)
- Circular polarizing lens filters (for cross-polarization)
- Set of lights with polarizing screen, such as laminated polarizing sheets (for cross-polarization)

As mentioned before, for very small objects, it can be useful to have a scale bar proportionate to the object, optimizing the frame space to narrow on the object and thus also on the scale bar, aiming for a high-resolution image (Bedford, 2017, 49). We used a scale bar of 0.025m.

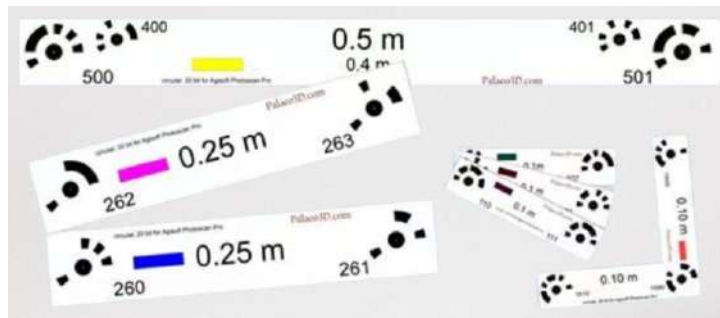


**Figure 31** Scale bars of different dimension.

Concerning the lens, a medium focal length (50mm for a full frame camera) is usually the best choice to reduce any perspective distortion (De Paolis et al., 2020, 378), but in some cases (very small objects, outdoor setting) there is a need to use other types of fixed lens (macro lens, wide-angle lens). The different optical lens components of such a camera lens define its individual features such as focal length. The interaction of focal length and imaging sensor size determines whether a lens is classified as wide-angle, standard, or long focus. All of them have unique applications and produce distinct effects (such as depth of field and perspective distortion) (Verhoeven, 2016, 163).

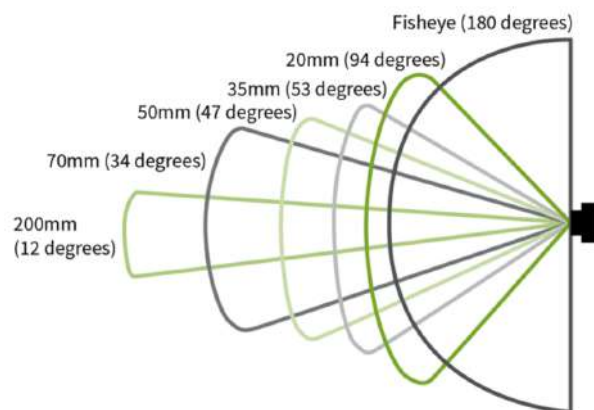


**Figure 32** Different optical lens.

A wide-angle lens must have a large Field of View (FoV), such as 90°, whereas a long focus lens must have a small FoV (say, 7°) (Verhoeven, 2016, 191). In recent years, fish-eye lens cameras, which were not formerly used for documenting CH resources, have been applied in a variety of industries, including indoor and outdoor 3D modelling. It can record a picture across a considerably larger area, but it exhibits significant geometric distortion in the image, which must be addressed using the self-calibration technique, as a result of compressively recording the image's outside part relative to the central component (Choi and Changjae, 2021). A macro lens, on the other hand, has traditionally been used to record cultural assets or for industrial measurement, and previous literature considered its use an optimal solution to perform digital very close-range photogrammetry for small

objects (Percoco and Sanchez Salmeron, 2015; Yanagi and Chikatsu, 2010; Gallo et al., 2014). Macro lenses can capture a sharp image of a small object from the working distance (Yanagi and Chikatsu, 2010, 617), but their main limitation is the very small DoF (Collins et al., 2019): only a tiny proportion of the image appears sharp enough to be used for 3D replicas, as image matching algorithms cannot operate on blurred regions (Gallo et al., 2014), 175). A higher  $f$ -number is one approach for extending the depth of field in macro photography. Thus, our reflex camera was equipped with a macro lens (Tamron SP 90mm f/2.8).

Thus, in accordance with what is explained in the chapter on the intrinsic and extrinsic aspects of artefacts, it may happen that objects with translucent or reflective materials are involved. One of the possible acquisition strategies is the use of polarizing filters to be applied to the lenses, which shall necessarily be prime lenses. Photographic filters can be circular or plate filters, and the polarizing filter is no exception. If it is plate-type, it is called a linear polarizer and has the abbreviation PL, if it is screw-type, it is called a circular polarizer and can be found under the abbreviations C-PL, PL-CIR or CPL (Hong, 2020). In our case studies, this solution proved particularly effective for the fibula, LUHM13188c, and titulus, LUHM21015.20, thus coinciding with the use of the Tamron 90mm macro lens. The filter used was therefore a Tiffen 62mm Circular Polarizing Filter.

To drive the distribution of the light source and obtain a correct cross polarization of the light (Miyazaki et al., 2004), it may be required to supplement the lighting set with new light sources placed on telescopic arms with the ability to pan and tilt symmetrically to the object (Fig. 33). It should be combined with laminated polarizing sheets as a polarized screen.

VILROX VL-200T Bi-Colour 3300K-5600K 30W Dimmable LED Video Light Panel Lighting Kit (3 Packs) was employed in our survey.

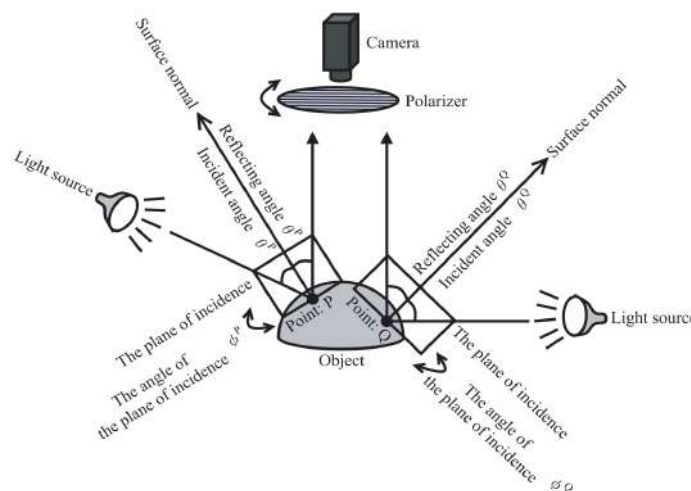


**Figure 33** Interaction of light sources, the object and the camera with polarizer (Miyazaki et al., 2004, 6).

In the following section, a brief analysis on light polarization also explores how to correctly arrange such a set of lights to obtain 2D polarized images.

## 4.2. The camera setting

Before beginning the acquisition process, some camera settings suited for the object in question should be carefully adjusted to provide images suitable for optimal 3D reconstruction in the subsequent stages (De Paolis et al., 2020). There is no "best" camera or "best" setting for all photogrammetric tasks, although a single high-quality camera can be a significantly more adaptable sensor in a range of settings than, for instance, a much more expensive 3D laser scanner (Bedford, 2017, 19).

The lighting condition of the object must be set. It is critical that the characteristics stay consistent as the item is rotated, which necessitates illumination conditions that are proportional to the rotational angle. As a result, consistent, diffuse light is typically recommended (Collins et al., 2019) and on this initial setting (which can however be changed later) the parameters of the camera are also set.

First and foremost, the camera should be set to manual mode, and electronic aids like auto-focus (AF) and image stabilization should be turned off, which can be done on both the camera and the lens in many current systems (Verhoever, 2016). Setting the focusing distance suitably (usually at infinity, or potentially for closer range work at 1m or 2m) and then keeping it from moving (with electrical tape or a locking screw, if available) will be required when utilizing calibrated primary focal length lenses (Verhoever, 2016).

The exposure components must then be set. In general, ideal exposure for photogrammetry is a balancing act between aperture, shutter speed, and sensor sensitivity, just like it is in 'regular' photography (Bedford, 2017).

### 4.2.1. Aperture, shutter speed and ISO

The aperture controls the quantity of light that passes through the lens, similar to the pupil of the human eye. In general, the aperture of the lens should be stopped down to provide enough depth of field (Bedford, 2017). Each of the numbers below represents a possible f-stop for that lens.

1 1.4 2.8 4 5.6 8 11 16 22 32

For instance, an  $f/11$  setting allows double the amount of light to pass, compared to an  $f/16$  aperture.

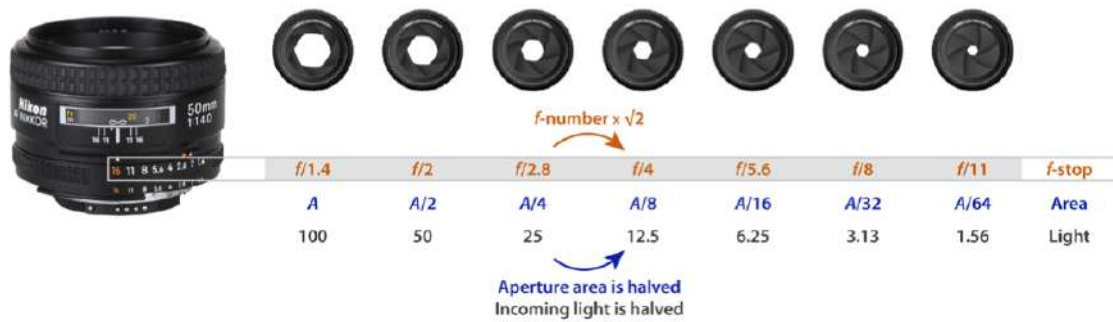


**Figure 34** Aperture measures and related image of the lens.

The shutter speed, on the other hand, controls how long the film is exposed to light passing through the lens. The shutter in a camera prevents all light rays from exposing the sensor until the shutter button is pressed. Then it opens and shuts again, enabling light to reach the image sensor for a set amount of time. This period is referred to as shutter speed. Seconds and fractions of a second are used to measure shutter speeds. A typical sequence is as follows:

2 seconds 1 second  $\frac{1}{2}$  second  $\frac{1}{4}$   $\frac{1}{8}$   $\frac{1}{15}$   
 $\frac{1}{30}$   $\frac{1}{60}$   $\frac{1}{125}$   $\frac{1}{250}$   $\frac{1}{500}$   $\frac{1}{1000}$

The interaction of aperture and shutter speed ensures that the proper amount of irradiance reaches the image sensor (Verhoever, 2016). They work together when the third value, ISO value, is left out of the exposure equation (as it happened with analog photography, when one has to physically switch the film to work with another ISO setting). Thus, changing one usually involves changing the other in the reverse way.

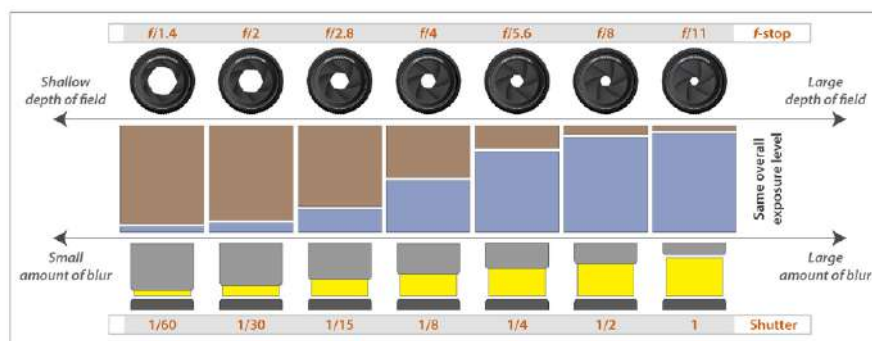


**Figure 35** Explanation of the reciprocal relationship with aperture and shutter speed (Verhoever, 2016).

Thus, the sensor sensitivity, ISO, describes the sensitivity of the film or sensor to incoming light. In digital imaging and so in photogrammetry, it really became an integral part of the whole exposure chain. The goal is to get clear, sharp photographs of the object. High ISO settings, however, give an

extremely light-sensitive device at the cost of grainy or noisy photos, that would require an image denoise process later (Apollonio et al., 2021). The higher the ISO, the greater the noise becomes. Compact camera photographs are frequently blurry from ISO 640 to ISO 800 due to their tiny photoites. The newest full frame D-SLRs, on the other hand, may readily be utilized up to ISO 3200 before noise becomes a concern (Verhoever, 2016).

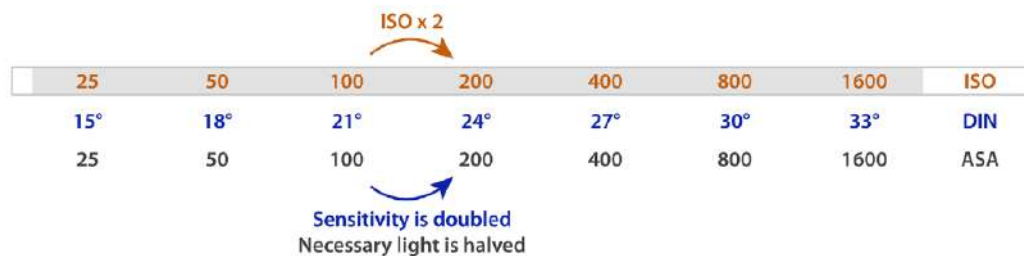


**Figure 36** Explanation of relative aperture and f-stop series.

Therefore, specific combinations of these three factors can produce distinct visual effects, even when the overall quantity of irradiance reaching the sensor remains constant. As the image noise is typical related to ISO value, Depth of Field (DoF) is strongly influenced by the aperture and the Motion blur, resulting from both subject movement as well as camera shake, by the shutter speed. The exposure triangle visually shows the ISO-A-S interplay.

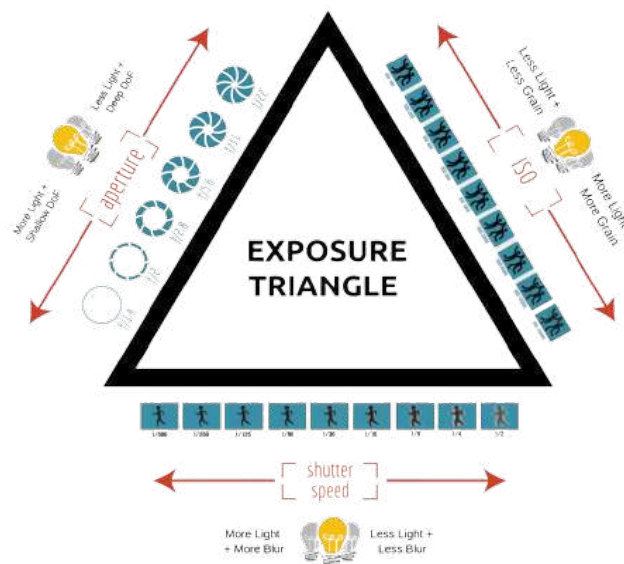


**Figure 37** The ISO-A-S triangle exposure.

Thus, the operator should select the quickest shutter speed allowed by the conditions (to limit the possibility of blurring), the lowest ISO setting feasible (to reduce picture noise), and the optimal aperture to keep sharpness and adequate depth of focus (typically between  $f/8$  and  $f/11$ ) throughout the subject (Bedford, 2017). This is a general rule, but specific cases involve specific issues and situations and thus rethinking camera parameters.

Macro photography, for example, generally suffers from restricted depth-of-field due to the low subject distances compared to the focal length of the camera lens. The options available to fill the image frame while keeping focus over the whole target region of the calibration plate are to reduce the aperture setting to a level where the depth-of-field is acceptable or to elevate the camera elevation such that the needed depth-of-field decreases (Collins et al., 2019, 4).

#### 4.2.2. Arrangement of lighting and associated filters

Now let us consider the case where the reflectivity of the artefact material requires the use of polarized lenses and polarized lights. Before beginning to photograph the artefact, it is also required to set up the lighting and associated filters, as well as configure the camera according to the precautions listed above. This technique impacted two of the objects in our inquiry sample (the titulus and the fibula).

Cross polarisation is a method that eliminates undesirable specular reflections by using two polarising filters, one on the light source and one on the camera lens (Ludwig, 1973).

As we mention in the section about object's intrinsic features (3.1.1. *Intrinsic aspects*), generally, natural light is unpolarized and becomes polarised once it goes through a polarisation material (*body reflection*) or it is reflected from a surface (*surface reflection*) (Miyazaki et al., 2004, 5). Thus, when light is reflected, it keeps its polarisation, whereas when it is dispersed, it loses its polarisation. Therefore, when we shine a polarised light onto an artefact, the glare is expressed through a polarized beam, while diffused light vibrates in any direction (Cosentino, 2013). The optical response to the beam emitted by the surface reflection in the forward direction is utilised in photography to reduce unwanted reflections in the image (Hong and Hilfiker, 2020).

In the case of fibula and titulus, we were interested in eliminating the glare produced by this surface reflected light, which can deform the representation of object topology and texture. To achieve this result, two lamps (with laminated polarising sheets in front) were placed symmetrically with respect to the object such that they formed a 45° angle with the object and the camera (placed in line, centre between the lamps) (Cosentino, 2013). Then, the final step is to attach a polarising filter to our camera and rotate the circular polarising filter to achieve the desired glare reduction. During the image acquisition, the rotating action of the filter should be repeated when the orientation of the object changes, and with it the direction of the beam from its surface (Miyazaki et al., 2004).

#### 4.2.3 Equipment and camera setting for the case studies

To summarise the experience with the selected four case studies with equipment and camera settings, I design the table below.

Model	Lens	Focal Length	Aperture	Shutter speed	ISO	Use of cross polarisation	Use of lights with polarised screen	Curtain made of black matte surfaces
Fibula LUHM13188c	Macro <sup>22</sup>	90mm	<i>f/32</i>	10sec	160	yes	yes	yes
Titulus LUHM21015.20	Macro	90mm	<i>f/32</i>	10sec	160	yes	yes	yes
Sword LUHM25561	Zoom lens <sup>23</sup>	70mm	<i>f/22</i>	1/4	800	no	no	yes
Vase LUHM32125.81	Zoom lens	55mm	<i>f/22</i>	1/4	1600	no	no	no

**Table 5** Equipment and camera setting for the four case studies.

---

<sup>22</sup> Tamron SP 90mm f/2.8

<sup>23</sup> Canon EF 24-105mm f/4L IS II USM



## 4.3. Image acquisition

«In photogrammetry, the quality of the output is almost wholly dependent on the quality of the input. Poor photography will inevitably lead to inaccurate results, so time spent familiarising yourself with the camera you intend to use, and considering the best image configurations for the subject, is seldom wasted. » (Bedford, 2017)

According to (Remondino and El-Hakim, 2006, 276) the accuracy of computed object coordinates is dependent on several factors:

- accuracy improves with the number of images in which a point appears, though measuring the point in more than four images' results in only slight improvement.
- accuracy is influenced by the number of measured points per image, with a more significant improvement if the geometric configuration is strong and the points are well defined and well distributed in the image.
- accuracy is also affected by image resolution, with a more noticeable improvement on natural features as compared to well-defined and resolved targets.

Thus, now it's time to focus on the capturing of the initial data, so the development of the images.

### 4.3.1. Turntable interval rotation

Thus, using the rotating table, the items were shot by slightly rotating it between each exposure, creating a circular camera network as the camera moved around the object (Apollonio et al., 2021; Bedford, 2017). Conventionally, a 10° interval rotation is used, producing 36 photographs per round (Apollonio et al., 2021). During the image acquisition of our four case studies, we tried to respect the interval of 10°. However, depending on the characteristics of the object and the accuracy of the model, the interval angle can be narrowed or widened, from 5° to 30°, but always allowing at least ⅔ overlapping between the previous and the next photograph, since photogrammetric reconstruction relies on the matching of features between pairs of photographs (Collins et al., 2019).

In this regard, (Barbieri and De Silva, 2019) revealed that significant overlap provided more 3D model features (with a lower rotation step). The findings of each mesh analysis were identical for models built with 40 and 20 photos (9° and 18° step). However, when the number of photos was lowered (step increased), the mistakes grew considerably. This is explained by a shortage of processing points and subsequent software interpolation. The best result (9°) demonstrated an average

inaccuracy of 7 m in a 2.4 mm length model, corresponding to a percentage error of 0.3%. The poorest result (27°) was off by 1.4% (Barbieri and De Silva, 2019).

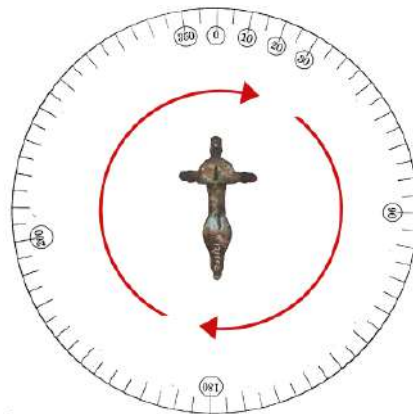


**Figure 38** Example of the turntable interval rotation with LUHM13188c.

#### 4.3.2. Camera height intervals

Furthermore, in order to photographically cover the entire object, the camera must be set at various heights (also depending on the height of the object) (Apollonio et al., 2021, 26). For small objects, images can be taken at **three height** intervals while the object rotates (Bedford, 2017; Collins et al., 2019). Calculating the angle based on the plane of the turntable, for our case studies, it was decided to shoot at 0°, so with the camera perfectly in front of the object, 30° and 60° (Fig. 39).

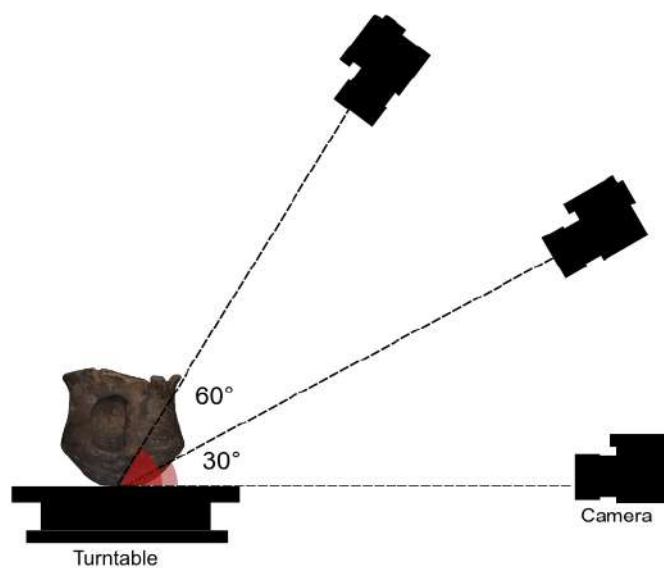


**Figure 39** Example of the camera height intervals with LUHM32125.81.

### 4.3.3. Artefact orientations

To achieve a photogrammetric reconstruction of small objects, it is necessary to place the object on a turntable in several different positions (Barbieri and Da Silva, 2019). Using only a single set of photographs gathered from a turntable will not provide enough information to completely reconstruct an artefact, as the underside of the object will not be visible (Collins et al., 2019, 2). The result of each turntable position will be a partial 3D model, which must then be registered and combined to form a complete 3D mesh through SFM processing (Pritchard et al., 2022). Moreover, to access a wider range of artefacts orientations, rubber pads can help (Fig. 42). It is also good to remember during acquisition to add the scalebar, such as the source of control data, that allow to scale the model subsequently. It is not necessary in every shot, but it is sufficient to integrate it into the context of the photo for at least one round (so in our case 36 photos). During our campaign, it was always added at the same time as the first orientation of the artefact, so as to be sure not to forget it later on.

However, planning the appropriate orientation for the artefact can sometimes be a challenging decision, especially if the object has thin sides, such as a card or a fibula, that has two main distinguishable faces (front and back) As a result, mistakes usually involve incorrect matching of points during automated alignment (Bedford, 2017, 13): sometimes precisely because of a failure to recognise the lateral conjunctions of two faces of the object.

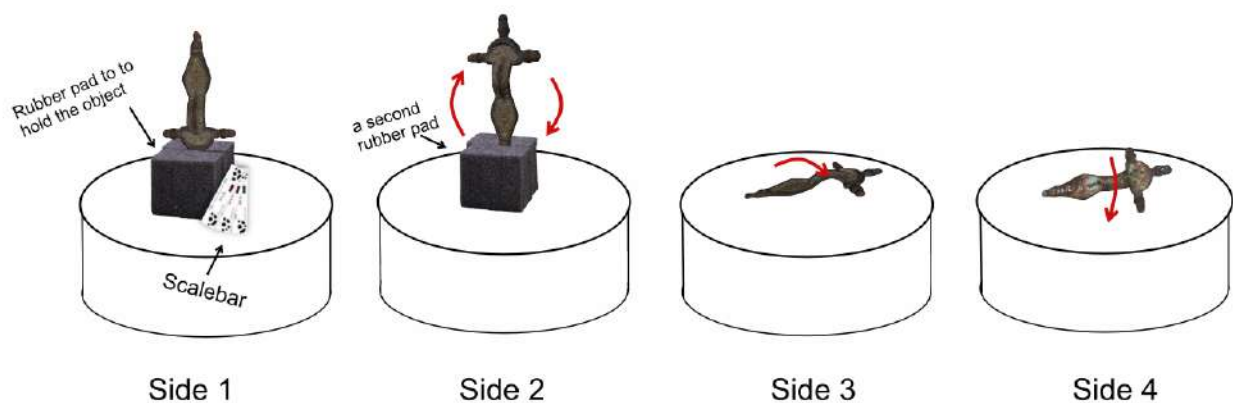


**Figure 40** The four artefact orientations used for LUHM13188c.

Hence, capturing both the upper and lower surfaces separately with adequate overlap between them is essential, and later merging the parts to create a single model. In certain cases, incorporating an additional set of images that cover the overlap area and are common to both sections of the model can enhance the reduction of noise in data along the edges of each half. (Bedford, 2017, 76)

Thus, to adhere to the statement of (Collins et al., 2019, 5), “during acquisition,  $M$  photographs are taken for each of  $N$  artefact orientations”. For the fibula, shown above (Fig. 40),  $N=4$  artefact orientations correspond to an  $M=36$ , so a degree of rotation of  $10^\circ$  was applied. But, while for *side 1* and *side 2* photographs were taken at three height intervals while the object rotates, in the case of *side 3* and *side 4* it was sufficient to take a single round of 36 photographs at a height of  $60^\circ$ , respectively, to allow a complete view (unobstructed by rubber pad) of the two main faces of the object, useful for the texture creation process.



**Figure 41** On the left, the frontal symmetric face of LUHM21015.20; on the right, its thin lateral side.

The alignment can be challenging sometimes if the face of the object is particularly symmetric and/or almost featureless (Koutsoudis et al., 2013) (Fig. 41). To prevent incorrect alignment and the need for a second acquisition campaign, the following strategy was employed. The rubber pads were changed for two different artefact orientations and, during a second round of photos (i.e. *side 2* of artefact orientation), an extra object was added to the close range area of the item on the turntable or directly on the object (as seen in Fig. 42).



**Figure 42** Disposition of LUHM21015.20 on the turntable with rubber pads. The first representation is relative to the first artefact orientation; the images on the centre and the right side are related to the second orientation.

The presence of a small rubber pad on the titulus helped accurately replicate its symmetrical geometry on the front and its subtitled lateral face (as shown in Fig. 43).

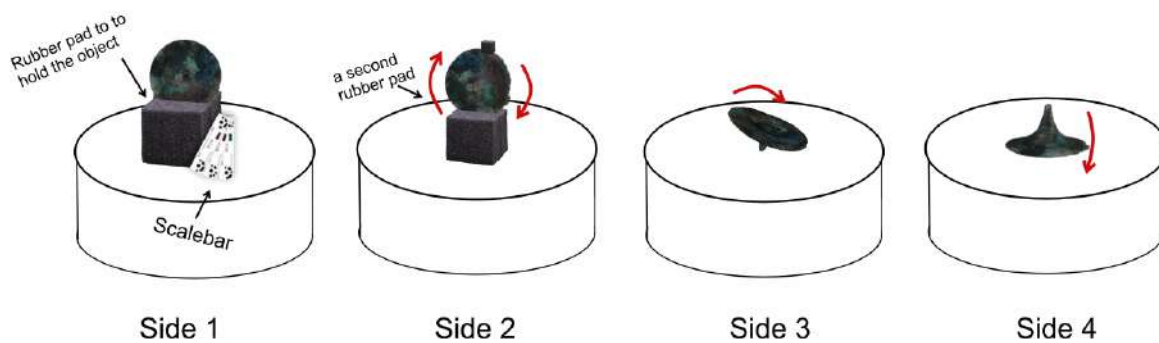


**Figure 43** The four artefact orientations used for LUHM21015.20.

So, to summarise the experience of these notions with the 4 case studies, the table below (Table 6) collects data on the number of photographs taken, the camera height intervals and the positions of artefacts during acquisition. The smaller objects needed a fourth position, already shown in the previous images, while the vase, having a relevant cavity in size, needed a few shots inside as well, reaching almost a 90° interval of the camera height with respect to the turntable.

	Fibula	Titulus	Sword	Vase
Photos	155	192	305 <sup>24</sup>	138
Camera height intervals	3	3	3	4
Artefact orientations	4	4	3	3

**Table 6** Number of photos, camera height intervals and orientations with different optical axis inclinations around the object.

#### 4.3.4. The use of polarized filter and lights with laminated polarizing sheets

“However, photogrammetric acquisition of ‘problematic’ artefacts such as small form-factor objects with challenging texture, optical properties or complex geometry can be achieved but requires *high attention and experience* to image acquisition.” (Collins et al., 2019, 2).

So, let us now turn to the cases where the characteristics of the surface and material require the cross polarisation of the light, so the use of a polarised filter (attached to the camera) and of lights with laminated polarising sheets (Fig. 44).

---

<sup>24</sup> I would like to explain, that in the case of the sword, the high number of photographs compared to the average is mainly due to my initial inexperience. It was in fact the first of these four objects on which I experimented, and having reached an optimal result, we did not consider the option of redoing the model with a reduced number of photographs, which is certainly possible.

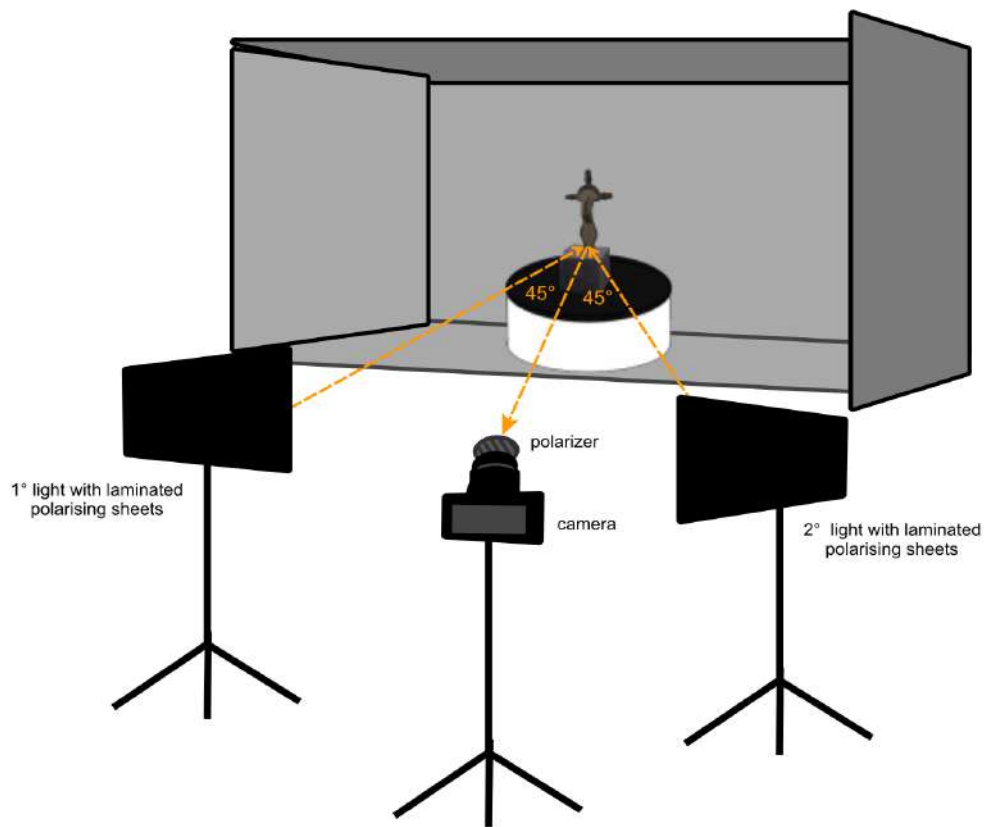


**Figure 44** Arrangement of the polarised filter (attached to the camera) and of lights with laminated polarising sheets, during the camera acquisition. The model shown in the figure is LUHM13188c.

Therefore, the application of polarised light to an artefact results in glare being expressed as a polarised beam and diffused light oscillating in any direction (Cosentino, 2013). To mitigate unwanted reflections in images, photography leverages the optical response of the surface reflection beam emitted in a forward direction (Hong and Hilfiker, 2020).

When you place the filter on the lens and view the framed scene, you will observe the change in colours in the image as you rotate the filter. By turning the filter by a quarter, you will achieve complete polarisation of the beam. If you rotate it by another quarter, for a total of half a rotation, you will return to the initial situation (Hong, 2020).

When the orientation of the object (Fig. 45), and therefore the direction of the beam from its surface, changes during picture capture, the rotating operation of the filter should be repeated (Miyazaki et al., 2004). Because the Brewster curve, which helps to explain the reflection and refraction of light as it passes through a medium, is affected by both surface normal and viewer direction, it is not invariant as the object rotates (Miyazaki et al., 2004, 13)

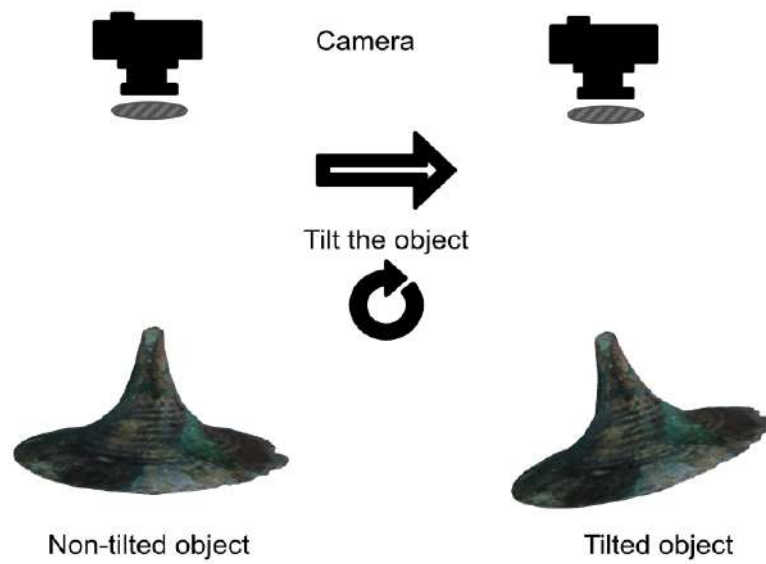


**Figure 45** Object rotation in relation to the camera and polarizer. The model used is LUHM21015.20.



## 5. Third phase of the survey: 3D photogrammetric processing

The camera acquisition process has produced its inputs. We now have 2D resources at our disposal and it's time to choose the software that will transform them into a 3D model. For the purpose of the four case studies presented, we utilized Metashape Agisoft Pro, a cost-effective 3D reconstruction software from Agisoft LLC in Russia. Agisoft has substituted Photoscan with Metashape, which also offers the option of cloud-based processing, allowing for cost savings on hardware (De Paolis et al., 2020). Metashape uses digital photos of objects or scenes, both metric and non-metric, to automatically generate precise textured 3D models and it is available in both Standard and Pro versions (Rahaman and Champion, 2019).

Comparisons of the various software options available for Structure from Motion (SfM) are well documented (Ronchi et al., 2022; Cotugno et al., 2022; Nguyen et al., 2012; Koutsoudis et al., 2013; Remondino et al., 2017; Nocerino et al., 2017; Rahaman and Champion, 2019).

In the following pages, we will provide a theoretical explanation of the main steps of image base modelling processing, with a focus on the practical examples demonstrated through the use of Metashape. The photogrammetric workflow typically consists of the following steps (Fig. 46).

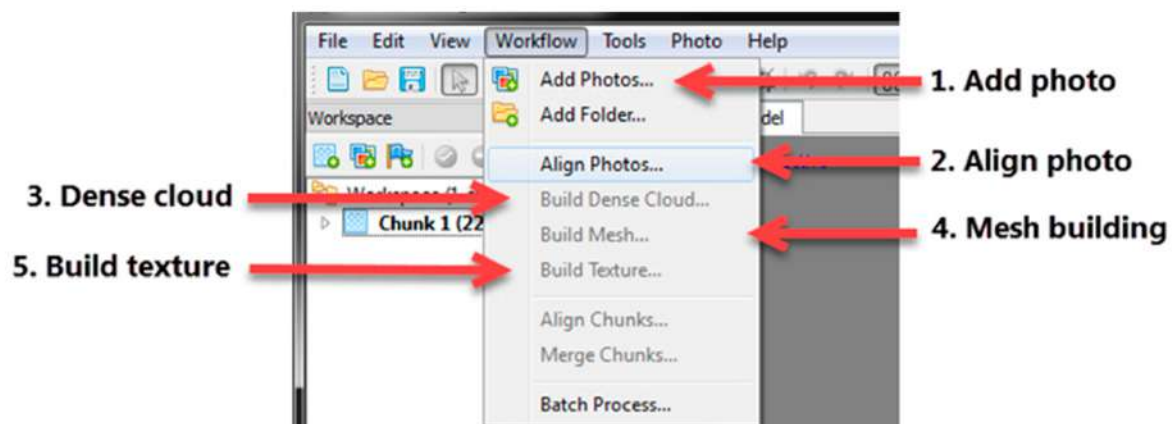


**Figure 46** A sample of typical workflow offered by Metashape (PhotoScan) GUI (Rahaman and Champion, 2019).

## 5.1. Feature matching

Thus, it is time to feed our input into the software that deals with image analysis, the definition of geometrical patterns and their reconstruction, summarised by (Rahaman and Champion, 2019, 1836) as *feature detections, matching, triangulation* (or align photos).

All photographs should be examined before going through the process, primarily to remove those of poor quality, typically those that are completely out of focus or display considerable motion blur because of either faulty camera settings or the usage of video frames (Bedford, 2017, 14). Some software has an estimating image quality functionality; however, none of their approaches are flawless, and a visual check of the inputs is always recommended before processing begins (Bedford, 2017, 14). Images having a quality value of less than 0.5 units should be deactivated and hence eliminated from the alignment and texture creation processes (Agisoft, 2023). On Metashape, you can use the *Deactivate button* on the *Photos pane toolbar* to disable a photo. Once the quality of the input has been verified, we can proceed with image alignment.

Regarding alignment, the software identifies stable points as potential points of interest in the source photographs by isolating points located at the extrema of the Difference-of-Gaussian function in scale space (Nguyen et al., 2012). These points are chosen as they remain unchanged despite changes in perspective and illumination. The software then generates a description for each point based on its surrounding area (Nguyen et al., 2012). These descriptors are then utilised to find correspondences across photographs. Image correspondences (or tie points) are therefore retrieved using the best detector and (float or binary) descriptor methods available: SIFT and all its variations (ASIFT, ColSIFT, PCA-SIFT, SIFT-GPU, DAISY, and so on), SURF, FAST, BRIEF, ORB, LDAHash, MSD, and so on (Remondino et al., 2017). In recent years, indeed, automatic photogrammetric matching algorithms created for terrestrial photos have largely replaced manual image measuring, which is today time-consuming and impracticable (Remondino and El-Hakim, 2006, 276).

The Agisoft Metashape technique uses the widely known SIFT approach to increase alignment quality by integrating several algorithms (Agisoft, 2023).

The Scale Invariant Feature Transform (SIFT) approach is a commonly used computer vision technique in photogrammetry for identifying and describing distinct features in photographs (Xu et al. 2022). The SIFT method identifies key points or regions of interest in a picture, such as corners and edges, and generates a descriptor vector that describes the geometric structure and appearance of these points. This approach is well-known for its ability to recognise and characterise features reliably and robustly in the presence of picture deformations such as rotations and scale shifts (Xu et al. 2022).

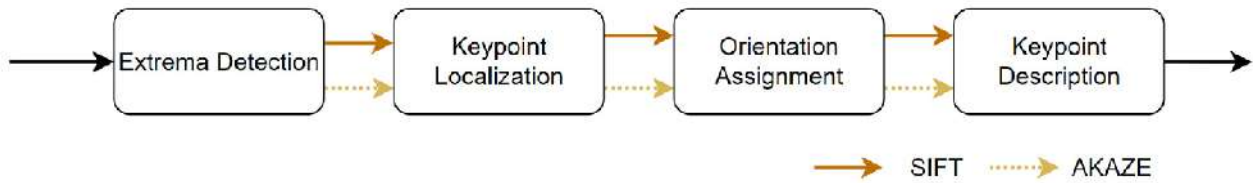


**Figure 47** Flowchart of feature extraction, in a comparison among SIFT and AKAZE (Xu et al., 2022, 5).

These (single or combined) approaches give a collection of key points together with a vector of information that may be used for successive matching and tie point identification (Remondino et al., 2017). The brute force method based on the Hamming distance, a conventional L2-Norm matching strategy, or the productive FLANN - Fast Library for Approximate Nearest Neighbours strategy, which is independent of the image acquisition protocol and implements a fast search structure, are commonly used for key point matching (e.g. based on kd-trees) (Remondino et al., 2017, 595).

In Metashape, the “*Align photos...*” command activate the algorithm.

One of the criteria in the alignment process is the level of accuracy. The "high accuracy" setting improves accuracy by processing photographs in their original size. The "medium accuracy," "low accuracy," and "lowest accuracy" choices, on the other hand, allow for a factor of 2, 4, and 8 downscaling along each picture dimension (De Paolis et al., 2020). For the purpose of efficient assessment, using “low” accuracy in the quality assessment of captured photos is often sufficient, especially when conducting on-site evaluations with the intention of later refining the model with higher accuracy (“high” or “medium”), which can require a very long-time processing (De Paolis et al., 2020). If the alignment produces satisfactory results with “low” accuracy, it is highly likely to perform even better with the higher accuracy settings.

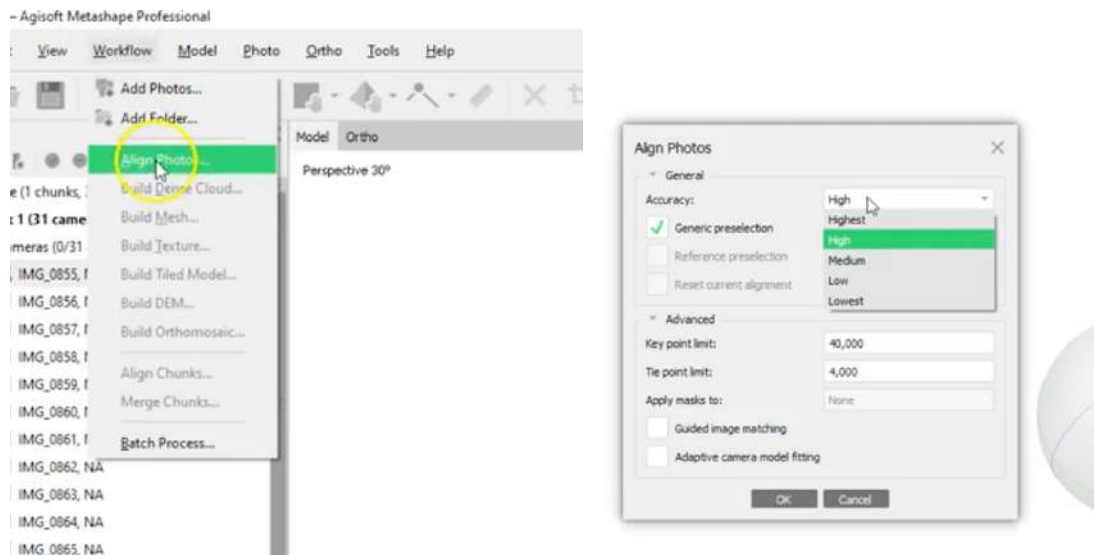


**Figure 48** Align photo menu of Agisoft Metashape Professional.

The feature matching process can be performed on both masked and unmasked photographs. Apply mask to tie points option means therefore that certain tie points are ignored from alignment procedure. As result, troublesome parts of photos can be masked in certain applications to remove aspects that do not need to be rebuilt, such as sky, logos, fiducial markers, or moving objects in a scene (Bedford, 2017). This can save a significant amount of time later on in the process (Bedford, 2017). Additionally, using a single-color background with good contrast, ideally a dark colour to eliminate shadows, can enhance the process (Kaufman et al., 2015). Research has shown that the time required to mask each digital image is significantly reduced when using a uniform and recognizable background (Kaufman et al., 2015).

Images that cannot be aligned correctly can be either removed if there is sufficient redundancy in the inputs, or manually aligned with the addition of local control points (Bedford, 2017, 14).

## 5.2. Bundle adjustment

The tie points extracted from the images are utilized to determine all unknown parameters, including camera positions and angles, camera interior parameters, and 3D coordinates of image points, through a process known as Bundle Adjustment (BA) (Remondino et al., 2017).

(Rahaman and Champion, 2019, 1836) refers to this step as *sparse reconstruction*, *bundle adjustment*, or *point cloud generation*. The term "bundle" refers to the set of optical rays that connect the camera

projection center, the measured image point, and the corresponding 3D point in object space, based on the collinearity condition or central perspective camera model (Remondino et al., 2017).

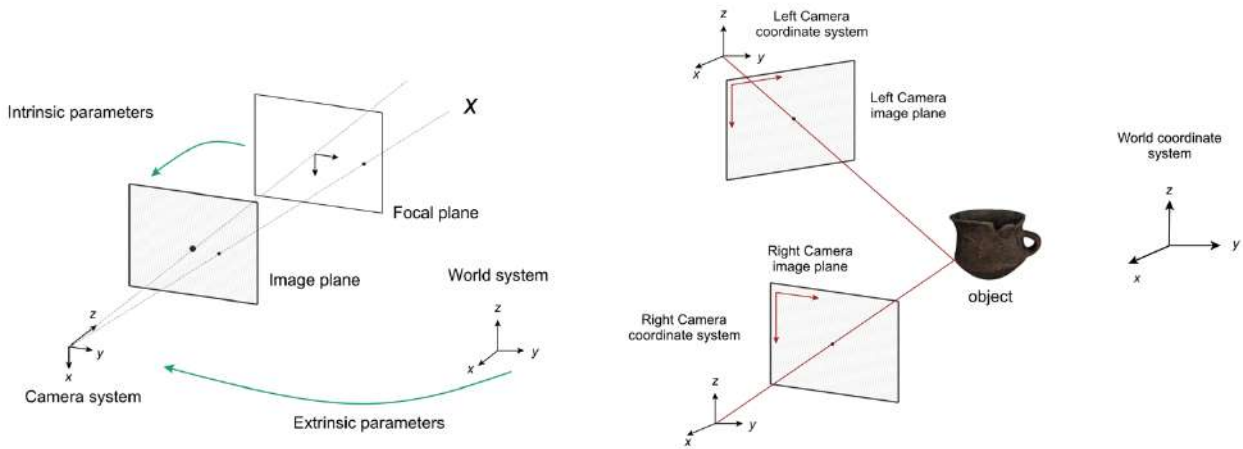


**Figure 49** Camera calibration mechanism.

Hence, Bundle Adjustment refers to the process of optimally and jointly arranging the bundle of optical rays from the images to the 3D object points to reconstruct both the 3D scene and camera parameters iteratively (Remondino et al., 2017). The objective of this stage is to determine the geometry of the scene and the camera's motion information, including its extrinsic parameters (position and orientation) and intrinsic parameters for the captured images (Nguyen et al., 2012, 4). This is accomplished using the Structure from Motion (SfM), the most common algorithm which find out correspondences among features in multiple images (feature matches) (De Paolis et al., 2020).

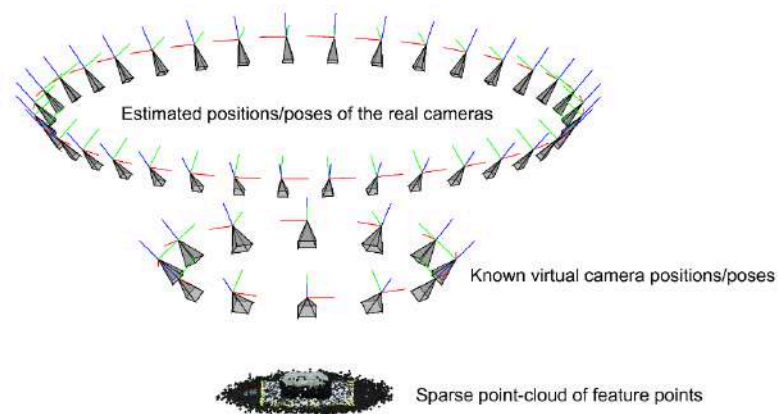


**Figure 50** Results from the estimation of camera properties and geometry. At the bottom of the figure, the sparse point-cloud formed from the feature points matching (Collins et al., 2019, 7).

The Levenberg-Marquardt method has been widely regarded as a top-performing solution for the Bundle Adjustment (BA) process due to its ease of implementation and its efficient damping strategy, which allows for quick convergence from a broad range of starting points (Remondino et al., 2017). By determining the actual camera positions relative to a fixed, calibrated set of features, accurate scale factors are automatically established. In the final step, virtual images are removed from the image set, and only the actual images and their corresponding calibrated camera parameters are used for the dense point-cloud reconstruction (Collins et al., 2019).

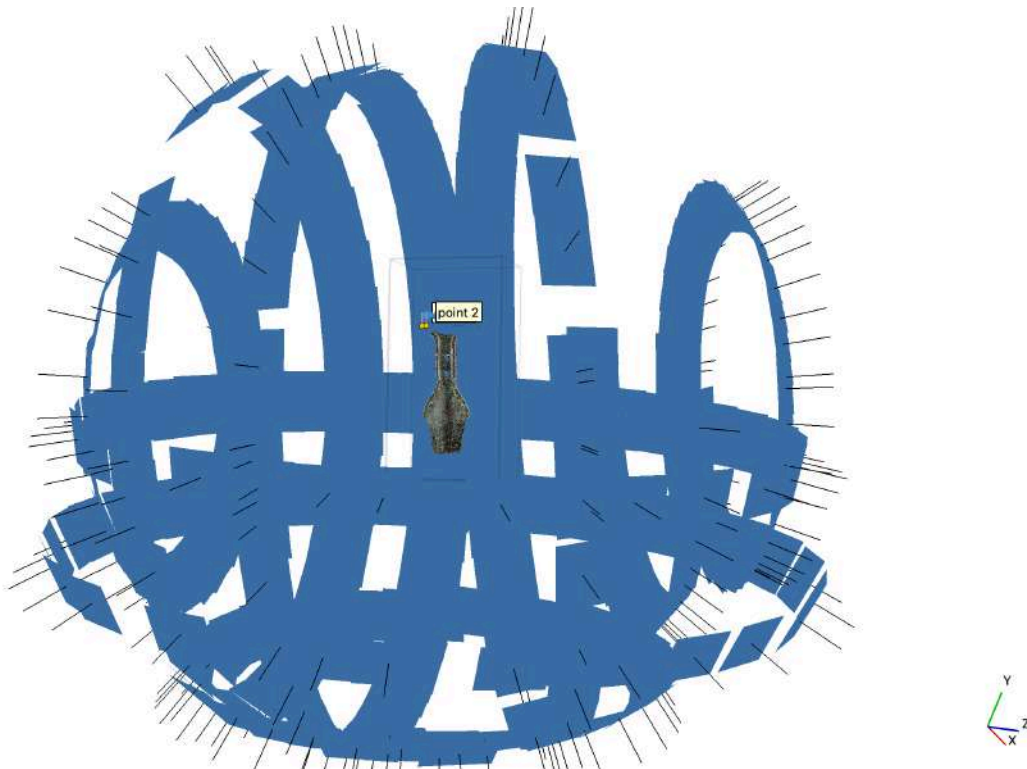


**Figure 51** Result of the camera calibration and the generation of the sparse cloud.

In some photogrammetry software, sparse point clouds can be refined by filtering out points with significant re-projection errors or low accuracy in their reconstruction (Bedford, 2017). The *re-projection error* refers to the discrepancy between the observed image coordinates of matched 2D points and the calculated values derived from the adjustment process. It can be represented as the Euclidean distance between the manually or automatically recorded image point and the position of the corresponding 3D point, as projected back into the image (Remondino et al., 2017).

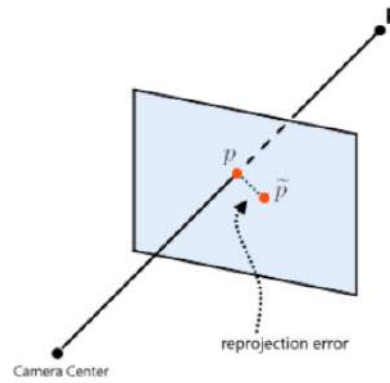


**Figure 52** The reprojection error is the distance between the projected image point  $p$  and the observed image point  $\tilde{p}$  (Nguyen et al., 2012).

In a perfect scenario, the reprojection error of a 3D point generated from only two images would be zero. However, factors such as noise in image measurements, inaccurate camera positions, and unmodeled lens distortions often result in deviations from zero (Nguyen et al., 2012). It is generally recommended that the Root Mean Square Error (RMSE) should be less than 1 pixel for accurate reconstruction, according to the rule “the smaller the value, the better the accuracy of the reconstruction” (Remondino et al., 2017). It's advisable to avoid filtering the sparse point clouds more than three times, as this may introduce a "stepping" effect into the model and, besides, removing too many points during filtering could compromise the reconstruction process (Bedford, 2017). If the input images produce high reprojection errors that cannot be reduced, it may indicate poor image quality or difficulties in accurately determining camera calibration parameters (Bedford, 2017).

In Metashape, therefore, there is the *Gradual Selection* command from the *Model* menu (Agisoft, 2023), to detect and delete the point with a high reprojection error.

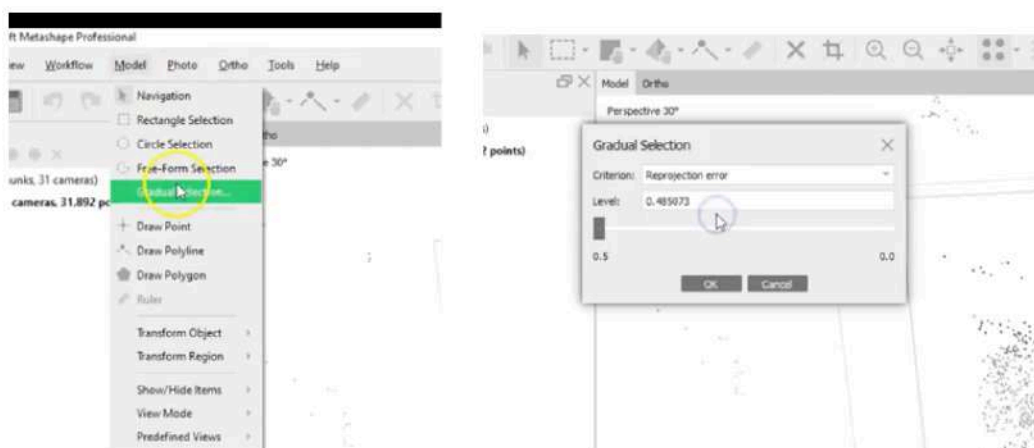


**Figure 53** Gradual selection and Reprojection error windows of Agisoft Metashape Professional.



Before going on, we decided to scale the cloud using a reference (i.e. the scalebar shot together with the artefact). In Metashape the user can create markers directly by pointing them on the images (Add Marker) and placing it in the correct position (Place Marker), also by moving and drag the point on the image (Agisoft, 2023). On the left, a window shows the markers, and from this section, the user can select the two points and create the scalebar, declaring the distance between them.

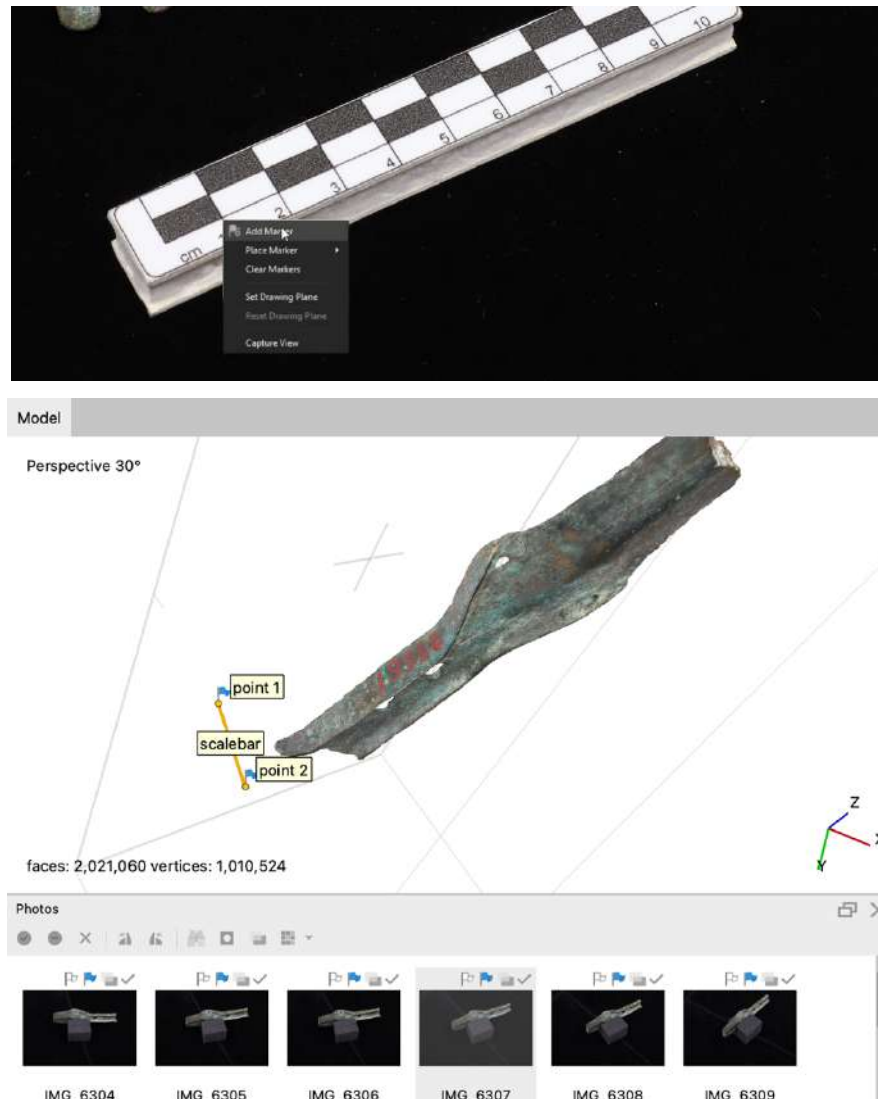


**Figure 54** Screenshot of *Add Marker* action, by pointing on the images and click right button on the mouse (top); result of the scaled model in Metashape (bottom).



### 5.3. Dense reconstruction

After obtaining the camera positions and the sparse set of 3D coordinates from triangulated tie points, the next step is to enhance the resolution of the 3D representation by applying a pixel-based matching algorithm to establish dense and colorized 3D point clouds (Remondino et al., 2017). This process, also known as *dense correspondence matching* (Rahaman and Champion, 2019), involves filling in the gaps in the sparse point cloud to create a denser and more comprehensive representation of the scene. The result of this densification process is a dense point cloud (Rahaman and Champion, 2019, 1836). The approach involved is the MVS (Multiview stereo) matching and reconstruction (Collins et al., 2019). PMVS2 (Patch Multi-View Stereo vision 2)<sup>25</sup> and CMVS (Clustering Views for Multi-view Stereo)<sup>26</sup> are algorithms used for large-scale, multi-view stereo reconstruction: the first one is included in the CMVS package, and they both were developed by Yasutaka Furukawa.

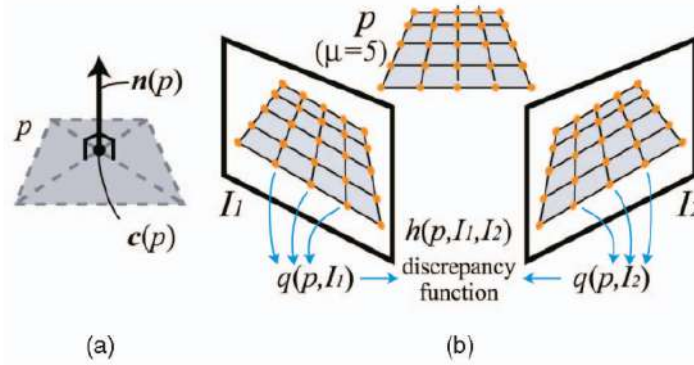


**Figure 55** (a) A patch  $p$  is a three-dimensional rectangle with centres and normal represented as  $c(p)$  and  $n(p)$ , respectively. (b) A patch's photometric discrepancy  $f(p, I_1, I_2)$  is equal to one minus the normalised cross correlation score between sets of sampled pixel colours  $q(p; I_i)$  (Furukawa and Ponce, 2010, 1364).

(Furukawa and Ponce, 2010) helped me to describe in the following line the functioning of the algorithms. Thus, the open sources PMVS2 and CMVS operate by utilizing the camera parameters, such as position, rotation, and focal length, which are outputted by the SfM (structure from motion) algorithm. PMVS2 specifically computes 3D vertices in regions that were not correctly detected or matched by descriptors. It does so by utilizing the known camera parameters to project pixels from one image onto lines in another image through a process known as *epipolar geometry*. This simplifies the matching process compared to SfM, which searches through the entire 2D image for matches. MVS also considers illumination and object materials in its optimization, whereas SfM does not.

<sup>25</sup> PMVS2. DIENS. <https://www.di.ens.fr/pmvs/>

<sup>26</sup> CMVS. (s.d.). DIENS. <https://www.di.ens.fr/cmvs/>

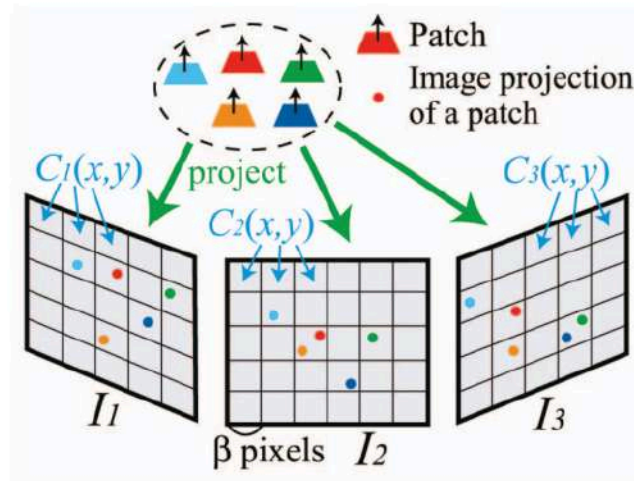


**Figure 56** They use visible pictures to keep track of image projections of reconstructed patches to execute essential tasks like as accessing nearby patches, enforcing regularization, and so on (Furukawa and Ponce, 2010).

However, PMVS2's complex optimization can be slow and consume a large amount of memory for large image sequences, leading to the use of CMVS. CMVS clusters the coarse 3D SfM output into regions, allowing PMVS2 to be executed on each cluster in parallel, and then merges the outputs into a unified detailed model (Collins et al., 2019).

The mechanism of the Metashape command “Build Dense Cloud” from the Workflow menu (Agisoft, 2023) follows these algorithms.

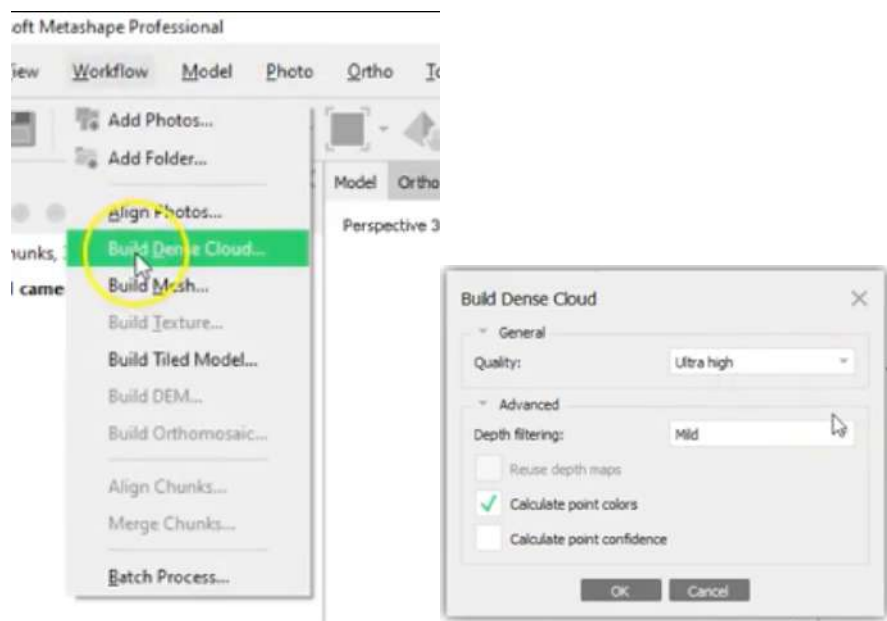


**Figure 57** Build Dense Cloud button and menu on Agisoft Metashape Professional.

## 5.4. Network triangulation

Following the above-described point-cloud registration and merging procedures, the points must be connected to form a surface mesh before texturing can be applied (Collins et al., 2019). The triangulation is the process of converting a given collection of points into a consistent polygonal representation. This method creates vertices, edges, and faces (representing the surface under consideration) that only intersect at common edges. Finite element techniques are used to partition the measured domain into many tiny elements, often triangles or quadrilaterals in two dimensions and tetrahedra in three dimensions (Remondino and El-Hakim, 2006).

Polygons are often the most adaptable approach to correctly capture the results of 3D measurements, offering the best surface description (Remondino and El-Hakim, 2006). Surface reconstruction is also known as surface triangulation or network (mesh) creation (Rahaman and Champion, 2019).

(Remondino and El-Hakim, 2006) broadly categorized the numerous techniques for surface generation basing on the way the input data is organized:

- *Unstructured point clouds*: These algorithms rely solely on the spatial position of the input data, without making use of any assumptions regarding the object geometry or the adjacency or connectivity of the points. Before generating a polygonal surface, the points are often structured based on their coherence. However, these algorithms require a well-distributed input data, and may not work well if the points are not uniformly distributed.
- *Structured point clouds*: In contrast, algorithms that work with structured data can take advantage of additional information about the points, such as breaklines or coplanarity.

For its relative simplicity and reliability, Poisson-based methods is at the core of almost all surface reconstruction programs, Metashape included<sup>27</sup> (Collins et al., 2019). Thus, the screened Poisson-based surface reconstruction method is used to create a smooth 3D geometry from an unstructured point cloud. It is the most popular technique but is sensitive to the normal of the input points (Xu et al., 2022, 8).

---

<sup>27</sup> This method corresponds to the “Build Mesh” command in the Workflow menu of the programme.

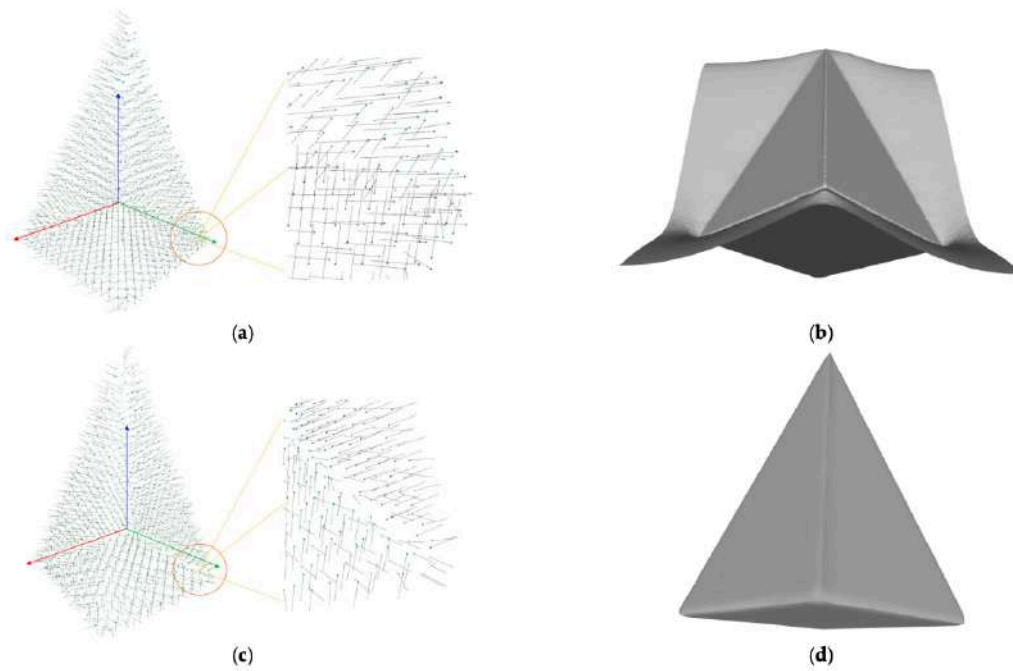


**Figure 58** The following are the results of normal orientation and meshing: (a) default point normals; (b) mesh before normal orienting; (c) point normals after orienting; and (d) mesh after normal orienting. (Xu et al., 2022, 8).

Furthermore, mesh creation can be followed by mesh editing. The user is taken through a series of automatic stages that run on the Cloud to delete triangles with edge lengths greater than the average mesh resolution and to reject isolated mesh components or islands, as well as self-intersecting and non-manifold triangles (Nocerino et al., 2017). Therefore, in certain circumstances, the mesh construction is followed by a technique to build a lighter geometry supported by a reduction criteria, more specifically the D/d ratio, and normal map, decreasing mesh complexity in terms of the number of vertices, the regularity of the connection, the quality of the triangular shape, and the sample distribution on the surface (Apollonio et al., 2021). Its polygon count is the result of several considerations based on the degree of proximity and the quality of perception that the final user needs to achieve inside the interactive application the asset is designed for (Apollonio et al., 2021).

## 5.5. Texturing

After the mesh has been built, the next phase is the texture generation (Rahaman and Champion, 2019), which includes the generation of the colour information necessary to represent the subject in a more realistic manner (Dischler and Ghazanfarpour, 2001). Additionally, the colour information offered by the dense point cloud and that generated by the texture should not be mixed up. Through the dense point cloud, we can see a colourful model that looks like a model but it is not. Rather, it is

merely a point cloud, which can be mistaken for a 3D object because of how many and how closely the dots are spaced (Fig. 59).

Instead, the software applies the texture by creating a 2D (bidimensional) object that represents the 3D one (Polo et al., 2022). In order to define the precise look (i.e. texture) of each face of the mesh, its building method really refers back to the original sets of images and the camera location information calculated during the sparse point-cloud reconstruction (Collins et al., 2019).

There are methods to optimize the texturing procedure in the image-based modelling pipeline to get a greater geometric definition in relation to the texture quality (Bolognesi and Fiorillo, 2018): The texture mapping is the one utilised by Metashape (Polo et al., 2022).

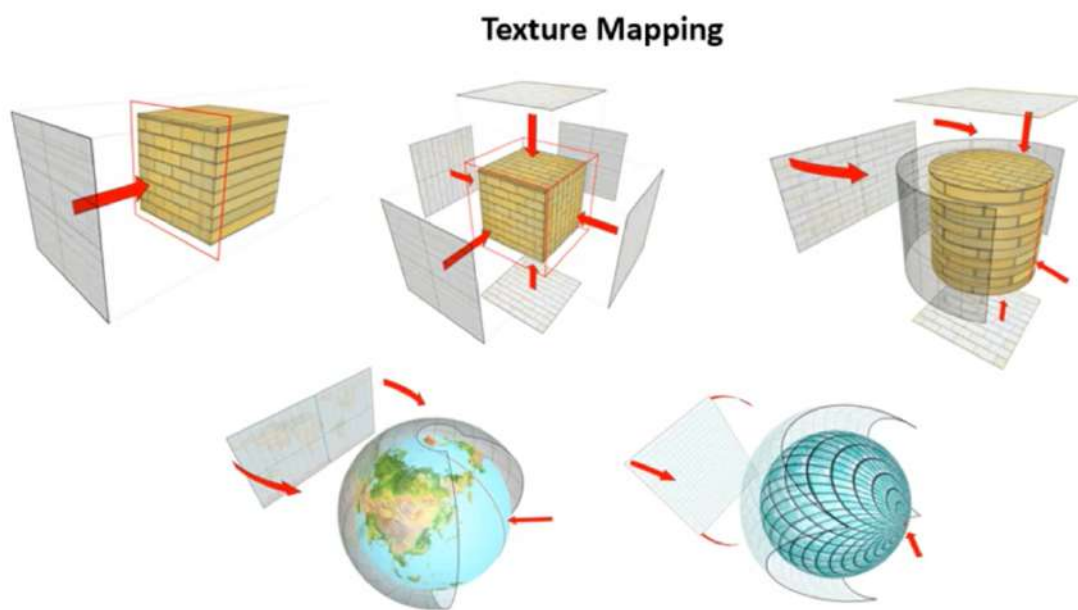


**Figure 59** Example of texture mapping mechanism.

When generating a texture map in Metashape, the software creates a photomosaic and applies it to the mesh geometry (Yamafune, 2016). The "Build Texture" stage of the workflow includes several adjustable settings that impact how the software works on the 2D sources to generate the texture map. One of these settings is the "Mapping Mode," which determines the orientation of the texture on the model. The available options are "Generic," "Adaptive Orthophoto," "Orthophoto," "Spherical," "Single Camera," and "Keep UV" (Agisoft, 2023).

The default setting is "Generic," which automatically selects the best photos for composing a UV atlas to convert the 3D mesh into a 2D texture canvas. This mode is ideal for models with complex 3D structures (Christopher and Yamafune, 2018). The "Orthophoto" setting creates a photomosaic from a top-down view plane and applies it to the mesh from one direction. The "Adaptive Orthophoto" setting specifically targets vertical surfaces and generates textures for those areas independently. The "Spherical" mode creates a UV map for spherical structures, while the "Single Photo" mode generates

a texture based on a single chosen photo. If a UV map, such as a 2D atlas for textures, or a canvas on which textures can be projected, has already been created in another program, the "Keep UV" option allows Metashape to import it (Agisoft, 2023).

The "Blending Mode" is another sub-setting in the "Build Texture" stage. It determines how the colour values of the texture map are calculated, whereas the mapping mode options determine the method for projecting the texture map onto the mesh (Christopher and Yamafune, 2018). The available options for blending mode are: "Mosaic," "Average," "Max Intensity," "Min Intensity," and "Disabled." By default, the blending mode is set to "Mosaic," which chooses pixels from the source photos that are closest to the centre of the images (Yamafune, 2016). The "Average" option calculates an average pixel value or RGB colour of the assigned photos and uses those values as textures. "Max Intensity" uses images with the brightest pixels to form the textures, while "Min Intensity" uses images with the darkest pixels. The "Disabled" option is used when the imported model already has suitable textures (Agisoft, 2023).

Once the photogrammetric mesh and texture are complete, the mesh model for each artifact should be exported as .stl or .obj file. (Christopher and Yamafune, 2018)



**Figure 60** Results of the four steps (feature matching, bundle adjustment, network triangulation and texturing) for the object LUHM25561. From left to right: sparse point cloud, dense point cloud, solid model (mesh), textured model.

## 6. Guiding the 3D photogrammetric survey

The steps, both theoretical and practical, that enable a good planning of a 3D photogrammetric acquisition campaign have been therefore analysed. As mentioned in the introductions, four case studies have guided us during this study and the following semi-automatic procedure is correctly applied to them, which is intended to be a widely extendable and improvable test sample. The graph path is divided into a few macro areas (Object description, Environment, Project purpose and definition) and is developed with closed questions and answers, which the users select according to the acquisition project they have in mind.

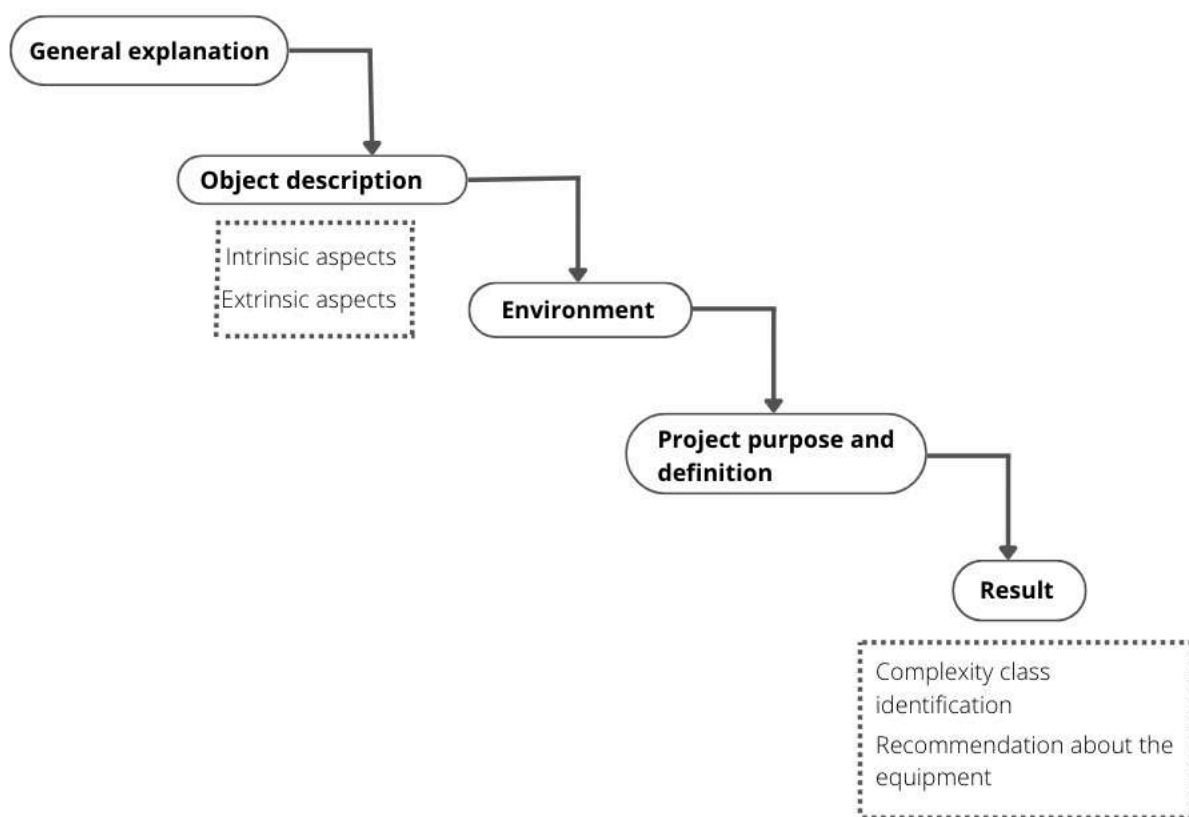


**Figure 61** Overview of the macro areas proposed by the semi-automatic procedure written with Twine.

The open-source program Twine, in its most recent release *version 2.6.1.*, has been used to create this interactive and nonlinear path. Chris Klimas developed the software tool Twine to make it easier to create interactive stories using cross-textual connections on web pages. Twine allows for the branching of lines in accordance with the format of book games and traditional adventures.

Because of its malleability and its highly interactive nature, it seemed to us to be the right tool to describe a process that is highly shaped by the needs of the user and his or her acquisition campaign, but nevertheless tied to objective evaluation parameters and set in a predetermined order, which is why we called it 'semi-automatic'.



## 6.1. Result of the semi-automatic procedure in Twine

The result of the adopted procedure was published through a Twine Html page in Github at the following link: <https://luisammi.github.io/Digital-Heritage-and-Multimedia-Thesis/main.html>

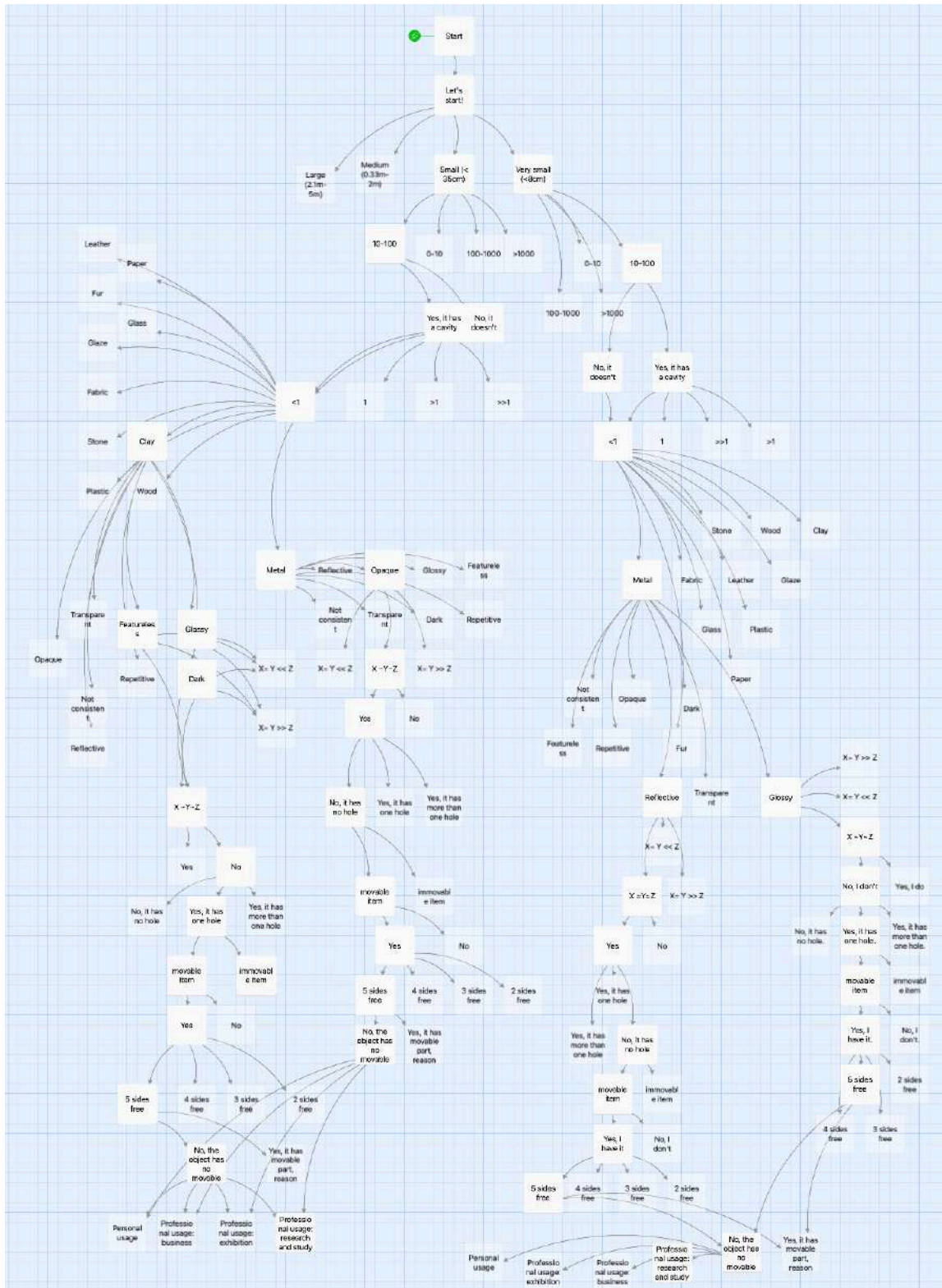


Figure 62 Structure of the decision tree (graph) obtained with Twine Version 2.6.0 (2.6.0).



# Conclusion

By presenting theoretical arguments and practical application examples, the thesis has demonstrated the importance of treating 3D digital data acquisition as a process with specific stages and interdependent parameters that require careful assessment and planning. The 3D modelling field has seen exponential growth in the last decades, leading to the emergence of various platforms for visualizing and studying three-dimensional objects. These applications have highlighted the impact of technology on the archaeological field, serving as both a "tool" to be passively deployed and a "medium" or "science" capable of influencing interpretation and research direction.

In the case of accurate 3D digitisation of movable cultural heritage objects, the process involves an initial classification phase of the artifact, followed by the planning phase of appropriate instrumentation based on the prior assessment, then the stage of setting study and image acquisition, and finally, data processing with reference software. The study emphasizes the importance of considering complexity (of the object and its 3D replica) as a critical factor in determining the necessary effort for a 3D digitisation project to achieve the desired output quality.

Moreover, the thesis highlights that there is a specific intentionality behind the 3D data acquisition process for cultural heritage artifacts, which influences the output quality and process complexity. In the absence of a comprehensive understanding of the project's objectives and the target audience, the investment and endeavour relating the technicalities becomes self-serving pursuit that fails to fully leverage the potential of new technological tools for enriching the value of the Cultural Heritage. Thus, it is impossible to separate the data acquisition stage from the previous cultural interpretation, which forms the basis of intervention choices and the theory of historical conservation and knowledge dissemination.

Furthermore, the context of constructing and implementing an acquisition campaign plays a vital role, and the reality is that not all museums and cultural institutions can keep up with the digitalisation of their heritage. The prototype proposed on Twine in this thesis proves how it may be feasible to cure a semi-automatic procedure for creating 3D models. It is designed to be an informative and guided path, which does not discriminate against inexperienced operators, but rather allows them to move around the field with greater confidence.

In conclusion, it demonstrates how to tailor the right outfit to a survey campaign through a matrix, of which the design of a branch has been traced, concerning a range of small-to-medium complexity objects, but which has the potential to be widely expanded and enriched.

# References

Addison, Alonso C.; Marco Gaiani. 2000. "Virtualized architectural heritage: New tools and techniques". *IEEE Multimed* 7, 26–31.

Agbe-Davies, Anna S., Jillian Galle, Mark W. Hauser and Fraser D. Neiman. 2014. "Teaching with digital archaeological data: A researcharchive in the university classroom". *Journal of Archaeological Method and Theory*, 21(4), 837–861. doi: 10.1007/s10816-013-9178-3.

Agisoft. 2023. "*Metashape User Manual. Professional Editio Version 2.0*".

Angulo, Antonieta and Vasquez de Velasco, Guillermo. 2007. "Digitally integrated practices: a new paradigm in the teaching of digital media in architecture". *Arquitetura Unisinos (Brasil)* Num.2, Vol.3.

Amico, Nicola, Paola Ronzino, Achille Felicetti and Franco Niccolucci. 2013. "Quality management of 3D cultural heritage replicas with CIDOC-CRM." *CRMEX@TPDL* (2013).

Apollonio, Fabrizio Ivan, Filippo Fantini, Simone Garagnani, and Marco Gaiani. 2021. "A Photogrammetry-Based Workflow for the Accurate 3D Construction and Visualization of Museums Assets" *Remote Sensing* 13, no. 3: 486. <https://doi.org/10.3390/rs13030486>

Arias, Francisco, Carlos Enríquez, Juan Manuel Jurado, Lidia Ortega, Antonio Romero-Manchado and Juan José Cubillas. 2022. "Use of 3D models as a didactic resource in archaeology. A case study analysis". *Herit Sci* 10, 112. <https://doi.org/10.1186/s40494-022-00738-x>

Atkinson, Gary A., and Edwin R. Hancock. 2005. "Analysis of Directional Reflectance and Surface Orientation Using Fresnel Theory." *Lecture Notes in Computer Science*, 103–11. doi:10.1007/11578079\_11.

Awati, Rahul. 2022. "What Is a Dielectric Material and How Does It Work?". *WhatIs.com*, June 1. <https://www.techtarget.com/whatis/definition/dielectric-material>.

Baldissini, Simone, Marco Gaiani and Remondino, Fabio. 2010. "Rilievo, gestione e mappatura del colore" in *Modelli Digitali 3D in archeologia: Il caso di Pompei*. Edizioni della Normale. Scuola Normale Superiore Pisa: 200-235

Barbieri, Gabriel, and Fabio Pinto da Silva. 2019. "Acquisition of 3D Models with Submillimeter-Sized Features from SEM Images by Use of Photogrammetry: A Dimensional Comparison to Microtomography." *Micron* 121: 26-32.

Barr, Robert B. and John R. Tagg. 1995. "From Teaching to Learning — A New Paradigm For Undergraduate Education." *Change: The Magazine of Higher Learning* 27: 12-26.

Bolognesi, Cecilia, Fausta Fiorillo. 2018. "Optimization of texture mapping process in the Reality-Based Modeling application". In Salerno, R. (Ed.), *Drawing as (In) Tangible Representation*. 40° Convegno Internazionale dei docenti delle discipline della Rappresentazione. Quindicesimo Congresso UID. Gangemi Editore, Milano. 337–342.

Chatterjee, Helen, Leonie Hannan and Linda Thomson. 2015. "An introduction to object-based learning and multisensory engagement" in Chatterjee, H. J. and Hannan, L. (eds.) *Engaging the senses: object-based learning in higher education*. Farnham, Surrey: Ashgate. 1-20.

Battini, Carlo. 2015. "Il colore come strumento di rilievo tridimensionale." in *Colore e Colorimetria. Contributi Multidisciplinari*, Vol. X A, Atti della Decima Conferenza del Colore, ISBN 978-88-916-0437-8.

Bedford, Jon. 2017. *Photogrammetric Applications for Cultural Heritage: Guidance for Good Practice*. Historic England Publishing. ISBN:9781848025028

Bitelli, Gabriele, Valentina A. Girelli, Fabio Remondino, and Luca Vittuari. 2007. "The Potential of 3D Techniques for Cultural Heritage Object Documentation." In *SPIE Proceedings*, doi:10.1117/12.705012.

Börjesson, Lisa, Olle Sköld, and Isto Huvila. 2020. "Paradata in Documentation Standards and Recommendations for Digital Archaeological Visualisations." *Digital Culture & Society* 6: 191-220.

Bourke, Paul. 2016. "Report: Comparing Laser Scanning to 3D Reconstruction".  
<http://paulbourke.net/miscellaneous/laservs3d/>

Budiono, Hendri Dwi Saptioratri and Hadiwardoyo, Finno Ariandiyudha. 2021. "Development of Product Complexity Index in 3D Models Using a Hybrid Feature Recognition Method with Rule-Based and Graph-Based Methods." *Eastern-European Journal of Enterprise Technologies* 3(1 (111)), 47–61. doi:10.15587/1729-4061.2021.227848.

Caine, Moshe, and Magen, Michael. 2017. "Low Cost Heritage Imaging Techniques Compared." In *Proceedings of the Electronic Visualisation and the Arts*, London, UK, 11-13 July.

Callieri, Marco, Nicolò Dell'Unto, Domenica Dininno, Fredrik Ekengren, F. 2020. Dynamic Collections: A 3D web infrastructure designed to support higher education and research in archaeology -<https://www.darklab.lu.se/digital-collections/dynamic-collections/> "

Carlucci, Renzo. 2016. "Dalla scomposizione della realtà alla memoria digitale preventiva", *Archeomatica Tecnologie per Beni Culturali* , no. 1.

Caroti, Gabriella, Isabel Martínez-Espejo Zaragoza, and Andrea Piemonte. 2015. "Range and Image Based Modelling: A Way for Frescoed Vault Texturing Optimization." In *3D Virtual Reconstruction and Visualization of Complex Architectures, Proceedings of the ISPRS-The International Archives of the Photogrammetry, Remote Sensing and Spatial Information Sciences*, vol. XL-5/W4: 285-2015. doi: 10.5194/isprsarchives-XL-5-W4-285-2015.

Champion, Erik. 2018. "The role of 3D models in virtual heritage infrastructures". In *Cultural Heritage Infrastructures in Digital Humanities*, edited by A. Benardou, E. Champion, C. Dallas, and L. Hughes. London: Routledge.

Chen, Yin, Zhan Song, Shuai Lin, Ralph R. Martin, and Zhi-Quan Cheng. 2018. "Capture of hair geometry using white structured light." *Computer-Aided Design* 96: 31-41. doi:10.1016/j.cad.2017.10.006.

Choi, Kang Hyeok and Changjae Kim. 2021. "Proposed New AV-Type Test-Bed for Accurate and Reliable Fish-Eye Lens Camera Self-Calibration". *Sensors* (Basel, Switzerland), 21. <https://doi.org/10.3390/s21040892>

Choudhury, Asim Kumar Roy. 2014. "Object Appearance and Colour." In *Principles of Colour and Appearance Measurement*, edited by Asim Kumar Roy Choudhury, 53-102. Woodhead Publishing, 2014. ISBN 9780857092298. <https://doi.org/10.1533/9780857099242.53>.

Cignoni, P., Rocchini, C., Roberto Scopigno. 1998: "Metro: measuring error on simplified surfaces". *Computer Graphics Forum*, vol. 17(2): 167-174. Blackwell Publishers.

Collins, Tim, Sandra I. Woolley, Erlend Gehlken and Eugene Ch'ng. 2019. "Automated low-cost photogrammetric acquisition of 3D models from small form-factor artefacts". *Electronics (Switzerland)*, 8(12). <https://doi.org/10.3390/electronics8121441>

Cosentino, Antonino. 2013. "Polarized light photography for art documentation." *Cultural Heritage Science Open Source*. <https://chsopensource.org/polarized-light-photography-for-art-documentation/>.

Cutugno, Matteo, Umberto Robustelli, Giovanni Pugliano. 2022. "Structure-from-Motion 3D Reconstruction of the Historical Overpass Ponte della Cerra: A Comparison between MicMac® Open-Source Software and Metashape". *Drones*. 10.3390/drones6090242.

Dang, Zheng, Fei Wang, and Mathieu Salzmann. 2020. "3D Registration for Self-Occluded Objects in Context." arXiv preprint arXiv:2011.11260.

Dell'Unto, Nicolò. 2018. "3D models and knowledge production" . In Y. Huvila(Ed.), *Archaeology and archaeological information in the digital society*. Abingdon, Oxon: Routledge: 54–69. doi: 10.4324/9781315225272-4.

De Paolis, Lucio Tommaso, Valerio De Luca, Carola Gatto, Giovanni D'Errico, and Giovanna Ilenia Paladini. 2020. "Photogrammetric 3D Reconstruction of Small Objects for a Real-Time Fruition." In *Augmented Reality, Virtual Reality, and Computer Graphics*, edited by L. De Paolis and P. Bourdot, 12242: Lecture Notes in Computer Science, Springer, Cham. [https://doi.org/10.1007/978-3-030-58465-8\\_28](https://doi.org/10.1007/978-3-030-58465-8_28).

Derudas, Paola and Berggren, Åsa. 2021. "Expanding Field-Archaeology Education: The Integration of 3D Technology into Archaeological Training". *Open Archaeology*. 7. 556-573. 10.1515/opar-2020-0146.

Di Giuseppantonio Di Franco, Paola, Carlo Camporesi, Fabrizio Galeazzi and Marcelo Kallmann. 2015. "3D Printing and Immersive Visualization for Improved Perception of Ancient Artifacts". *Presence: Teleoperators and Virtual Environments* 24(3), 243–264.

Di Giuseppantonio Di Franco, Paola, Fabrizio Galeazzi and Carlo Camporesi. 2012. "3D Virtual Dig: a 3D Application for Teaching Fieldwork in Archaeology". *Internet Archaeology*, 32. <http://dx.doi.org/10.11141/ia.32.4>

Dischler, Jean Michele and Djamchid Ghazanfarpour. 2001. "A survey of 3D texturing." *Computers & Graphics* 25, no. 1: 135-151. [https://doi.org/10.1016/S0097-8493\(00\)00113-8](https://doi.org/10.1016/S0097-8493(00)00113-8).

Dostal, Christopher and Kotaro Yamafune. 2018. "Photogrammetric texture mapping: a method for increasing the Fidelity of 3D models of cultural heritage materials". *J. Archaeol. Sci: Report* 18, 430–436. <https://doi.org/10.1016/j.jasrep.2018.01.024>.

Dudley, Sandra H. 2010. "Museum Materialities: Objects, Sense, and Feeling." In *Museum Materialities: Objects, Engagements, Interpretations*, edited by S. H. Dudley, 1-17. London and New York: Routledge.

"Dynamic Collections | Laboratoriet för Digital Arkeologi DARK Lab." Laboratoriet för Digital Arkeologi DARK Lab. <https://www.darklab.lu.se/digital-collections/dynamic-collections/>.

Edmond, Jennifer and Francesca Morselli. 2020. "Sustainability of digital humanities projects as a publication and documentation challenge". *JDOC* 76 (5):1019–1031.

Eldefrawy, Mahmoud, Scott King, Michael Starek. 2022. "Partial Scene Reconstruction for Close Range Photogrammetry Using Deep Learning Pipeline for Region Masking". *Remote Sensing*. 14. 3199. [10.3390/rs14133199](https://doi.org/10.3390/rs14133199).

Elkhrachy, Ismail. 2022. "3D Structure from 2D Dimensional Images Using Structure from Motion Algorithms" *Sustainability* 14, no. 9: 5399. <https://doi.org/10.3390/su14095399>

Ekengren, Fredrik, Marco Callieri, Domenica Dinunno, Åsa Berggren., MacHeridis, S., Nicolò Dell'Unto. 2021. "Dynamic Collections: A 3D Web Infrastructure for Artifact Engagement". *Open Archaeology*, 7(1), 337-352. <https://doi.org/10.1515/opar-2020-0139>

- Eros, Agosto, and Leandro Bornaz. 2017. "3D Models in Cultural Heritage: Approaches for Their Creation and Use." *International Journal of Computational Methods in Heritage Science* 1, no. 1: 1-9. doi:10.4018/IJCMHS.2017010101.
- Fiorillo, Fausta, Marco Limongiello, and Cecilia Bolognesi. 2021. "Image-Based and Range-Based Dataset Integration for an Efficient 3D Representation." In *3D Research*, vol. 6, no. 9, pp. 130. doi: 10.3280/oa-693.130.
- Fryer, John G. 1986. "Lens Distortion for Close Range Photogrammetry." *International Archives of Photogrammetry and Remote Sensing* 26, no. 5: 30-37.
- Furukawa, Yasutaka and Jean Ponce. 2010. "Accurate, Dense, and Robust Multiview Stereopsis," in *IEEE Transactions on Pattern Analysis and Machine Intelligence*, vol. 32, no. 8:1362-1376. doi:10.1109/TPAMI.2009.161.
- Galeazzi, Fabrizio, Paola Franco and Justin Matthews. 2015. "Comparing 2D Pictures with 3D Replicas for the Digital Preservation and Analysis of Tangible Heritage". *Museum Management and Curatorship*. 30. 10.1080/09647775.2015.1042515.
- Gallo, Alessandro, Maurizio Muzzupappa, and Fabio Bruno. 2014. "3D Reconstruction of Small Sized Objects from a Sequence of Multi-Focused Images." *Journal of Cultural Heritage* 15, no. 2: 173-182. doi:10.1016/j.culher.2013.04.009.
- Gebhard, Rupert. 2003. "Material Analysis in Archaeology." *Hyperfine Interactions* 150, no. 1-4: 1-5. doi:10.1023/B:HYPE.00000007175.85659.15.
- Gonizzi Barsanti, Sara, Fabio Remondino, Belén Jiménez Fernández-Palacios and Visintini, Domenico. 2014. "Critical Factors and Guidelines for 3D Surveying and Modelling in Cultural Heritage". *International Journal of Heritage in the Digital Era*. 3: 141-158. 10.1260/2047-4970.3.1.141.
- Goral, Cindy M., Kenneth E. Torrance, Donald P. Greenberg and Bennett Battaile. 1984. "Modeling the interaction of light between diffuse surfaces." *Proceedings of the 11th annual conference on Computer graphics and interactive techniques*.



Grassi, Caterina, Diego Ronchi, Daniele Ferdani, Giorgio Franco Pocobelli, Rachele Manganelli Del Fà. 2022. "A 3D survey in archaeology. Comparison among software for image and range-based data integration." *D-SITE Drones. System of Information on Cultural Heritage for a Spatial and Social Investigation*. Volume 2.

Guarnera, Daniele, Giuseppe Claudio Guarnera, Ghosh, A., Denk, C., and Glencross, M. 2016. "BRDF Representation and Acquisition." *Comput. Graph. Forum* 35, 625–650.

Guidi, Gabriele, Michele Russo, Jean Angelo Beraldin. 2010. *Acquisizione 3D e modellazione poligonale*. McGraw-Hill. Italia.

Hagg, Alexander, Frederik Hegger and Paul Plöger. 2017. "On Recognizing Transparent Objects in Domestic Environments Using Fusion of Multiple Sensor Modalities." In: Behnke, S., Sheh, R., Sariel, S., Lee, D. (eds) *RoboCup 2016: Robot World Cup XX*. Springer, Cham. [https://doi.org/10.1007/978-3-319-68792-6\\_1](https://doi.org/10.1007/978-3-319-68792-6_1).

Håkansson, Inga, Thörn, Raimond and Linde, Petter. 1999. *Bildkompendium: Bronsåldern*. Lund: Institutionen för arkeologi och antikens historia, Lunds universitet. (Kompendium, säljs i receptionen på LUX) <https://www.ht.lu.se/serie/3052249/>

Hong, Nina, and James Hilfiker. 2020. "Mueller matrix ellipsometry study of a circular polarizing filter." *Journal of Vacuum Science & Technology B* 38, no. 1: 014012. <https://doi.org/10.1116/1.5129691>.

Hilfiker, James, Nina Hong, and Stefan Schoeche. 2022. "Mueller matrix spectroscopic ellipsometry." *Advanced Optical Technologies* 11. <https://doi.org/10.1515/aot-2022-0008>.

Kaufman, John, Allan EW Rennie, Morag Clement. 2015. "Single Camera Photogrammetry for Reverse Engineering and Fabrication of Ancient and Modern Artifacts". *Procedia CIRP* 36. ISSN 2212-8271. 223-229. <https://doi.org/10.1016/j.procir.2015.01.073>.

Koshikawa, Kazutada and Yoshiaki Shirai. 1987. "A Model-Based Recognition of Glossy Objects Using their Polarimetrical Properties." *Adv. Robotics* 2, 137-147.

Lelkes, Jenny. 2019. "How inclusive is object-based learning?" In *Spark: UAL Creative Teaching and Learning Journal*, 4 No. 1, 76-82.

- Lock, Gary. 2006. "Computers, learning and teaching in archaeology: Life past and present on the screen". In T. L. Evans & P. T. Daly (Eds.). *Digital archaeology: Bridging method and theory*. Abingdon, Oxon: Routledge. <http://site.ebrary.com/id/10163521572>
- Lu, Renfu. 2016. "Light Scattering Technology for Food Property, Quality, and Safety Assessment." CRC Press. ISBN1482263351, 483.
- Ludwig, Arthur. 1973. "The definition of cross polarization." *IEEE Transactions on Antennas and Propagation* 21, no. 1: 116-119. <https://doi.org/10.1109/TAP.1973.1140406>.
- Maksimovic, Nikola. 2020. "Methods to Digitizing Physical Properties of Fabric for Virtual Simulation."
- Marín-Buzón, Carmen, Antonio Pérez-Romero, José Luis López-Castro, Imed Ben Jerbania, and Francisco Manzano-Agugliaro. 2021. "Photogrammetry as a New Scientific Tool in Archaeology: Worldwide Research Trends" *Sustainability* 13, no. 9: 5319. <https://doi.org/10.3390/su13095319>
- Marroquim, Ricardo, Asla S., Karina Rodrigues, Vitor Balbio, and Rafael Zamorano. 2017. "Digitizing ivory artifacts at the National History Museum in Brazil." In *GCH 2017 - Eurographics Workshop on Graphics and Cultural Heritage*, 11-18.
- Marshall, Matt, Johnson, Andrew, Summerskill, Steve, Quinner Baird, and Enrique Esteban. 2019. "Automating Photogrammetry for the 3D Digitisation of Small Artefact Collections. ISPRS - International Archives of the Photogrammetry", *Remote Sensing and Spatial Information Sciences*, XLII-2/W15, 751-757. <https://doi.org/10.5194/isprs-archives-XLII-2-W15-751-2019>.
- Menna, Fabio, Erica Nocerino, Daniele Morabito, Elisa Mariarosaria Farella, M. Perini, Fabio Remondino. 2017. "An open source low-cost automatic system for image-based 3D digitization". *Int. Arch. Photogramm. Remote Sens. Spat. Inf. Sci. - ISPRS Arch.* 42, 155–162. <https://doi.org/10.5194/isprs-archives-XLII-2-W8-155-2017>
- Mi, Xiying, and Bonita M. Pollock. 2018. "Metadata Schema to Facilitate Linked Data for 3D Digital Models of Cultural Heritage Collections: A University of South Florida Libraries Case Study." *Cataloging & Classification Quarterly* 56 (2-3): 273-86. <https://doi.org/10.1080/01639374.2017.1388894>.

- Miyazaki, Daisuke, Masataka Kagesawa, and Katsushi Ikeuchi. 2004. "Transparent Surface Modelling from a Pair of Polarization Images." *IEEE Trans. Patt. Anal. Mach. Intell.*, 26:73–82.
- Morelli, Luca, Ali Karami, Fabio Menna, and Fabio Remondino. 2022. "Orientation of Images with Low Contrast Textures and Transparent Objects." *International Archives of Photogrammetry, Remote Sensing and Spatial Information Sciences XLVIII-2/W2-2022*: 77-84. doi:10.5194/isprs-archives-XLVIII-2-W2-2022-77-2022.
- Morena, Sara, Salvatore Barba, and Antonio Álvaro-Tordesillas. 2019. "Shining 3D Einscan-Pro Application and Validation in the Field of Cultural Heritage, from the Chillida-Leku Museum to the Archaeological Museum of Sarno". *The International Archives of the Photogrammetry, Remote Sensing and Spatial Information Sciences XLII-2/W18*: 135–42. doi:10.5194/ISPRS-ARCHIVES-XLII-2-W18-135-2019.
- Morris, Christine, Alan Peatfield, and Brendan O'Neill. 2018. "'Figures in 3D': Digital Perspectives on Cretan Bronze Age Figurines." *Open Archaeology* 4, no. 1: 50–61. doi:10.1515/OPAR-2018-0003.
- Moskvin, Aleksei, Victor Kuzmichev, and Mariia Moskvina. 2019. "Digital Replicas of Historical Skirts." *The Journal of The Textile Institute* 110, no. 12: 1810-1826. doi:10.1080/00405000.2019.1621042.
- Nguyen, Hoang Minh, Burkhard Wünsche, Patrice Delmas and Christof Lutteroth. 2012. "3D models from the black box: investigating the current state of image-based modeling". In *Proceedings of the 20th International Conference on Computer Graphics, Visualisation and Computer Vision (WSCG), 2012*. 249-258.
- Nicolae, C.; Enica Nocerino, Fabio Menna, Fabio Remondino. 2014. "Photogrammetry Applied to Problematic Artefacts". *Int. Arch. Photogramm. Remote Sens. Spat. Inf. Sci.* 40, 451–456.
- Nobles, Gary, Canan Çakırlar and Pjotr Svetachov. 2019. "Bonify 1.0: Evaluating virtual reference collections in teaching and research". *Archaeological and Anthropological Sciences* 11. 5705–5716. doi: 10.1007/s12520-019-00898-1.

Nocerino, Erica, Fabio Menna and Fabio Remondino. 2014. "Accuracy of typical photogrammetric networks in cultural heritage 3D modeling projects." *ISPRS International Archives of the Photogrammetry, Remote Sensing and Spatial Information Sciences* 40, no. 4: 465-472.

Nocerino, Erica, Lago, F., Morabito, Daniele, Fabio Remondino, Porzi, L., Fabio Poiesi, Rota Bulò, S., Paul Chippendale, Alex Locher, Havlena, M., and others. 2017. "A Smartphone-Based 3D Pipeline for the Creative Industry—The REPLICATE EU Project." *International Archives of the Photogrammetry, Remote Sensing & Spatial Information Sciences* 42: 535–541.

Parente, Luigi, Jim H. Chandler. and Neil Dixon. 2019. "Optimising the quality of an SfM-MVS slope monitoring system using fixed cameras". *Photogram Rec*, 34: 408-427. <https://doi.org/10.1111/phor.12288>

Percoco, Gianluca, and A.J. Sanchez Salmeron. 2015. "Photogrammetric measurement of 3D freeform millimetre-sized objects with micro features: an experimental validation of the close-range camera calibration model for narrow angles of view". *Measurement Science and Technology*, 26. <https://doi.org/10.1088/0957-0233/26/6/065602>

Piccoli, Chiara. 2017. "Visualizing antiquity before the digital age: Early and late modern reconstruction drawings of Greek and Roman cityscapes". *Analecta Praehistorica Leidensia* 47:225–257.

Poiesi, Fabio, Alex Locher, Paul Chippendale, Erica Nocerino, Fabio Remondino and Luc Van Gool. "Cloud-Based Collaborative 3D Reconstruction Using Smartphones." 2017. In *Proceedings of the 14th European Conference on Visual Media Production (CVMP 2017)*, 1–9. Association for Computing Machinery. <https://doi.org/10.1145/3150165.3150166>.

Polo, María-Eugenia, Ángel M. Felicísimo, and Guadalupe Durán-Domínguez. 2022. "Accurate 3D models in both geometry and texture: An archaeological application." *Digital Applications in Archaeology and Cultural Heritage* 27: e00248. doi:10.1016/j.daach.2022.e00248.

Ponchio, Federico, Marco Callieri, Matteo Dellepiane and Roberto Scopigno. 2020, "Effective Annotations Over 3D Models". *Computer Graphics Forum*, 39: 89-105. <https://doi.org/10.1111/cgf.13664>

Pont, Sylvia C., and Koenderink, Jan J. 2005. "Reflectance from Locally Glossy Thoroughly Pitted Surfaces." *Computer Vision and Image Understanding* 98, no. 2: 211-222. doi:10.1016/j.cviu.2004.10.004.

Potenziani, Marco, Marco Callieri, Matteo Dellepiane, Corsini, M., Federico Ponchio, and Roberto Scopigno. 2015. "3DHOP: 3D Heritage Online Presenter". *Computers & Graphics*, 52, 129–141. doi: 10.1016/j.cag.2015.07.001.

Preim, Bernhard, Charl Botha. 2014. "Chapter 6 - Surface Rendering", in *Visual Computing for Medicine (Second Edition)*, Morgan Kaufmann,,: 229-267 ISBN 9780124158733, <https://doi.org/10.1016/B978-0-12-415873-3.00006-7>.

Pritchard, Douglas, Ripanti, Francesco, Rigauts, Thomas, Joncic, Nenad, Davies, Robert, and Ioannides, Marinos. 2022. "Study on Quality in 3D Digitisation of Tangible Cultural Heritage: Mapping Parameters, Formats, Standards, Benchmarks, Methodologies, and Guidelines VIGIE 2020/654 Final Study Report."

Rahaman, Hafizur, and Erik Champion. 2019. "To 3D or Not 3D: Choosing a Photogrammetry Workflow for Cultural Heritage Groups". *Heritage* 2, no. 3: 1835-1851. <https://doi.org/10.3390/heritage2030112>

Remondino, Fabio and El-Hakim, S. 2006. "Image-based 3D Modelling: A Review". *The Photogrammetric Record*, 21: 269-291. <https://doi.org/10.1111/j.1477-9730.2006.00383.x>

Remondino, Fabio, Erica Nocerino, Isabella Toschi, and Fabio Menna. 2017. "A Critical Review of Automated Photogrammetric Processing of Large Datasets." *The International Archives of the Photogrammetry, Remote Sensing and Spatial Information Sciences*, vol. XLII XLII 2/W5. 26th International CIPA Symposium. Ottawa, Canada.

Szeliski, Richard. 2011. "Image-based rendering". In: *Computer Vision. Texts in Computer Science*. Springer, London. [https://doi.org/10.1007/978-1-84882-935-0\\_13](https://doi.org/10.1007/978-1-84882-935-0_13)

Robinson, Martin P., Laura C. Fitton, Aimée Little, Samuel N. F. Cobb, and Steven P. Ashby. 2019. "Dielectric Replica Measurement: A New Technique for Obtaining the Complex Permittivity of Irregularly Shaped Objects." *Measurement Science and Technology* 30.

Ronchi, Diego, Daniele Ferdani, Giorgio Franco Pocobelli, and Rachele Manganelli Del Fà. 2022. "A 3D Survey in Archaeology: Comparison among software for image and range-based data integration." In *D-SITE Drones: Systems of Information on Cultural Heritage for a Spatial and Social Investigation*, edited by Sandro Parrinello, Salvatore Barba, Anna Dell'Amico, Andrea di Filippo. Pavia University Press.

Thomas, Adrian, Mohd Fahrul Hassan, Al Emran Ismail, Reazul Haq, Ahmad Arifin, M. Ahmad. 2019. "Portable Mini Turntable for Close-Range Photogrammetry: A Preliminary Study". *IOP Conference Series: Materials Science and Engineering*. 607. 012011. 10.1088/1757-899X/607/1/012011.

Verhoeven, Geert. 2016. "Basics of Photography for Cultural Heritage Imaging." In *3D Recording, Documentation and Management of Cultural Heritage*, edited by Efstratios Stylianidis and Fabio Remondino. Caithness: Whittles Publishing. 127–251.

Vitelli, Gian Paolo. 2011. "Potenzialità e prospettive delle tecnologie avanzate di rilevamento per la conservazione dell'architettura storica". University of Naples Federico II. Retrieved from <http://www.fedoa.unina.it/8851/>.

Wang, Zheng, Jon P. Mills, Wen Xiao, Rongyong Huang, Shunyi Zheng and Zhenhong Li. 2017. "A Flexible, Generic Photogrammetric Approach to Zoom Lens Calibration." *Remote. Sens.* 9: 244.

Wilkinson, Mark D., Michel Dumontier, IJsbrand Jan Aalbersberg, Appleton, G., Axton, M., Baak, A., ... Mons, B. 2016. The FAIR guiding principles for scientific data management and stewardship. *Scientific Data*, 3. 160018. doi: 10.1038/sdata.2016.18.

Willcocks, J. 2015. 'The power of concrete experience: museum collections, touch and meaning making in art and design pedagogy' in Chatterjee, H. J. and Hannan, L. (eds.) *Engaging the senses: object-based learning in higher education*. Farnham, Surrey: Ashgate. 43-56.

Xu, Yanan, Yohwan So, and Sanghyuk Woo. 2022. "Plane Fitting in 3D Reconstruction to Preserve Smooth Homogeneous Surfaces." *Sensors* 22, no. 23: 9391. doi:10.3390/s22239391.

Yamafune, Kotaro. 2016. "Using Computer Vision Photogrammetry (Agisoft PhotoScan) to Record and Analyze Underwater Shipwreck Sites."

Yanagi, Hideharu, and Hirofumi Chikatsu. 2010. "Modeling of small objects using macro lens in digital very close range photogrammetry". *International Archives of Photogrammetry, Remote Sensing and Spatial Information Sciences*. Vol. XXXVIII.

Yu, Chih-Hao. 2014. "Semantic annotation services for 3D models of cultural heritage artefacts". PhD Thesis, School of Information Technology and Electrical Engineering, The University of Queensland. <https://doi.org/10.14264/uql.2014.617>

Yu, Chih-Hao and Jane Hunter. 2013. "Documenting and sharing comparative analyses of 3D digital museum artifacts through semantic web annotations." *ACM Journal on Computing and Cultural Heritage* 6: 18:1-18:20.

Zhang, Chuchu, and Richard W. Neu. 2021. "Understanding the Role of Glaze Layer with Aligned Images from Multiple Surface Characterization Techniques." *Wear*. vol. 477. doi:10.1016/j.wear.2021.203837.

Zlatanova, Siyka, Alias Abdul Rahman and Wenzhong Shi. 2004. "Topological models and frameworks for 3D spatial objects". *Computers & Geosciences*. 30(4). 419-428.





# Sitography

"3D Digitization |." 3D Digitization |. Accessed February 2023. <https://3d.si.edu/>.

"3D Virtual Museum - Il Museo Virtuale del patrimonio culturale italiano." 3D Virtual Museum. Accessed February 2023. <http://www.3d-virtualmuseum.it/>.

"Agisoft Metashape: Agisoft Metashape." Agisoft Metashape: Agisoft Metashape. Accessed February 2023. <https://www.agisoft.com/>.

"Archaeology: Level 2 | The joint faculties of humanities and theology." Humanistiska och teologiska fakulteterna. Accessed February 2023. <https://www.ht.lu.se/en/course/ARKA22/VT2016/>.

"The Arc/k Project | To save and to keep safe ..." Arc/k Project. Accessed February 2023. <https://arck-project.org/>.

"CMVS." DIENS. Accessed February 2023. <https://www.di.ens.fr/cmvs/>.

"CyArk." CyArk. Accessed February 2023. <https://cyark.org/>.

Cardinal, David. "Smartphones vs Cameras: Closing the gap on image quality - DXOMARK." DXOMARK, March 19, 2020. <https://www.dxomark.com/smartphones-vs-cameras-closing-the-gap-on-image-quality/>.

"Discover Europe's digital cultural heritage." Discover Europe's digital cultural heritage | Europeana. Accessed February 2023. <https://www.europeana.eu/en>.

"Dynamic Collections." 403 Forbidden. Accessed February 2023. [https://models.darklab.lu.se/dynmcoll/Dynamic\\_Collections/single\\_viewer.html?obj=DC354\\_LUHM13188c](https://models.darklab.lu.se/dynmcoll/Dynamic_Collections/single_viewer.html?obj=DC354_LUHM13188c).

"Dynamic Collections." Accessed February 2023. [https://models.darklab.lu.se/dynmcoll/Dynamic\\_Collections/single\\_viewer.html?obj=DC351\\_LUHM21015.20](https://models.darklab.lu.se/dynmcoll/Dynamic_Collections/single_viewer.html?obj=DC351_LUHM21015.20).

"Dynamic Collections." Accessed February 2023. [https://models.darklab.lu.se/dynmcoll/Dynamic\\_Collections/single\\_viewer.html?obj=DC352\\_LUHM25561](https://models.darklab.lu.se/dynmcoll/Dynamic_Collections/single_viewer.html?obj=DC352_LUHM25561).

"Dynamic Collections." Accessed February 2023. [https://models.darklab.lu.se/dynmcoll/Dynamic\\_Collections/single\\_viewer.html?obj=DC358\\_LUHM32125.81](https://models.darklab.lu.se/dynmcoll/Dynamic_Collections/single_viewer.html?obj=DC358_LUHM32125.81).

"Global Digital Heritage." Global Digital Heritage. Accessed February 2023. <https://globaldigitalheritage.org/>.

"MeshLab." MeshLab. Accessed February 2023. <https://www.meshlab.net/>.

"Photogrammetry: the technology behind the magic." Photogrammetry: the technology behind the magic. Accessed February 2023. <https://www.photogrammetry.technology/>.

"PMVS2." DIENS. Accessed February 2023. <https://www.di.ens.fr/pmvs/>.

"Sketchfab - The best 3D viewer on the web." Sketchfab. Accessed February 2023. <https://sketchfab.com/>.

"Survey on museums and other cultural institutions: public use micro.stat files." Istat.it. Accessed February 2023. <https://www.istat.it/it/archivio/167568>.





# Ringraziamenti

Vorrei ringraziare la mia relatrice Sofia Pescarin per avermi seguito in questo percorso tesi e avermi avvicinato al mondo affascinante dell'archeologia digitale.

Ringrazio il mio correlatore Diego Ronchi, per la sapienza, l'esperienza trasmessa e la grande disponibilità di tempo e attenzione dimostratami, che non era scontata e ho capito essere preziosa.

Ringrazio il mio tutor Nicolò Dell'Unto per avermi infuso energia e speranza per il futuro e aver stimolato spirito critico, in un momento di formazione che considero altissimo.

Voglio esprimere la mia gratitudine a Domenica Dinunno, per lo scambio stimolante di esperienze durante le uggiose giornate svedesi e le passeggiate al parco in quelle sporadiche di sole. Per la professionalità e l'amicizia, grazie.

Grazie ad entrambi per avermi dato prova concreta del fatto che si lavora e si vive meglio se circondati da menti gentili in un ambiente sereno.

Vorrei ringraziare i miei genitori che per non deludermi sanno mettere in discussione le proprie convinzioni ed abitudini, senza tradire sé stessi. A loro devo il senso della giustizia e la capacità d'amare incondizionatamente. A mia sorella Anna, per avermi precluso dalla nascita il senso di solitudine ed essere sempre il mio saldo modello di coraggio, grazie.

A Giulia, *funicoletto*<sup>28</sup> nel mondo che ci vedrà crescere insieme; a Consti, che ha il dono dell'ascolto e quello della distruzione (di oggetti); ad Alice, che ha una forza di volontà inversamente proporzionale al suo senso dell'orientamento.

A Lorenza, che racchiude la fulgida tenerezza del mondo in cui vorrei abitare.

A Nico, Enrico e Daniele.

A Lia, per la mano sempre tesa.

Ad i miei amici e agli animi buoni che ho incontrato e che mi sono accanto.

A chi ha smesso di combattere la propria vulnerabilità, a cui non si fa la guerra, ma l'amnistia.

Grazie.

---

<sup>28</sup> funicoletto: /funiko'let:0/ [dal dialetto menniano, voce di origine molisana] - *spazio di comfort, generalmente di piccole dimensioni, generato da una fenditura ospitale ed accogliente*. Rientra, insieme a parole come "Mozzafiato", "Roccambolesco" e "Merigliare", nella lista di parole italiane intraducibili in altre lingue.